Universidade do Minho
Escola de Engenharia

Bárbara Guerra Nogueira

Developing and validation of a novel antimicrobial coating strategy for endotracheal tubes to prevent ventilator-associated pneumonia

October 2023

Developing and validation of a novel antimicrobial coating strategy for endotracheal tubes to prevent ventilator-associated pneumonia
Bárbara Guerra Nogueira
UMinho | 2023

Universidade do Minho
Escola de Engenharia

Bárbara Guerra Nogueira

Developing and validation of a novel antimicrobial coating strategy for endotracheal tubes to prevent ventilator-associated pneumonia

Dissertação de Mestrado
Mestrado em Biotecnologia

Trabalho efetuado sob a orientação da
Doutora Susana Patrícia Peixoto Lopes

October 2023

DIREITOS DE AUTOR E CONDIÇÕES DE UTILIZAÇÃO DO TRABALHO POR TERCEIROS

Este é um trabalho académico que pode ser utilizado por terceiros desde que respeitadas as regras e boas práticas internacionalmente aceites, no que concerne aos direitos de autor e direitos conexos.

Assim, o presente trabalho pode ser utilizado nos termos previstos na licença abaixo indicada.

Caso o utilizador necessite de permissão para poder fazer um uso do trabalho em condições não previstas no licenciamento indicado, deverá contactar o autor, através do RepositóriUM da Universidade do Minho.

Licença concedida aos utilizadores deste trabalho:



Atribuição
CC BY
https://creativecommons.org/licenses/by/4.0/

AGRADECIMENTOS

A realização desta dissertação contou com o apoio de um grande número de pessoas, que se mostraram sempre disponíveis para o esclarecimento de dúvidas e que me acompanharam incondicionalmente durante estes quatro meses. A todas elas, eu presto o meu sincero agradecimento!

Um muito obrigado à Dr.ª Susana Lopes, orientadora desta dissertação, pela sua simpatia, orientação, dedicação e empatia. De igual forma, agradeço a todos os membros do Laboratório de Investigação de Biofilmes Rosário Oliveira, por me terem acolhido e por se terem demonstrado sempre disponíveis para me esclarecerem as dúvidas surgidas ao longo do deste percurso.

À minha família, em especial aos meus pais, por ter proporcionado as melhores condições para a minha evolução cívica e académica, pelos valores transmitidos e o apoio incondicional, ao longo de todos estes anos.

Aos meus amigos, Alda Ferreira, Ana Luísa Monteiro, Beatriz Peixoto, Beatriz Ribeiro, Carlos Botelho, Maria João Costa, Maria José Ferreira, Vera Mendes pela partilha de momentos inesquecíveis, motivação e paciência no decorrer deste percurso.

A todos, um sincero, muito obrigada!

STATEMENT OF INTEGRITY

I hereby declare having conducted this academic work with integrity. I confirm that I have not used plagiarism or any form of undue use of information or falsification of results along the process leading to its elaboration.

I further declare that I have fully acknowledged the Code of Ethical Conduct of the University of Minho.

RESUMO

A pneumonia associada à ventilação mecânica (VAP), infeção nosocomial com elevada mortalidade, é causada principalmente pelo desenvolvimento de biofilmes nos tubos endotraqueais (ETT). Os atuais métodos de diagnóstico de VAP são imprecisos devido à existência de várias doenças que se assemelham a esta infeção. Este trabalho teve como principais objetivos: desenvolver um método de Hibridação *In Situ* por Fluorescência de Ácidos Nucleicos Peptídicos (PNA-FISH) para o diagnóstico de VAP; avaliar a formação de biofilmes por espécies relacionadas com VAP em superfícies de materiais distintas (poliestireno vs. PVC); e estudar um novo revestimento de PVC para prevenir a adesão de biofilmes.

No estudo do PNA-FISH, foi examinado o efeito da temperatura (52°C, 58°C, 60°C e 62°C) e da concentração de formamida (30% vs. e 5% v/v) na especificidade de cinco sondas PNA concebidas para a deteção de *Pseudomonas aeruginosa*, *Staphylococcus aureus*, *Klebsiella pneumoniae*, *Staphylococcus epidermidis* e *Acinetobacter baumannii*. A sonda de *P. aeruginosa* apresentou hibridação de forma consistente, independentemente das condições testadas; o sinal da sonda de *K. pneumoniae* variou com a estirpe alvo, apresentando um sinal mais elevado a 52°C e 60°C. Por sua vez, as restantes sondas apresentaram sinal fraco ou nulo no microscópio de fluorescência. Relativamente ao efeito da formamida, em geral, verificou-se uma melhor hibridação quando se utilizou HS2 (solução de hibridação com 5% (v/v) de formamida). Porém, este parâmetro também foi influenciado pela sonda utilizada, havendo casos em que ocorreu hibridação mesmo utilizando-se HS1 (solução de hibridação com 30% (v/v) de formamida).

Para impedir a formação de biofilmes compostos por *P. aeruginosa*, *S. aureus* e *Candida albicans* SC 5314 em ETTs, foi explorada uma estratégia inovadora para o revestimento de PVC. Esta abordagem implica a imobilização da ciprofloxacina (CIP) e da clorexidina (CHX) através da funcionalização da polidopamina (pDA) na superfície do PVC.

P. aeruginosa e *S. aureus* apresentaram a maior capacidade de formar biofilmes em poliestireno (8,0 $\log_{10}$ CFU/mL), seguidos por *C. albicans* (6,7 $\log_{10}$ CFU/mL). Quando cultivadas em biofilmes de duas espécies com *P. aeruginosa*, *S. aureus* diminuiu 1,3 $\log_{10}$ CFU/mL o seu número de células, enquanto *C. albicans* permaneceu inalterada. Nos biofilmes de três espécies, *P. aeruginosa*, *S. aureus* e *C. albicans* podiam coexistir, apresentando 6,8 $\log_{10}$ UFC/mL, 7,1 $\log_{10}$ UFC/mL e 6,5 $\log_{10}$ UFC/mL, respetivamente. No entanto, verificou-se uma diminuição do número

de células em cada um dos microrganismos quando comparado com os seus biofilmes uma espécie.

As três espécies apresentaram padrões distintos na formação de biofilme nas superfícies de PVC, com predominância de *C. albicans* (7,2 $\log_{10}$ CFU/mL), seguida de *S. aureus* (6,2 $\log_{10}$ CFU/mL) e *P. aeruginosa* (5,5 $\log_{10}$ CFU/mL). Curiosamente, a superfície de PVC modificada com CIP/CHX resultou numa diminuição drástica do número de células bacterianas/fúngicas cultiváveis. O FISH utilizado nestes consórcios mostrou, no entanto, a presença e a discriminação de todas as espécies nos biofilmes em superfícies não revestidas e a população bacteriana no biofilme formado em PVC revestido. Assim, a imobilização do PVC com CIP e CHX permitiu que *P. aeruginosa*, *S. aureus* e *C. albicans* passassem para um estado de células não cultiváveis.

Palavras-Chave: Pneumonia Associada à Ventilação Mecânica; Tubo Endotraqueal; PNA-FISH; Ciprofloxacina; Clorexidina

ABSTRACT

Ventilator-associated pneumonia (VAP), a nosocomial infection with high mortality, is primarily caused by biofilm development on endotracheal tubes (ETT). Current diagnostic methods for VAP are imprecise due to the presence of similar diseases. This work had as its main goals: to develop a Peptide Nucleic Acid Fluorescence *In Situ* Hybridization (PNA-FISH) method for VAP diagnosis; to evaluate the biofilm formation by VAP-related species on distinct material surfaces (polystyrene vs. PVC); and to address a novel PVC coating for preventing biofilm adhesion.

In the PNA-FISH study, the effect of temperature (52°C, 58°C, 60°C, and 62°C) and formamide concentration (30% vs. and 5% v/v) was examined on the specificity of five PNA probes designed for detection of *Pseudomonas aeruginosa*, *Staphylococcus aureus*, *Klebsiella pneumoniae*, *Staphylococcus epidermidis*, and *Acinetobacter baumannii*. The *P. aeruginosa* probe consistently showed hybridization, regardless of the conditions tested; the *K. pneumoniae* probe signal varied with the target strain, showing a higher signal at 52°C and 60°C. In turn, the remaining probes showed weak or no signal under a fluorescence microscope. Regarding the effect of formamide, in general, better hybridization was seen when HS2 (hybridization solution with 5% (v/v) formamide) was used. However, this parameter was also influenced by the probe used, and there were cases where hybridization occurred even when HS1 (hybridization solution with 30% (v/v) formamide) was used.

To hinder the formation of biofilms comprising *P. aeruginosa*, *S. aureus*, and *Candida albicans* SC 5314 on ETTs, an innovative strategy for PVC coating was explored. This approach entails the immobilisation of ciprofloxacin (CIP) and chlorhexidine (CHX) via polydopamine (pDA) functionalization on the PVC surface.

P. aeruginosa and *S. aureus* showed the highest ability to form biofilms on polystyrene (8.0 $\log_{10}$ CFU/mL), followed by *C. albicans* (6.7 $\log_{10}$ CFU/mL). When grown in dual-species biofilms with *P. aeruginosa*, *S. aureus* decreased by 1.3 $\log_{10}$ CFU/mL in its number of cells, whereas *C. albicans* remained unchanged. In triple-species biofilms, *P. aeruginosa, S. aureus*, and *C. albicans* could co-exist together, presenting 6.8 $\log_{10}$ CFU/mL, 7.1 $\log_{10}$ CFU/mL, and 6.5 $\log_{10}$ CFU/mL, respectively. However, there was a decrease in the number of cells in each of the microorganisms when compared to their single-species biofilms.

All three species showed distinct patterns of biofilm formation on PVC surfaces, with *C. albicans* prevailing (7.2 $\log_{10}$ CFU/mL), followed by *S. aureus* (6.2 $\log_{10}$ CFU/mL) and *P. aeruginosa*

(5.5 $\log_{10}$ CFU/mL). Intriguingly, the CIP/CHX-modified PVC surface resulted in a drastic decrease in the number of cultivable bacterial/fungal cells. FISH employed in these consortia showed, however, the presence and discrimination of all species within biofilms on uncoated surfaces and the bacterial population in biofilm formed on coated PVC. Thus, immobilising PVC with CIP and CHX allowed *P. aeruginosa*, *S. aureus*, and *C. albicans* to switch into a state of non-culturable cells.

Keywords: Ventilator-associated pneumonia; Endotracheal tubes; PNA-FISH; Ciprofloxacin; Chlorhexidine

TABLE OF CONTENTS

AGRADECIMENTOS iii
RESUMO v
ABSTRACT vii
LIST OF ABBREVIATIONS, AND SYMBOLS xi
LIST OF FIGURES xv
LIST OF TABLES xviii
CHAPTER 1: INTRODUCTION 1
1.1. Background 2
1.2. Motivation 2
1.3. Aims of this Dissertation 3
1.4. Thesis Outline 4
CHAPTER 2: LITERATURE REVIEW 5
2.1. Ventilator-Associated Pneumonia 6
2.1.1. VAP Pathogenesis 7
2.1.2. Microbial Contributors to VAP 9
2.1.2.1. *P. aeruginosa* 10
2.1.2.2. *S. aureus* 11
2.1.2.3. S. epidermidis 11
2.1.1.1. *A. baumannii* 11
2.1.1.2. *K. pneumoniae* 12
2.1.1.3. *C. albicans* 12
2.1.2. Diagnosis of VAP 13
2.1.2.1. Radiographic Criteria for VAP Diagnosis 14
2.1.2.2. Microbiological Criteria for VAP Diagnosis 15
2.1.2.3. Molecular-based VAP diagnostic technologies 15
2.1.2.3.1. PNA-FISH method for VAP diagnosis 16
2.1.3. Treatment of VAP 17
2.1.4. Prevention of VAP 20
2.2. Endotracheal Tubes 21
2.2.1. Biofilms on ETTs 22
2.2.2. Prevention of Biofilm Development in ETTs 24

CHAPTER 3: MATERIALS AND METHODS 27
3.1. Microorganisms and Culture Conditions 28
3.2. PNA-FISH Method 28
3.2.1. Sample Preparation, Fixation and Permeabilization 28
3.2.2. Probes Preparation 29
3.2.3. Hybridization and Washing 30
3.2.4. Sample Counterstaining 31
3.2.5. Sample Visualization 31
3.3. Biofilm Assay 31
3.3.2. Biofilm Analysis 32
3.3.3. Biofilm Formation on PVC 33
3.4. Data analysis and Statistics 34
CHAPTER 4: RESULTS AND DISCUSSION 36
4.1. PNA-FISH Experimental Specificity Testing 37
4.2. Assessment of Biofilm Formation 50
CHAPTER 5: CONCLUSION AND FUTURE PERSPECTIVES 60
CHAPTER 6: BIBLIOGRAPHY 63

LIST OF ABBREVIATIONS, AND SYMBOLS

#

% | Percentage

°C | Degrees Celsius

µL | Microliter(s)

µM | Micromolar

A

A. baumannii | *Acinetobacter baumannii*,

ACN | Acetonitrile

AMR | Antimicrobial Resistance

B

BAL | Bronchoalveolar Lavage

BP | Bandpass

C

C. albicans | *Candida albicans*

CFU | Colony-Forming Units

CFU/mL | Colony-Forming Units per Millilitre(s)

CHX | Chlorhexidine

CIP | Ciprofloxacin

cm | Centimetre(s)

COPD | Chronic Obstructive Pulmonary Disease

CV | Crystal Violet

D

DAPI | 4',6-Diamidino-2-Phenylindole

DNA | Deoxyribonucleic Acid

E

ECDC | Centre for Disease Prevention and Control

EDTA | Disodium Ethylenediaminetetraacetic Acid

Escherichia coli | *E. coli*

ETT | Endotracheal Tube

F

FITC | Fluorescein Isothiocyanate

G

g | Gravitational Acceleration

H

h | Hour(s)

HAI | Healthcare-Associated Infection

HAP | Hospital-Acquired Pneumonia

HS | Hybridization Solution

HS1 | Hybridization Solution with 30% (v/v) Formamide

HS1 | Hybridization Solution with 5% (v/v) Formamide

I

ICU | Intensive Care Units

K

K. pneumoniae | *Klebsiella pneumoniae*

L

LP | Long pass

LRTI | Lower Respiratory Tract Infection

M

MALDI-TOF MS | Matrix-Assisted Laser Desorption/Ionization Time-of-Flight Mass Spectrometry

MDR | Multidrug-Resistant

mg/L | Milligram(s) per Litre(s)

mg/mL | Miligram(s) per Mililitre(s)

min | Minute(s)

mL | Milliliter(s)

mm | Millimetre(s)

MRSA | Methicillin-Resistant *S. aureus*

MSA | Mannitol Salt Agar

N

nm | Nanometer(s)

nM | Nanomolar

O

OD | Optical Density

P

P. aeruginosa | *Pseudomonas aeruginosa*

PCR | Polymerase Chain Reaction

pDA | Polydopamine

PNA | Peptide Nucleic Acid

PNA-FISH | Peptide Nucleic Acid Fluorescence *in situ* Hybridization

PSB | Protected Specimen Brush

PVC | Polyvinyl Chloride

Q

qPCR | Quantitative Polymerase Chain Reaction

R

rpm | Revolutions Per Minute

RPMI | Roswell Park Memorial Institute 1640

rRNA | Ribosomal Ribonucleic Acid

S

S. aureus | *Staphylococcus aureus*

S. epidermidis / *Staphylococcus epidermidis*

SC | Silicone-Coated Polyvinyl Chloride

SDA | Sabouraud Dextrose Agar

SDB | Sabouraud Dextrose Broth

T

T3SS | Type III Secretion System

TFA | Trifluoroacetic Acid

TRITC | Tetramethylrhodamine isothiocyanate

TSA | Tryptic Soy Agar

TSB | Tryptic Soy Broth

U

USA | United States of America

UV | Ultraviolet

V

v/v | Volume/Volume

VAP | Ventilator-Associated Pneumonia



w/v | Weight/Volume

LIST OF FIGURES

Figure 1: Risk factors of VAP. Created with BioRender.com. **8**

Figure 2: The actions of microorganisms within a host who is placed on mechanical ventilation using an ETT [66]..... **22**

Figure 3: Life cycle of biofilms. Created with BioRender.com. **23**

Figure 4: Examples of strategies involving antimicrobial materials reported as coatings on endotracheal tubes [9], [67]..... **25**

Figure 5: Detection of *P. aeruginosa* ATCC 27853 by the red fluorescent probe Paer565 in a pure smear of the organism under different hybridization temperatures (52°C, 58°C, 60°C, and 62°C) and using HSs with distinct percentages of formamide (30% (v/v) (HS1) and 5% (v/v) (HS2)). . **38**

Figure 6: Detection of *S. aureus* ATCC 25923 by the green fluorescent probe Saur1 in a pure smear of the organism under different hybridization temperatures (52°C, 58°C, 60°C, and 62°C) and using HSs with distinct percentages of formamide (30% (v/v) (HS1) and 5% (v/v) (HS2)). . **40**

Figure 7: Detection of *K. pneumoniae* ATCC 11296 by the blue fluorescent probe Kpneu1 in a pure smear of the organism under different hybridization temperatures (52°C, 58°C, 60°C, and 62°C) and using HSs with distinct percentages of formamide (30% (v/v) (HS1) and 5% (v/v) (HS2)). **41**

Figure 8: Detection of *K. pneumoniae* ATCC 43216 by the blue fluorescent probe Kpneu1 in a pure smear of the organism under different hybridization temperatures (52°C, 58°C, 60°C, and 62°C) and using HSs with distinct percentages of formamide (30% (v/v) (HS1) and 5% (v/v) (HS2)). **43**

Figure 9: Detection of *S. epidermidis* CECT 4183 by the orange fluorescent probe Sepi1 in a pure smear of the organism under different hybridization temperatures (52°C, 58°C, 60°C, and 62°C) and using HSs with distinct percentages of formamide (30% (v/v) (HS1) and 5% (v/v) (HS2)). A shows the image in the green filter depicted, while image B portrays the red filter. **45**

Figure 10: Detection of *A. baumannii* ATCC 19106 by the green fluorescent probe Abau1 in a pure smear of the organism under different hybridization temperatures (52°C, 58°C, 60°C, and

62°C) and using HSs with distinct percentages of formamide (30% (v/v) (HS1) and 5% (v/v) (HS2)). A shows the image in the green filter depicted, while image B portrays the red filter. **48**

Figure 11: PNA-FISH results, made at a hybridization temperature of 65°C and involving the PNA probes Paer565, Saur1, Kpneu1, Sepi1, and Abau1, that were designed for the specific targeting of *P. aeruginosa* ATCC 27853, *S. aureus* ATCC 25923, *K. pneumoniae* ATCC 11296, *K. pneumoniae* ATCC 43216, *S. epidermidis* CECT 4183, and *A. baumannii* ATCC 19106, respectively. In the case of *S. epidermidis* and *A. baumannii*, Image A illustrates the results in the green filter, while Image B presents the results in the red filter. **50**

Figure 12: Quantification of cultivable cells by CFU counting, expressed in log10 CFU/mL, within single-, dual-, and triple-species biofilms of *P. aeruginosa* ATCC 27853 (Pa), *S. aureus* ATCC 25923 (Sa), and *C. albicans* SC 5314 (Ca) for 24h at 37°C. The results are presented as mean±SD from three independent assays. Statistical analysis was conducted using ANOVA followed by a Kruskal-Wallis multiple comparisons test, comparing (*) significant differences between single-species *P. aeruginosa* biofilms and other *P. aeruginosa* biofilm types ($p<0.05$) and (#) significant differences between single-species *S. aureus* biofilms and other *S. aureus* biofilm types (#<0.05). No significant differences were observed between single-species *C. albicans* biofilms and other *C. albicans* biofilm types. **51**

Figure 13: Biofilm biomass, expressed as OD 570 nm values, obtained for single-, dual-, and triple-species of biofims developed by *P. aeruginosa* ATCC 27853 (Pa), *S. aureus* ATCC 25923 (Sa), and *C. albicans* SC 5314 (Sa) for 24h at 37°C. The results are presented as mean±SD from three independent assays. Statistical analysis was conducted using ANOVA followed by a Kruskal-Wallis multiple comparisons test, comparing (*) significant differences between single-species *P. aeruginosa* biofilms and other *P. aeruginosa* biofilm types ($p<0.05$) and (#) significant differences between single-species *S. aureus* biofilms and other *S. aureus* biofilm types (#<0.05). No significant differences were observed between single-species *C. albicans* biofilms and other *C. albicans* biofilm types. **54**

Figure 14: Biofilm quantification by plate count of triple-species 24h biofilms of *P. aeruginosa* ATCC 27853 (Pa), *S. aureus* ATCC 25923 (Sa), and *C. albicans* SC 5314 (Ca) formed in PVC and PVC that had been previously functionalized with pDA to immobilise CIP and CHX. The results are presented as mean±SD from two independent assays. Statistical analysis was conducted using ANOVA followed by a Kruskal-Wallis multiple comparisons test, comparing (*) significant differences

between *S. aureus* biofilms ($p<0.05$) and (#) significant differences between *C. albicans* biofilms (#<0.05). No significant differences were observed between *P. aeruginosa* biofilms. **57**

Figure 15: Detection of *P. aeruginosa* ATCC 27853 (Red), *S. aureus* ATCC 25923 (Blue), and *C. albicans* SC 5314 (White) in 24h triple-species biofilms formed in PVC (A) and PVC that had been previously functionalized with pDA to immobilise CIP and CHX (B), by using FISH technique. ...**58**

LIST OF TABLES

Table 1: Summary of the thesis structure **4**

Table 2: The prevalence of the most frequently isolated microorganisms associated with VAP in different countries, including Portugal [4], Spain [4], Turkey [24], Thailand [21], and the United States of America (USA) [25], as well as their average distribution [20]. This data is presented in the form of percentages..... **10**

Table 3: Diagnostic Criteria for VAP as defined by the ECDC. Adapted: [45], [46] **13**

Table 4: Suggested initial empiric antibiotic treatment for both early- and late-onset VAP [15], [61], [63] **18**

Table 5: Name and oligonucleotide sequences of PNA probes designed for the specific detection of the species selected for this study..... **29**

Table 6: Constituents of the HSs, HS1 and HS2, and respective final concentration **30**

Table 7: Constituents of the washing solution and respective final concentration **30**

CHAPTER 1: INTRODUCTION

1.1. Background

In recent centuries, advancements in medical technology have significantly contributed to an increase in human life expectancy. Nevertheless, challenges persist regarding medical device application, leading to the development as infections related to these devices [1]. Particularly, intensive care units (ICU) stand out as the primary environment for such infections to manifest [2], [3]. According to the European Centre for Disease Prevention and Control (ECDC), statistics from 2019 reveal that approximately 7.4% of patients admitted to ICUs for more than two days experienced at least one healthcare-associated infection (HAI). Among the most prominent HAIs, healthcare-associated pneumonia accounts for 4% of patients with ICU stays exceeding two days, as outlined by the ECDC [4].

Critically ill patients admitted to the ICU typically require mechanical ventilation. The primary risk factor for ventilator-associated pneumonia (VAP) is the endotracheal intubation [2], [3]. ECDC reveals that about 95.8% of pneumonia occurrences within hospital ICUs were related with use of an endotracheal tube (ETT) to assist ventilation. Furthermore, the average incidence of VAP raised to 4.4 episodes per 1000 patient days [4].

Endotracheal intubation leads to the development of VAP after a 48-hours (h) intubation period [3], [5]. On one side, the presence of the ETT contributes to the accumulation of secretions in the tracheobronchial region, while on the other hand, it provides a gateway for various microorganisms to infiltrate the lower airways and cause VAP. Consequently, mechanical ventilation promotes the adherence of different microorganisms, including pathogens, onto the tube surfaces, thereby accelerating the formation of multi-species biofilms [3], [6].

Several microorganisms contribute to VAP pathogenesis, with Gram-negative bacteria like *Klebsiella spp.*, *Pseudomonas aeruginosa (P. aeruginosa)*, and *Acinetobacter spp.*, but also Gram-positive bacteria (*Staphylococcus aureus* (*S. aureus*)) and fungi (*Candida spp.*) prevailing [4], [7], [8]. According to ECDC, the predominant causative agents in VAP instances within ICUs are *Klebsiella spp.*, followed by *S. aureus* and *P. aeruginosa* [4]. However, the presence of these microorganisms is reliant upon factors such as the patient's underlying health condition, the hospital environment, and the duration of mechanical ventilation [8].

1.2. Motivation

The prevailing strategies for infection control in hospitals involve various practises such as surface cleaning, disinfection, and pre-conditioning. Nevertheless, their effectiveness in achieving the desired

control remains considerably limited, given that infections originating from biofilm formation continue to manifest repeatedly. As a result, it is imperative to formulate innovative strategies to effectively address and manage this problem.

Typically, ETTs used in mechanical ventilation are made of polyvinyl chloride (PVC), a thermoplastic material known for its susceptibility to microorganism adhesion and subsequent biofilm formation on its surface [3]. Numerous studies have been conducted to explore the coating of PVC surfaces or the development of novel materials to take the place of this polymer. However, most of the antimicrobial strategies under investigation have remained in the pre-clinical stage, lacking progress to the clinical phase. Among the most promising investigations is the application of a silver coating to ETTs. Yet, several concerns have been raised regarding the potential toxicity and stability of this approach [9].

Currently, the diagnostic techniques employed to identify VAP lack the precision required to effectively recognise the existence of biofilm formations *in vivo*. Diagnostic methods for VAP include radiological techniques like plain radiography and computed tomography, ultrasound imaging, microbiological procedures, non-quantitative or semi-quantitative airway sampling, and quantitative cultures of airway samples. As a result, the limitations intrinsic to these approaches, coupled with the applied criteria, can lead to the generation of inaccurate VAP rates [5].

1.3. Aims of this Dissertation

The aim of this thesis is to design and optimize a novel molecular diagnostic technology for VAP based on peptide nucleic acid fluorescence *in situ* hybridization (PNA-FISH). PNA-FISH is a molecular technique employing synthetic peptide nucleic acid (PNA) probes to identify specific bacterial species by targeting their unique ribosomal RNA (rRNA) sequences. Thus, this method will make it possible to detect multiple VAP-associated pathogens, namely the bacteria *S. aureus*, *P. aeruginosa, Acinetobacter baumannii* (*A. baumannii*), *K. pneumoniae*, and *Staphylococcus epidermidis* (*S. epidermidis*) and the fungus *Candida albicans* (*C. albicans*).

To achieve the main goal, three tasks were established. The initial task involved the development and validation of a PNA-FISH methodology for the rapid and accurate detection of VAP-related species. This assessment focused on PVC surfaces that had been previously functionalized with polydopamine (pDA) to immobilise two antibacterial compounds, ciprofloxacin (CIP) and chlorhexidine (CHX). This evaluation included a comparison of how effectively the VAP-causing microorganisms adhered to different surfaces, first on polystyrene 96-well plates and then on PVC coupons and functionalized PVC coupons.

Lastly, the biofilms formed on conventional microtiter plates and on PVC coupons were then characterised using traditional methods to assess cell cultivability and quantify biomass and using advanced techniques, specifically PNA-FISH.

1.4. Thesis Outline

This master dissertation was divided into four main sections to facilitate the understanding of the subject matter. The sections are distributed according to **Table 1**.

Table 1: Summary of the thesis structure

MAIN SECTION	DESCRIPTION
1. Introduction	This section includes a description of the objectives and the aim of the work, the context, and motivations behind it.
2. Literature Review	This section conducts an in-depth analysis of the existing literature related to VAP. In addition to covering topics such as VAP's pathogenesis, the responsible pathogens, methods of diagnosis, and preventive measures, it also explores the role of endotracheal tubes and the development of biofilms on their surfaces. Furthermore, it explores novel strategies for preventing the formation of these biofilms.
3. Materials and Methods	This section provides a detailed description of the materials, equipment, experimental procedures, and data analysis methods employed in this study.
4. Results and Discussion	This section describes the outcomes achieved through the optimisation of a PNA-FISH as a diagnosis technology for VAP species, along with the results obtained from the characterization of biofilms (single and multi-species) developed on conventional microtiter plates and on PVC surfaces, uncoated and coated with CIP and CHX. Furthermore, it encompasses the interpretation and analysis of the results obtained in the context of the existing literature and the objectives of this work.
5. Conclusion	This section delivers a summary of the key conclusions and ideas of the current work.

CHAPTER 2: LITERATURE REVIEW

A lower respiratory tract infection (LRTI) refers to any infection that impacts the lower parts of the respiratory system, encompassing the airways and lungs. LRTI is a broad term encompassing a range of illnesses such as bronchiolitis, bronchitis, tracheitis, pneumonia, and respiratory conditions that exhibit a worsened clinical presentation, such as cystic fibrosis and chronic obstructive pulmonary disease (COPD) [10]–[12].

LRTIs represent the most prevalent diseases globally and rank as the fourth leading cause of death, following ischemic heart disease, cerebrovascular disease, and COPD. Approximately 2.74M deaths occur annually across the globe because of this pathology. The incidence and mortality associated with LRTIs can be influenced by various factors, including age, gender, season, and population demographics, but most significantly by antibiotic therapy, causative agent distribution, and antimicrobial resistance (AMR) prevalence. Regarding the microbial aetiology of LRTIs, the susceptibility of pathogens to antibiotics can vary by geographical region. Common microorganisms involved in these infections are Gram-positive bacteria such as *Staphylococcus* spp. and *Enterococcus* spp., as well as Gram-negative bacteria like *Pseudomonas* spp., *K. pneumoniae*, and *Acinetobacter* spp. [11]–[13].

2.1. Ventilator-Associated Pneumonia

Nosocomial pneumonia, also known as hospital-acquired pneumonia (HAP), is a prevalent infection acquired in medical facilities, particularly in ICUs, posing a significant risk to patients' lives [2]. HAP is defined as a lung parenchyma infection that occurs at least 48-h after a patient has been admitted to the hospital [3], [14], [15]. Among various types of hospital-acquired infections, VAP ranks as the most prevalent one [2]. VAP refers to a lung parenchyma infection that develops in patients who have been subjected to mechanical ventilation for a duration exceeding 48-h [14], [15].

VAP has been linked with long stays in the ICU, prolonged periods of mechanical ventilation, and high inpatient mortality rates [2], [3], [16]. In fact, it is believed that VAP contributes to about a 30% increase in the mortality rate associated with the underlying illness [16]. The incidence of VAP varies from 2 to 16 episodes for every 1000 days of ventilator use [3], [14], [17]. VAP mortality rates range generally between 3% and 17% [3]; however, they may vary across studies due to certain factors (e.g., a specific patient cohort, the effectiveness of infection control practices within healthcare units, and the duration of mechanical ventilation).

There are two definitions for VAP, depending on the start of mechanical ventilation: early-onset VAP and late-onset VAP. Early-onset VAP occurs within the initial days of mechanical ventilation, up to

the fourth day, whereas late-onset VAP develops after five days of endotracheal intubation [9], [17], [18]. The prognosis of early-onset VAP is relatively better, as the causative bacteria are usually more susceptible to antibiotic treatment [14], [17], [18]. On the contrary, late-onset VAP is associated with higher mortality rates as the main causative pathogens are generally resistant to multiple drugs [14], [17], [18].

2.1.1. VAP Pathogenesis

The physiological mechanisms inherent in the respiratory system encompass a diverse range of defence strategies that collectively serve to support its health and operational efficiency. These mechanisms effectively prevent lung infections and maintain optimal lung function [3], [17]. Coughing and sneezing, the production of tracheobronchial secretions, the efficiency of mucociliary clearance, the presence of macrophages in the alveoli, and the inflammatory response orchestrated by the immune system are examples of these defensive mechanisms against foreign particles and pathogens [3], [17]. However, the introduction of a foreign device, an ETT, to a patient disrupts the equilibrium of the respiratory system, which leads to an increased susceptibility for microbial colonisation within the lower respiratory tract [3], [17].

In intubated patients, microbial infiltration into the airways can manifest through two distinct routes: exogenous and endogenous [14], [19]. Exogenous contamination occurs when pathogens are introduced through events like micro- and macro-aspiration during intubation, respiratory endoscopy, or when disconnecting the ventilator circuit for tasks such as administering aerosols or transferring the patient [3], [14], [19]. Conversely, endogenous contamination arises when pathogens originate from oropharyngeal secretions or contaminated gastric contents [3], [17]. In the context of ICU patients, factors like gastric alkalinization due to enteric nutrition and the administration of specific medications foster the colonisation of diverse pathogens in the stomach [3], [19]. As a result, when patients are placed in a supine position while mechanically ventilated and equipped with a nasogastric tube, the risk of respiratory tract contamination escalates [3], [19]. Although micro-aspiration, involving the inhalation of contaminated secretions from the subglottic area above the tracheal balloon into the lower respiratory tract (exogenous route), is a prevalent occurrence, it is the endogenous pathways that primarily contribute to contamination [3], [14], [19].

Hence, after endogenous or exogenous contamination, there is a proliferation in the number of pathogenic microorganisms. These colonisers, together with accumulated secretions, traverse the ETT

and potentially develop a biofilm [3], [14], [19]. This biofilm has the potential to spread towards the lung parenchyma, consequently culminating in the onset of pneumonia.

Given these considerations, there are several factors that contribute to the development of VAP in patients who are undergoing mechanical ventilation in ICUs. These risk factors increase the probability of pathogenic microorganisms colonising and leading to infection within the respiratory tract [14], [17]. VAP risk factors can be classified into two distinct categories: host factors and intervention factors (**Figure 1**). Host factors pertain to the patient's response when subjected to mechanical ventilation, while intervention factors relate to events occurring during ventilation intervention [17].

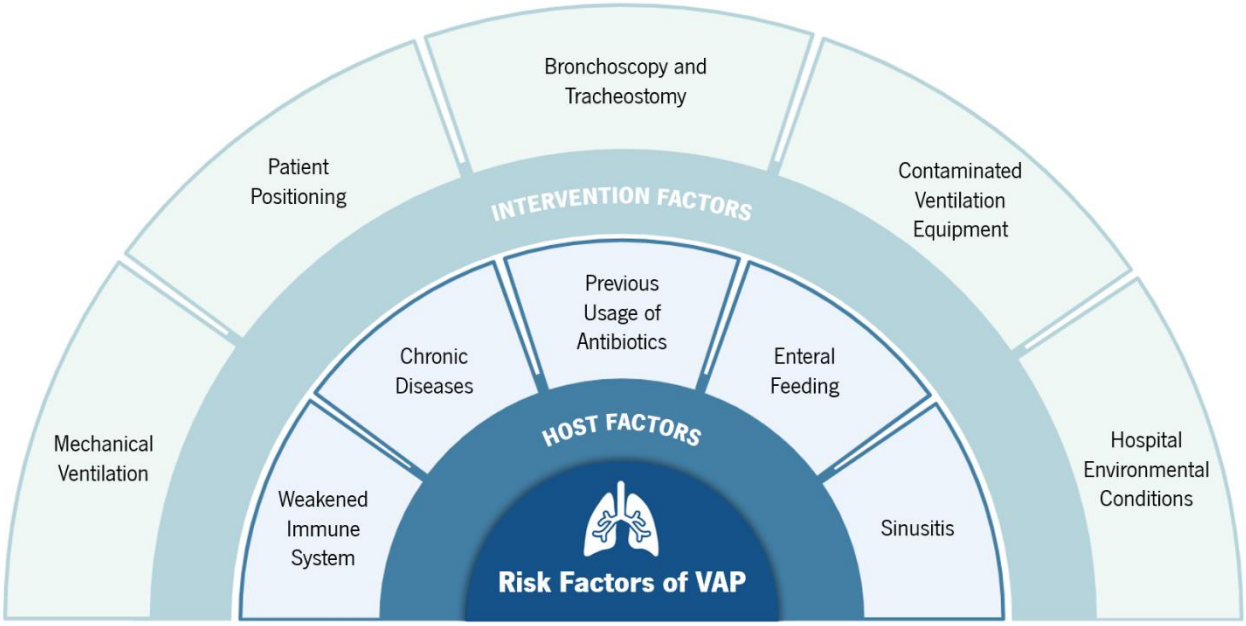


Figure 1: Risk factors of VAP. Created with BioRender.com.

Host factors include the patient's age and medical history. Patients with weakened immune systems, underlying health conditions like COPD, diabetes, or heart disease, and a history of prior antibiotic use are more susceptible to contracting VAP [14], [17]. Moreover, when a patient undergoes mechanical ventilation, inadequate oral hygiene and enteral feeding via a nasogastric tube also contribute to an increased probability of VAP incidence [14], [17]. It is noteworthy that patients with sinusitis exhibit a heightened susceptibility to developing LRTIs when subjected to this condition [14], [17].

Intervention factors encompass the duration of mechanical ventilation, the frequency of ventilator circuit changes, and the type of circuit used (which can include heat and moisture exchange humidifiers or passive devices designed to maintain heat and humidity) [14], [17]. Ventilation methods also play a crucial role; closed ventilation isolates the patient's airway from the external environment to minimise

contamination and infection risk, while open ventilation allows for a more direct connection to the patient's airway but carries a higher infection risk [14], [17]. Other intervention factors include the patient's position during ventilation, the use of invasive procedures like bronchoscopy or tracheostomy, the administration of paralytic agents or sedative drugs, contaminated ventilator equipment, and the overall healthcare environment [14], [17].

2.1.2. Microbial Contributors to VAP

VAP infections can be instigated by either a single pathogen or multiple pathogens, a condition referred to as a polymicrobial infection [20], [21]. Furthermore, a range of microorganisms are associated with this condition, with bacteria being the most prevalent causative agents [20], [22]. Nevertheless, it is important to note that viruses and fungi can also play a role in the onset of this pathology. In general, among the bacterial pathogens, the most frequently Gram-negative species include *P. aeruginosa*, *Escherichia coli* (*E. coli*), *K. pneumoniae*, and *Acinetobacter* spp.. Additionally, *S. aureus* stands out as the principal Gram-positive bacterial pathogen in VAP [20]–[22].

The microorganisms responsible for VAP can vary depending on when the infection occurs, whether it is early-onset or late-onset. Early-onset VAP is typically associated with pathogens that are more susceptible to antibiotic treatment, such as *Streptococcus pneumoniae*, *Haemophilus influenzae*, and methicillin-susceptible *S. aureus.* In contrast, late-onset VAP is often linked to multidrug-resistant (MDR) pathogens, such as *P. aeruginosa*, *Acinetobacter* spp., methicillin-resistant *S. aureus* (MRSA), and *Enterobacteriaceae* that produce broad-spectrum β-lactamases, like *K. pneumoniae*, *E. coli*, and *Enterobacter* spp.. Nevertheless, it is important to acknowledge that certain research studies have reported that both susceptible and antibiotic-resistant microorganisms can exhibit similar frequencies in both early-onset and late-onset VAP cases [20], [22], [23].

The variance associated with the microorganisms that cause this pathology depends on the geographical location of the ICU. These variations can occur between different countries but also within different areas within the same city [20], [22]. Additionally, this diversity is also influenced by specific patient populations and the distinct sections or departments within the same hospital that are associated with the risk factors outlined in **Section 3.1.1.** [20], [22]. **Table 2** provides an overview of frequencies of the pathogens frequently isolated in cases of VAP, across different regions of the globe.

Table 2: The prevalence of the most frequently isolated microorganisms associated with VAP in different countries, including Portugal [4], Spain [4], Turkey [24], Thailand [21], and the United States of America (USA) [25], as well as their average distribution [20]. This data is presented in the form of percentages

MICROORGANISM	COUNTRY					AVERAGE FREQUENCY
	Portugal	Spain	Turkey	Thailand	USA	
Gram-Negative Bacteria:						
E. coli	5.6	7.1	1.8	2.9	5.4	4-10
P. aeruginosa	27.4	26.8	6.1	22.0	16.5	20-28
Acinetobacter spp.	-	-	4.7	38.9	-	4-13
Klebsiella spp.	25.4	15.2	-	12.3	10.2	-
K. pneumoniae	-	-	1.9	-	-	8-12
Enterobacter spp.	9.0	12.7	1.1	6.3	8.3	6-7
Gram-Positive Bacteria:						
S. aureus	15.0	15.8	2.1	6.0	24.7	20-32
Streptococus pneumoniae	-	-	0.3	-	-	2-8
Yeast:						
Candida spp.	2.5	0.6	0.4	-	0.4	<1
C. albicans	-	-	-	-	2.2	<1

Notably, *P. aeruginosa*, *K. pneumoniae*, *Acinetobacter* spp. and *S. aureus* are the predominant pathogens. Regarding fungi, *C. albicans* is the most encountered species.

2.1.2.1. *P. aeruginosa*

P. aeruginosa is a Gram-negative bacterium with a rod-shaped morphology characterised by polar flagella that enable unipolar motility. Like *S. aureus*, this microorganism exhibits adaptability, thriving in both aerobic and anaerobic environments. It is recognised as a nosocomial pathogen and is associated with a wide range of acute and chronic infections. It often assumes an opportunistic role, particularly in critically ill and immunocompromised patients [20], [26], [27]. Remarkably, infections caused by *P. aeruginosa* are linked to a high morbidity rate, and it holds the highest mortality rate among bacteria [20].

This opportunistic pathogen possesses virulence factors on its cell surface, including flagella, pili, or fimbriae, lipopolysaccharide, and the type III secretion system (T3SS). The T3SS is responsible for the direct secretion of toxins into host cells, making it a prominent contributor to acute invasive infections. Additionally, *P. aeruginosa* produces various proteases, such as pyocyanin, pyoverdine, protease IV,

elastase, and metalloproteinases, as well as exotoxin A. These enzymes have the capability to hydrolyse immunoglobulin, fibrin, and fibrinogen and to disrupt epithelial tight junctions. This array of virulence factors facilitates the bacterium's colonisation of the lower respiratory tract [20].

2.1.2.2. *S. aureus*

S. aureus, a Gram-positive bacterium with a spherical morphology, is typically found in the respiratory tract and on the skin. It exhibits adaptability in both aerobic and anaerobic environments [28]. Various strains of *S. aureus* produce an array of virulence factors that can either induce pathological conditions or exacerbate the severity of LRTIs. Certain virulence factors have the capacity to inhibit them, including proteins such as protein A, coagulase, leukocidin, and γ-toxin. Conversely, others facilitate the bacterium's invasion into infected tissue by releasing enzymes such as proteases, nucleases, lipases, hyaluronidase, and staphylokinase, thus promoting tissue invasion [20].

S. aureus possesses a notable ability to destabilise both innate and adaptive immune responses, promoting its replication within the host. In individuals with compromised immune systems, particularly among patients in ICUs, there is an elevated susceptibility to *S. aureus* infections. Of particular concern is the MRSA strain, which is a significant contributor to severe necrotizing pneumonia. This severity is attributed to the production of Panton-Valentine leukocidin by MRSA, making it a particularly virulent pathogen in certain clinical settings [20].

2.1.2.3. S. epidermidis

S. epidermidis, a coagulase-negative bacterium with a spherical shape, is typically present on the skin and mucous membranes of humans as part of the normal flora, thus being generally harmless. Nevertheless, in the context of VAP, it can pose a significant concern [29], [30].

The primary pathogenic mechanism of this microorganism relies on its capacity to create biofilms on both medical device surfaces and host tissues. Through its adhesins and extracellular polysaccharides, *S. epidermidis* can adhere to surfaces, establish biofilms, and elude the host's immune defences [29], [30].

2.1.1.1. *A. baumannii*

There are numerous *Acinetobacter* species; however, the most frequently isolated within hospital settings is *A. baumannii* [20], a Gram-negative bacterium with a preference for aerobic conditions. It

possesses particular characteristics, including non-fermentative metabolism, lack of motility, absence of pigmentation, and positive catalase activity, resulting in its *coccobacillus* shape [31].

While the typical presence of *A. baumannii* is on human skin, in the throat, and as part of the rectal flora, this microorganism is also an opportunistic pathogen. In individuals with compromised immune systems, it has the potential to induce severe and occasionally lethal infections, making it a notable contributor to HAI. *A. baumannii* has the capability to adhere to and colonise particularly moist tissues, such as mucous membranes or skin, which have been compromised due to accidents or injuries. More specifically, this microorganism can adhere to, colonise, and invade human epithelial cells. Furthermore, it produces an exopolysaccharide that acts as a protective shield, enabling it to evade host immune defences [20]. Another attribute of *A. baumannii* is its high genetic adaptability, which enables rapid mutations and the integration of exogenous genetic material into its genome via mobile elements like insertion sequences [32].

2.1.1.2. *K. pneumoniae*

K. pneumoniae is a Gram-negative bacterium with a non-motile, rod-shaped morphology [33]. It is typically present in the intestines, oral cavity, and skin, as well as in hospital environments and medical devices. This opportunistic pathogen primarily affects individuals with compromised immune systems, leading to severe lung infections like VAP [20], [33].

K. pneumoniae exhibits multiple capsular serotypes, known as K antigens, which result in the formation of hypermucoviscous colonies. These microorganisms are particularly concerning because of the presence of a capsule, which functions as a barrier to opsonization and phagocytes and inhibits dendritic cell maturation, which in turn suppresses the production of pro-Th1 cytokines mediated by dendritic cells. Additionally, the capsule exerts an anti-inflammatory effect by inhibiting the expression of interleukin-8. It also reduces the number of antimicrobial peptides reaching the bacterial surface, thereby promoting resistance, and facilitating the acquisition of iron, an essential component for *K. pneumoniae* growth [20].

2.1.1.3. *C. albicans*

C. albicans is a dimorphic fungus, possessing the unique ability to exist in two distinct forms: as a yeast or as a filamentous cell [34]. This fungal organism is commonly used as a harmless commensal, specifically in the gastrointestinal tract and oral cavity [34], [35]. However, it can lead to severe skin infections and even progress to potentially life-threatening systemic infections in immunocompromised hosts [35], [36].

Notably, *C. albicans* often co-occurs with bacteria such as *P. aeruginosa* and *S. aureus* in infections, with VAP being an example of this polymicrobial infection [35].

One significant virulence factor associated with *C. albicans* is its capacity to undergo a morphological transition, shifting between yeast and hyphal forms. The filamentous forms of yeast, including hyphae and pseudohyphae, are responsible for tissue penetration and macrophage destruction, while the yeast form is primarily involved in dissemination [37], [38]. Other virulence factors encompass the expression of adhesins and invasins, facilitating adherence to other cells (including *C. albicans* cells, other microorganisms, or host cells) and abiotic surfaces [39]. Furthermore, *C. albicans* secretes hydrolases, further enhancing its pathogenicity [35].

In the respiratory tract, the presence of *Candida* spp. is often associated with an increased disease burden. Nevertheless, it remains uncertain whether the colonisation of respiratory tract secretions by this fungus serves as an indicator of disease severity or if it genuinely contributes to adverse clinical outcomes [40].

2.1.2. Diagnosis of VAP

Early detection of VAP is crucial as it enables the prompt administration of treatment, leading to a decrease in both morbidity and mortality [41], [42]. Given the absence of a universally recognised gold standard for diagnosing VAP, reported VAP rates and associated outcomes can vary substantially depending on the adopted diagnostic criteria. It is important to note that two-thirds of patients treated for VAP may not actually have the condition. Therefore, there is a pressing need to enhance VAP diagnostic methods to facilitate informed decisions regarding empirical antibiotic treatment [41], [43], [44]. Currently, the diagnosis of VAP relies on an evaluation incorporating clinical, radiological, and microbiological criteria, requiring 24 to 48h to obtain preliminary or definitive results [42], [45], [46].

According to the ECDC, a patient is suspected of having acquired VAP if he is mechanically ventilated for over 48h and if he meets a minimum of two radiographic criteria, one systemic criterion, and two pulmonary criteria, as detailed in **Table 3** [16], [45], [47], [48].

Table 3: Diagnostic Criteria for VAP as defined by the ECDC. Adapted: [45], [46]

CRITERIA	DESCRIPTION
Radiographic	1. New or progressive and persistent infiltrate. 2. Consolidation. 3. Cavitation.

CRITERIA	DESCRIPTION
Systemic	1. Fever (>38°C). 2. Leukopenia (4000 WBC/mm³) or leukocytosis (>12000 WBC/mm³). 3. For adults older than 70 years old, altered mental status with no other recognized cause.
Pulmonary	1. New onset of purulent sputum or alteration in sputum characteristics, increased respiratory secretions, or an elevated demand for aspiration. 2. Deterioration in gas exchange, such as desaturation, heightened oxygen demands, or an increased necessity for ventilation. 3. New-onset or aggravated cough, dyspnea, or tachypnea. 4. Detection of rales or bronchial breath sounds.

It has been proposed to obtain quantitative samples from the lower respiratory tract using techniques like protected specimen brush (PSB), bronchoalveolar lavage (BAL), or endotracheal aspiration in conjunction with the beginning of a mechanical ventilation system due to the potential for various conditions occurring in mechanically ventilated patients that resemble pneumonia, such as acute respiratory distress syndrome, pulmonary edema, pulmonary contusion, tracheobronchitis, and thromboembolic disease [15], [16], [42], [45], [46]. Despite the widespread application of these techniques, their accuracy in VAP diagnosis remains inadequately characterised, and studies have indicated that their utilisation is highly subjective, resulting in low specificity and sensitivity [15], [16], [46].

2.1.2.1. Radiographic Criteria for VAP Diagnosis

As previously mentioned, diagnosing VAP involves the evaluation of radiographic criteria, characterised by the presence of new or progressively persistent infiltrates on imaging. Conventional chest X-rays, however, often fail to distinguish between the various causes of pulmonary opacities in critically ill patients, limiting their sensitivity and specificity in VAP diagnosis [15], [49], [50]. To address this limitation, advanced diagnostic tools like lung ultrasound and biomarkers have been developed.

Lung ultrasound offers benefits including real-time bedside applicability, the absence of radiation exposure, and the precise identification of underlying causes of opacities observed on chest X-rays [49]. Yet, its effectiveness in diagnosing VAP, particularly in patients with pre-existing lung abnormalities, remains uncertain [46], [49], [50].

Biomarkers, on the other hand, have the purpose of detecting and identifying specific indicators of alveolar infection, potentially expediting, and enhancing VAP diagnosis [51], [52]. However, despite extensive research into various biomarkers, no perfect biomarker has been identified. Studies assessing their utility

in VAP diagnosis have produced conflicting results and have not met the necessary specificity and sensitivity criteria for routine clinical application [43], [51], [52].

2.1.2.2. Microbiological Criteria for VAP Diagnosis

To enhance the viability and speed of diagnosing VAP, alongside clinical and radiographic techniques, microbiological tests based on culture (quantitative or semi-quantitative) are also conducted [53]. This approach is justified by its significant impact on diagnostic accuracy and the reduction in unnecessary antimicrobial use. Using this method, pathogens are identified by sampling the lower respiratory tract [22], [53]. Sample collection methods can be either invasive, such as BAL, mini-BAL, and PSB, or non-invasive, such as endotracheal aspiration [16], [22].

When conducting quantitative cultures, it is imperative to carefully evaluate the predetermined cut-off thresholds to prevent the omission of VAP cases or the occurrence of false positives, which could result in unjustified treatment [16]. Therefore, specific thresholds have been established: 10^6 or higher Colony-Forming Units (CFU)/mL for endotracheal aspirates and 10^4 CFU/mL or higher for mini-BAL, BAL, and PSB [16], [22], [46]. The threshold for bronchial sampling is set higher due to the possibility that the sampled area may not always represent the most affected region, potentially affecting test sensitivity while preserving an elevated level of specificity. It is essential to acknowledge that, from a laboratory standpoint, conducting quantitative cultures using this method is more labour-intensive, time-consuming, and costly compared to semi-quantitative cultures [16], [22].

2.1.2.3. Molecular-based VAP diagnostic technologies

In recent years, novel molecular-based methods have emerged for the identification of pathogens within the respiratory tract. These innovative techniques have been designed to enhance the precision, speed, and reliability of VAP diagnosis. Moreover, they aim to detect various pathogens, including antibiotic-resistant microorganisms, while upholding diagnostic sensitivity and specificity. Consequently, methods employing nucleic acids for microorganism identification, such as Polymerase Chain Reaction (PCR), and, more recently, mass spectrometry techniques, present higher sensitivity and specificity compared to conventional diagnostic approaches [15], [53].

PCR is a methodology employed to amplify and identify distinct deoxyribonucleic acid (DNA) sequences from bacteria and fungi in respiratory tract samples, such as those obtained through BAL [15], [54]. This enables a rapid and cost-effective diagnosis of VAP compared to the traditional culture methods currently in use. Additionally, PCR can identify viral targets, toxins, and specific antibiotic resistance

(AMR) genes in bacteria, simplifying the selection of appropriate antibiotics for VAP treatment by clinicians [54].

A crucial aspect for diagnosing polymicrobial infections like VAP is the detection and characterization of several pathogens, which is made achievable by multiplex assays that allow the identification of several microorganisms simultaneously. Multiplex PCR allows the simultaneous amplification and detection of multiple target DNA sequences within a single reaction. Consequently, multiplex PCR accelerates the VAP diagnosis process, providing rapid and precise results, often in a few hours [42], [53], [54]. However, this method has limitations, including cost implications and the requirement for specialised equipment and expertise [22], [54].

Quantitative PCR (qPCR), a variation of PCR, is another valuable tool, providing quantitative information regarding the amount of DNA within a sample through a calibration curve established from serially diluted standard samples with established concentrations or copy numbers. Nevertheless, it is important to note that, despite their advantages, these techniques have limitations. They are unable to detect Gram-negative bacteria with newly developed antibiotic AMR mechanisms and cannot distinguish between live and inactive pathogens, often leading to false-negatives results [54].

As previously mentioned, mass spectrometry represents an alternative approach for diagnosing VAP. This technology facilitates the rapid and highly accurate identification of pathogens based on the mass-to-charge ratio of their biomolecules, including proteins and peptides. In a hospital context, Matrix-Assisted Laser Desorption/Ionization Time-of-Flight Mass Spectrometry (MALDI-TOF MS) is typically the most employed method for identifying microorganisms, whether from solid culture media or directly from clinical samples, including those collected from the lower respiratory tract, positive blood cultures, and urine. This method can detect various bacteria, encompassing Gram-negative and Gram-positive species, with a more pronounced capability to characterise Gram-negative bacteria as well as fungi. It also has the capability to identify resistance markers like β-lactamases by assessing bacterial growth in the presence of antibiotics. However, it is important to note that MALDI-TOF MS has limitations, including its ability to identify only a limited range of resistance mechanisms and its sensitivity, which requires a bacterial concentration exceeding 10^5 CFU/mL for accurate detection in clinical samples [54], [55].

2.1.2.3.1. PNA-FISH method for VAP diagnosis

Another promising method for diagnosing VAP is PNA-FISH. Like the aforementioned technologies, it enables the rapid, specific, and sensitive detection and identification of microorganisms within polymicrobial communities without relying on traditional cultures. PNA-FISH relies on fluorescently

labelled oligonucleotide probes that selectively bind to specific rRNA target sequences found in bacteria, yeasts, or other microorganisms. These PNA oligonucleotide probes are typically small, ranging from 13 to 18 base pairs in length, and they are chemically labelled with fluorescent dyes such as fluorescein or carbocyanine, enabling easy detection through techniques such as epifluorescence microscopy or flow cytometry. A particular characteristic of PNA probes is their neutral charge, which significantly enhances their ability to penetrate the cell wall or cell membrane of the target microorganism, facilitating specific binding to complementary rRNA sequences. This is due to the unique molecular structure of PNA probes, which is composed of repeated N-(2-aminoethyl) glycine units, resulting in a neutral and achiral backbone [54], [56], [57].

PNA-FISH effectively mitigates certain drawbacks associated with PCR, qPCR, multiplex PCR, and MALDI-TOF. One notable advantage is that PNA-FISH operates independently of pathogenic material amplification, eliminating the need for DNA extraction and purification steps as required in PCR. This inherent feature reduces the susceptibility to contamination in clinical samples. Additionally, unlike PCR, PNA-FISH enables *in situ* analyses, proving particularly valuable for biofilm studies [54], [56].

Some limitations are associated with MALDI-TOF. Firstly, it requires subculturing to identify pathogens since it relies on intact whole cells for analysis, demanding a substantial quantity of bacterial cells. Secondly, it has constraints in detecting AMR determinants due to the labour-intensive analysis and the small size of the sequenced DNA fragments. Conversely, FISH-based methods have shown promise in identifying intact bacterial cells in various clinical samples like tissues, blood, and sputum, enabling direct identification and localization of resistant bacteria in biological samples. Thus, PNA-FISH provides a suitable and reasonable choice for integration into clinical microbiology laboratories, requiring only an epifluorescence microscope equipped with suitable fluorochrome filters [56]. The use of confocal microscopy in the PNA-FISH technique improves the visualisation of fluorescence images by enabling clear and precise imaging of target cells or structures in different focal planes within three-dimensional samples, reducing background noise. Additionally, confocal microscopy minimises photobleaching in fluorophores, extending the time available for image acquisition and ensuring stable and long-lasting fluorescence signals [58], [59].

2.1.3. Treatment of VAP

Antimicrobials comprise a category of synthetic compounds derived from various chemical sources, whereas antibiotics represent a subset of antimicrobials originating from living microorganisms. Among antibiotics, there exists a subgroup that forms irreversible bonds with bacterial binding sites,

known as bacteriostatic antibiotics. Examples of such bacteriostatic antibiotics include aminoglycosides, fluoroquinolones, polymyxin, colistin, and cotrimoxazole. The efficacy of these drugs within tissues relies on two critical factors: the maximum drug concentration achieved and the rate at which the drug is eliminated from the body. To maximise effectiveness, drugs with concentration-dependent killing and extended post-antibiotic effects should be administered in large, less frequent doses [17].

Apart from being the most isolated bacteria in VAP diagnoses, *S. aureus*, *P. aeruginosa*, *A. Baumannii*, *K. pneumonia*, and *S. epidermidis* share another concerning characteristic. They all possess AMR mechanisms, making treatment challenging [15], [20]. Due to the pressing issue of AMR, VAP treatment is guided by two fundamental principles. The first involves the administration of empirical antimicrobial treatment, which is determined by factors such as infection severity, underlying medical conditions, the presence of MDR pathogen risk factors, and local antimicrobial susceptibility patterns. The second principle comprises definitive treatment, emphasising the prudent use of antibiotics to minimise overuse and treatment duration while closely monitoring clinical improvement [15], [20], [60].

The selection of an appropriate empirical antimicrobial agent for the treatment of VAP is critical, as it can significantly reduce mortality rates. Hence, the choice of antibiotic and the timing of administration should be based on local prevalence and the antimicrobial susceptibility profile of the common pathogens [15], [20], [60], [61]. It should be noted that when the prompt administration of antibiotics is carried out, it must be balanced due to the potential adverse effects of unnecessary usage, such as AMR and superinfections, particularly within the ICU environment [41], [42], [44].

To guide an appropriate initial treatment for clinically suspected VAP, the American Thoracic Society/Infectious Disease Society of America has developed evidence-based guidelines for nosocomial pneumonia. These guidelines recommend a combination of antimicrobial agents that effectively target the most prevalent bacterial pathogens associated with both early- and late-onset VAP, as outlined in **Table 4** [15], [60]–[62].

Table 4: Suggested initial empiric antibiotic treatment for both early- and late-onset VAP [15], [61], [63]

CASE	EXEMPLES OF ANTIMICROBIAL AGENT
Early-VAP (≤ 4 days of mechanical ventilation), without risk factors associated with MDR pathogens	Non-antipseudomonal β-lactam: • Amoxicillin/Clavulanic acid • Ampicillin-sulbactam • Second or third generation cephalosporin antibiotic (e.g., ceftriaxone) • Fluoroquinolones (e.g., moxifloxacin, ciprofloxacin, or levofloxacin)

CASE	EXEMPLES OF ANTIMICROBIAL AGENT
Late-VAP (≥ 5 days of mechanical ventilation), with risk factors associated with MDR pathogens *	β-lactam active against *P. aeruginosa*: • Ceftazidime (third-generation cephalosporin antibiotic) • Cefepime (fourth-generation cephalosporin antibiotic) • Piperacillin–tazobactam • Carbapenem (e.g., imipenem, and meropenem) Non β-lactam antipseudomonal agent: • Aminoglycosides (e.g., amikacin or tobramycin) • Fluoroquinolones (e.g., moxifloxacin, ciprofloxacin, or levofloxacin)
Late-VAP (≥ 5 days of mechanical ventilation), associated with colonization of carbapenem-resistant *Enterobacteriaceae* or *P. aeruginosa* susceptible solely to novel β-lactam drugs	New β-lactam agent: • Ceftolozane–tazobactam • Ceftazidime–avibactam • Meropenem–vaborbactam • Imipenem–relebactam
Late-VAP (≥ 5 days of mechanical ventilation), associated with colonization of MRSA in patients who have been treated with antibiotics within the last 90 days or who have been hospitalised in units with a high (>20%) or unknown prevalence of MRSA among VAP patients	Agent active against MRSA: • Glycopeptide (e.g., vancomycin or teicoplanin) • Oxazolidinone (e.g., linezolid)

* This treatment should encompass antibiotics belonging to the two categories of antibiotics mentioned.

In cases where a high prevalence of pathogens with elevated minimum inhibitory concentrations is observed, even with efforts to tailor initial empirical antibiotic therapy using local antibiograms and standardise these choices through VAP treatment protocols, the available options are limited [61].

Both European and USA guidelines harmonise the duration of antimicrobial therapy for VAP, which should not surpass 7 days. This guideline applies universally, including to patients infected with non-fermenting Gram-negative *bacilli* like *P. aeruginosa* and *Acinetobacter spp.* Extended treatment durations are suggested for specific cases, such as immunocompromised patients and those with conditions like empyema, lung abscess, or necrotizing pneumonia [15], [17].

In addition to prescribing appropriate initial antibiotic therapy, it is important to consider the practice of antimicrobial de-escalation whenever feasible. Antimicrobial de-escalation involves narrowing or reducing the spectrum of antibiotics and shortening the duration of therapy based on the patient's clinical response to empirical treatment and the results of microbiological tests. This may include, e.g., switching from combination therapy to monotherapy based on the sensitivity results of the identified

organisms. It is worth noting that de-escalation does not impact in-hospital mortality, ICU and hospital length of stay, duration of mechanical ventilation, or the occurrence of a second VAP episode. The primary objective of this approach is to minimise the use of unnecessary antibiotic therapy, thereby preventing the emergence of AMR, reducing potential side effects, and avoiding unnecessary synergistic effects [17], [60], [61].

2.1.4. Prevention of VAP

The most effective approach to preventing the occurrence of VAP is to minimise the potential exposure of ventilated patients to risk factors. Thus, preventive measures such as thorough hand hygiene practices, isolating patients who are colonised with MDR microorganisms from those who are not, and exercising caution in the use of antimicrobial agents to reduce the emergence of drug-resistant pathogens are fundamental strategies for preventing VAP.

Aiming at preventing VAP, a multidimensional approach combining non-pharmacological and pharmacological measures has been established, with a primary focus on preventing aspiration, controlling microbial colonization in the aerodigestive tract, and minimizing contamination of ventilation equipment. Non-pharmacological preventive strategies involve various hospital care practices, including efforts to reduce mechanical ventilation through alternative methods like non-invasive positive-pressure ventilation, sedation, and weaning protocols. Other non-pharmacological procedures include maintaining a semi-upright patient position, employing continuous aspiration of subglottic secretions, using EET coatings, employing closed suctioning systems, and incorporating passive humidifiers or heat-moisture exchangers [14], [60], [61].

On the other hand, pharmacological prevention strategies primarily involve the use of antimicrobial or antiseptic agents to mitigate the risk of bacterial colonisation and infection. Examples of these pharmacological preventive measures include the application of oral CHX, selective digestive decontamination, and selective oral decontamination [60], [61].

CHX, used as an oral decontaminant, has demonstrated remarkable effectiveness in reducing the risk of VAP as well as mortality rate, duration of mechanical ventilation, and ICU length of stay. CHX exhibits a wide spectrum of activity against common VAP-causing pathogens, including *P. aeruginosa*, *Acinetobacter* spp., and MRSA. Its mechanism of action involves interaction with the anionic receptors present on bacterial cell surfaces, subsequently enhancing cell wall permeability and growth inhibition. Its better efficacy is likely related to bacterial growth inhibition when applied to contaminated surfaces, rather than preventing the growth of bacteria in initially pathogen-free tissues [60], [61].

2.2. Endotracheal Tubes

Mechanical ventilation using an ETT has emerged as an essential intervention for enabling the delivery of oxygen and inhaled gases to the lungs of patients recovering from surgery or trauma. While mechanical ventilation is a life-saving measure, the process of endotracheal intubation itself presents potential risks when applied to critically ill patients. In addition to its invasive placement, which involves either nasotracheal intubation via the nasal passages or oro-tracheal intubation through the mouth into the trachea, the presence of an ETT can elevate the risk of VAP by a factor ranging from 6 to 20 times [9], [64]–[66].

In line with the interaction of any medical device implanted within the body, the ETT is exposed to a range of pathogens. In the context of mechanical ventilation, the host organism undergoes several changes. These changes include the compromise of natural defence mechanisms such as coughing and mucociliary movement in the trachea. Furthermore, alteration of tracheobronchial cells, disturbance in the pulmonary microbiome, the introduction of endogenous flora from the oropharynx into the lower airway tract, and the establishment of bacterial attachment sites due to potential airway damage during intubation. Additionally, the ETT's surface offers an ideal environment for bacterial and fungal colonisation, resulting in the formation of biofilms on both its internal and external luminal surfaces. Another contributing factor to pathogen colonisation within the ETT and respiratory tract is the accumulation of contaminated secretions from the oropharynx or gastrointestinal tract in the subglottic space located above the inflated ETT cuff (**Figure 2**) [9], [64], [65], [67].

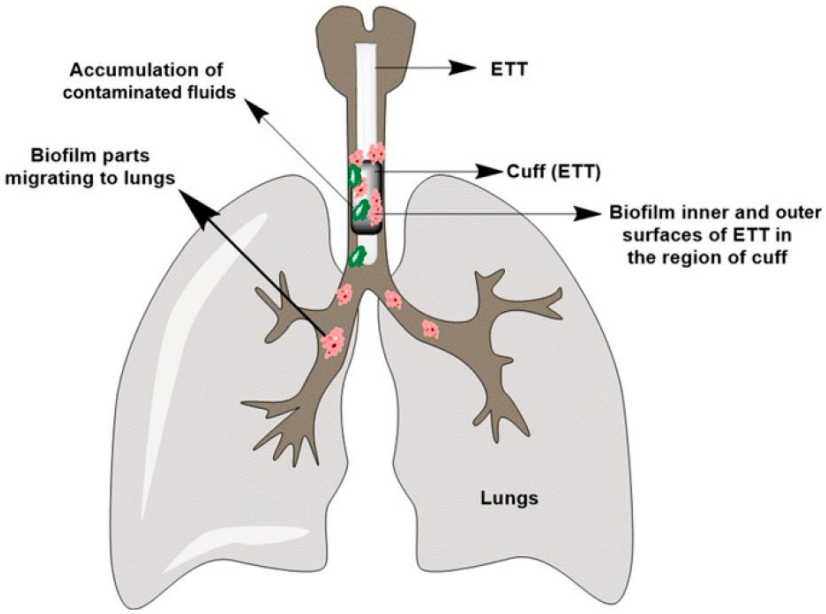


Figure 2: The actions of microorganisms within a host who is placed on mechanical ventilation using an ETT [66].

ETTs are known to function as reservoirs for microbial pathogens. This phenomenon is primarily associated with the prevalent use of materials such as PVC, which is the most common, and silicone-coated PVC (SC). These materials possess hydrophobic surfaces that create favourable conditions for microbial attachment and biofilm growth. Consequently, this leads to persistent microbial colonisation on both the inner and outer surfaces of the ETT. Notably, when comparing PVC to SC, it is evident that PVC exhibits a greater propensity for the formation of high-grade biofilms [9], [68], [69].

2.2.1. Biofilms on ETTs

Around 65% to 80% of human infections are related to biofilms, particularly those concerning respiratory diseases and infections associated with catheters, medical implants, and prosthetic devices. A biofilm is a structured, three-dimensional community of cells enclosed within a matrix of extracellular polymeric substances. This matrix includes polysaccharides, proteins, lipids, and extracellular DNA, all of which are produced by the microorganisms within the biofilm. This consortium of diverse microorganisms cooperates to survive in hostile environments. It adheres to moist surfaces, whether inert or living, and remains stationary due to its reduced metabolic activity, making it less susceptible to the effects of antimicrobial agents [3], [64], [68], [70].

The polymeric matrix of the biofilm serves multiple functions. It acts as a protective barrier against antibiotics and immune cells, either deactivating them or preventing direct contact with their target. As a

result, biofilms exhibit significantly higher tolerance to antimicrobial agents when compared to their planktonic counterparts [3], [64], [68], [70].

The functional and structural arrangement of microorganisms within biofilms is intricate and controlled by a process known as quorum sensing. Quorum sensing serves as a communication mechanism among microorganisms to coordinate their actions within a population. This communication relies on the production, release, and detection of signalling molecules known as autoinducers. These autoinducers enable bacteria to assess the density of their population and, consequently, adjust the activation of specific genes. Consequently, the proliferation of resistance genes among bacterial cells through horizontal gene transfer can lead to an escalation in antibiotic resistance [3], [68], [71].

After intubation, the formation of biofilms is a rapid and dynamic process that involves four distinct phases: the initial phase, the log phase, the stationary phase, apoptosis, and the dissemination phase, as illustrated in **Figure 3**.

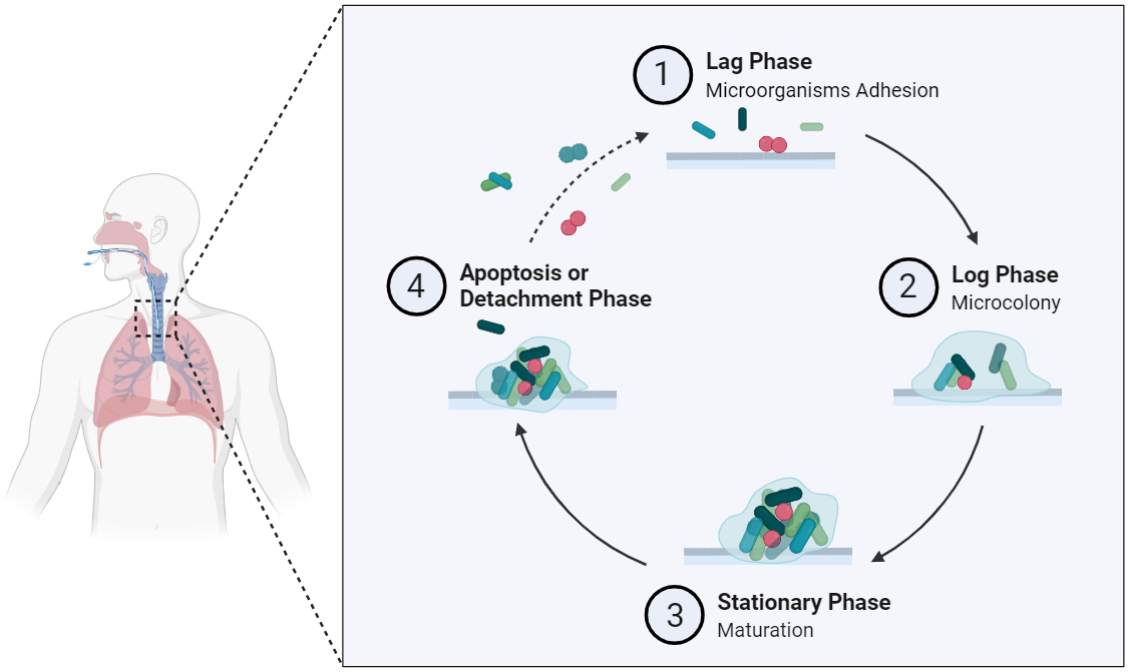


Figure 3: Life cycle of biofilms. *Created with BioRender.com*.

In the initial phase (**1**), known as the lag phase, microorganisms adhere to the surface of the ETT and adapt to their new environment. This initial stage holds particular significance because several pathogens, such as *P. aeruginosa*, switch from a mobile to a sessile state and undergo metabolic reprogramming favouring sessile growth. The subsequent phase, referred to as the log phase (**2**), is characterised by the proliferation of adhered microorganisms and the production of the polymeric matrix.

Following this, the stationary phase (**3**) is related to biofilm maturation and the consolidation of its architectural structure. During this third phase, there is the creation of microenvironments, including various species or varying levels of activity. Lastly, in the apoptosis and dissemination phases (**4**), the proximity of bacterial cells within the matrix facilitates the exchange of molecular signals that regulate behaviour. Some cells specialise in the production of polysaccharides, while others adopt different forms of phenotypic resistance and continue to propagate. Biofilm aggregates can detach from the initial matrix and migrate into the airways, often pushed by airflow or invasive medical procedures [3], [9].

Biofilms that develop on the ETTs of ventilated patients are composed of a complex mixture of various microorganisms and polysaccharides, as well as cellular residues and respiratory secretions from the host. In general, these biofilms are polymicrobial, comprising multiple microorganisms. Consequently, VAP is characterised as a polymicrobial infection, exhibiting significant variability between different patients and even within the same patient over time. This collective assembly of microorganisms within the ETT contributes to the pathogenesis of VAP through various mechanisms, including the passive dispersal of biofilm fragments, the aerosolization and subsequent aspiration of biofilm cells into the lungs due to gas flow during mechanical ventilation, and the potential dislodgment of individual cells by liquids [3], [9], [64].

2.2.2. Prevention of Biofilm Development in ETTs

Preventing microbial colonisation on the ETT is the most reliable method to avoid the proliferation of biofilms and, consequently, the development of VAP. Using strategies such as modifying the medical device, which may involve cuff control or altering the material and surface of the ETT, can be highly beneficial in achieving this goal [9], [72], [73].

Recent developments have introduced a range of material coating strategies for ETTs. These approaches can be divided into active, which targets the direct eradication of pathogens on the ETT surfaces; passive, which involves modifying the composition and surface properties of ETTs to create surfaces resistant to contamination; and hybrid approaches that combine active antimicrobial and passive antifouling features within ETT designs (**Figure 4**) [9], [74].

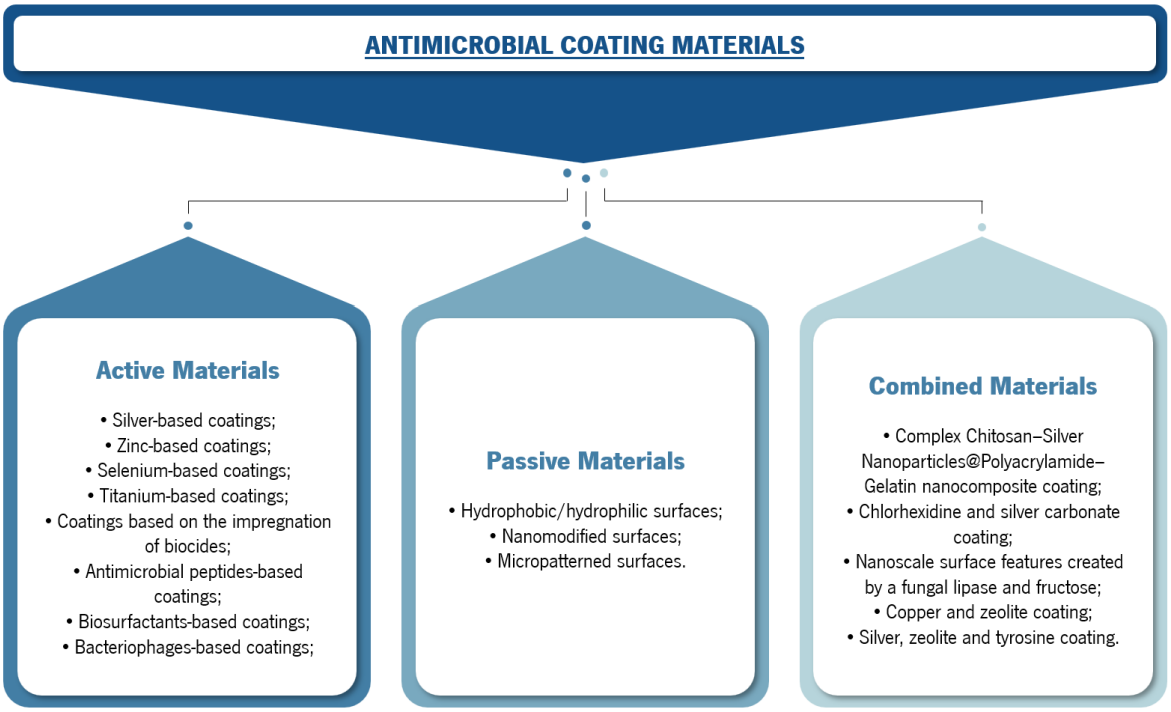


Figure 4: Examples of strategies involving antimicrobial materials reported as coatings on endotracheal tubes [9], [67].

Among the strategies outlined in **Figure 4**, the most extensively studied is the silver-based antimicrobial coating. This includes coatings with silver ions, silver nanoparticles, and even combined approaches with noble metal alloys like silver-gold-palladium. The versatility of silver-based coatings arises from silver's well-known broad-spectrum antimicrobial properties and its ability to reduce biofilm formation on ETTs. However, despite promising outcomes, data regarding the safety and efficacy of silver remain limited and sometimes inconsistent, making it challenging to draw definitive conclusions about its safety and clinical utility. Additionally, it is important to note that silver coated ETTs tend to be more expensive than traditional ETTs, which could hinder their widespread use in healthcare facilities [9], [67], [75].

Despite numerous research efforts aimed at developing new materials capable of inhibiting microbial proliferation in ETTs, combating polymicrobial biofilms is still a big challenge, and no study has reported an optimal material holding high efficiency, broad-spectrum antimicrobial/antibiofilm activity, biocompatibility, and economic viability.

Several reports have described a surface-coating strategy that imparts antimicrobial properties to biomaterial surfaces. This technique involves surface functionalization through the application of a bio-inspired pDA coating. The process entails immersing substrates in an alkaline dopamine solution, resulting in the formation of an ultrathin adhesive film with nanoscale dimensions due to dopamine's self-polymerization. This approach is characterised by its simplicity, applicability to various materials,

strong reactivity for additional functional modifications, and biocompatible properties. Its use in immobilisation allows biomaterial surfaces to acquire anti-infectious properties [75]–[77].

Through this method, the surface of ETT can be functionalized using pDA. This allows for the immobilisation of antimicrobial agents like CHX and CIP, which are effective in preventing the development of polymicrobial biofilms. CHX, recognised for its antiseptic properties, can be successfully affixed to biomaterial surfaces, and demonstrates promising efficacy against various microorganisms, including Gram-positive and Gram-negative bacteria, as well as yeasts [74]. CIP, a second-generation fluoroquinolone, possesses well-established broad-spectrum activity against both Gram-negative and Gram-positive bacteria [63].

CHAPTER 3: MATERIALS AND METHODS

3.1. Microorganisms and Culture Conditions

In the present research, several microorganisms were used, consisting of five bacterial strains, *P. aeruginosa* ATCC 27853, *S. aureus* ATCC 25923, *K. pneumoniae* ATCC 11296, *K. pneumoniae* ATCC 43216, *S. epidermidis* CECT 4183, and *A. baumannii* ATCC 19106, as well as one fungal species, *C. albicans* SC5314.

All microorganisms were stored at -80 ± 2°C in cryovials containing broth medium, Tryptic Soy Broth (TSB) (Liofilchem, Italy) or Sabouraud Dextrose Broth (SDB) (Liofilchem), supplemented with 20% (v/v) glycerol (Janssen Pharmaceuticals, Belgium), respectively, for the bacterial and the fungal strains. Every month, the frozen stocks were used to prepare the respective first cultures on a solid growth medium. For bacterial species, Tryptic Soy Agar (TSA), corresponding to TSB (Liofilchem) supplemented with 1.2% (w/v) agar (Liofilchem), was used, whereas Sabouraud Dextrose Agar (SDA), which is SDB (Liofilchem) supplemented with 1.2% (v/v) agar (Liofilchem), was used for *C. albicans*. The plates were incubated at 37°C for 18-24h. Subsequently, the plates were kept at 4°C for further studies.

3.2. PNA-FISH Method

The PNA-FISH technique involved the following steps: sample preparation, fixation and permeabilization, hybridization, washing, and visualisation of the results.

3.2.1. Sample Preparation, Fixation and Permeabilization

To ensure the microorganisms' maximum metabolic activity and to enhance the hybridization rate, a new solid microbial culture was prepared from the respective first solid cultures. This involved the preparation of a second microbial culture (subculture) by transferring a few colonies from the first cultures onto fresh Petri dishes containing the respective agar media. Subsequently, subcultures were incubated at 37°C for 18-24h.

Then, several colonies were collected into Eppendorf tubes from the subcultures and resuspended in ultrapure sterile water, following vortex to homogenize and disaggregate any microbial cluster. Afterward, 50 µL of each microbial suspension was placed onto microscope slides with reaction wells and let to dry in an incubator (37°C) for approximately 30 min.

For the fixation and permeabilization step, 50 µL of pure methanol (Fisher Bioreagents; UK) was added to each well for 10 min, and the excess of the fixative agent was removed to an absorbent paper. Then, 50 µL of a 4% (w/v) paraformaldehyde solution was applied for 10 min, and the reminiscent

solution was again removed, followed by 50 µL of 50% (v/v) ethanol, which was applied for 10 min and removed with absorbent paper. The samples were allowed to air dry before hybridization.

3.2.2. Probes Preparation

For each species, PNA probes were previously specifically designed using appropriate software and theoretical calculations [56]. Afterward, the oligonucleotides were synthesized by an external company. Accordingly, the name and respective oligonucleotide sequences for each selected/synthesized probe are summarised in **Table 5**.

Table 5: Name and oligonucleotide sequences of PNA probes designed for the specific detection of the species selected for this study

MICROBIAL SPECIES	PNA PROBE	
	Name	Sequence 5`- 3`
P. aeruginosa	Paer565	Alexa Fluor 594-OO-GCTGAACCACCTACG
S. aureus	Saur1	Alexa Fluor 488-OO-AGGCAACGATGCAT
K. pneumoniae	Kpneu1	Alexa Fluor 405-OO-TGTGAGACAGGTGC
S. epidermidis	Sepi1	ATTO 550-OO-CACGTCTTGACGGTA
A. baumannii	Abau1	ATTO 532-OO-GGTGAGCTAGAGTATG
C. albicans	Calb1	ATTO 633-OO-CCAAGGCTTATACTCG

After synthesis, it was crucial to optimise and validate the PNA probes experimentally so that they could be further applied to a multiplex PNA-FISH approach. It should be noted that any step involving the handling of the PNA probes was always performed in the dark. Once arrived, original probe aliquots (powder) were resuspended in 1% trifluoroacetic acid (TFA) (Sigma-Aldrich; USA) and 10% acetonitrile (ACN) (Sigma) solution, resulting in original aliquots (100 µM). Stock aliquots (4 µM) were prepared from the original aliquots in ultrapure water. Then, stock aliquots were used to prepare working aliquots (200 nM PNA), which were diluted in the hybridization solution (HS). The original and stock aliquots were preserved at -20°C, whereas the working probe solutions were kept at 4°C for further hybridization studies. Two HS were used, HS1 and HS2, differing in the formamide concentration. **Table 6** provides details of the component concentrations for both HS.

Table 6: Constituents of the HSs, HS1 and HS2, and respective final concentration

CONSTITUENTS OF HYBRIDIZATION SOLUTION	FINAL CONCENTRATION	
	HS1	HS2
Sodium Chloride	10 mM	10 mM
Sodium Pyrophosphate Decahydrate (Thermo Scientific Chemicals; USA)	0.1% (w/v)	0.1% (w/v)
Polyvinylpyrrolidone (Thermo Scientific)	0.2% (w/v)	0.2% (w/v)
Ficoll (Sigma)	0.2% (w/v)	0.2% (w/v)
Disodium Ethylenediaminetetraacetic Acid (EDTA) (PanReac AppliChem ITW Reagents; EUA)	5 mM	5 mM
Tris Hydrochloride	50 mM	50 mM
Dextran Sulphate (Sigma)	10% (w/v)	10% (w/v)
Formamide (Fisher Bioreagents)	30% (v/v)	5% (v/v)
Triton X-100 (Fisher Bioreagents)	0.1% (v/v)	0.1% (v/v)
Sodium Hydroxide (Sigma)	1 mM	1 mM

3.2.3. Hybridization and Washing

Following cell fixation and permeabilization on microscope slides with reaction wells, the subsequent step involved the preparation of samples for the hybridization process, as well as samples as a negative control (without a probe). In the dark, 20 µL of the working aliquot containing the PNA probe was added to each sample, while 20 µL of the HS was added to the negative control samples. The plates were incubated at 52°C, 58°C, 60°C, 62°C, and 65°C for 90 min to allow probe hybridization with their specific microbial target. The abovementioned temperature and incubation time were selected as the optimal conditions for the hybridization of most of the probes in previous testing.

Next, the probe washing was carried out by immersing the microscope slides into a washing solution (pre-heated to the same hybridization temperature) for 30 min. The constituents and their final concentration in the washing solution are summarised in **Table 7**. The pH of the solution was adjusted to 10.

Table 7: Constituents of the washing solution and respective final concentration

CONSTITUENTS OF WASHING SOLUTION	FINAL CONCENTRATION
Tris Base	5 mM
Sodium Chloride	15 mM

CONSTITUENTS OF WASHING SOLUTION	FINAL CONCENTRATION
Triton-X	1% (v/v)

3.2.4. Sample Counterstaining

Prior to sample visualisation, 20 µL of two distinct fluorescent dyes, SYTO BC and DAPI (4',6-Diamidino-2-Phenylindole), were added for counterstaining. SYTO BC (green) was applied to *K. pneumoniae* samples to be distinct from the Alexa Fluor 405 blue fluorochrome linked to the N-terminal of the PNA probe Kpneu. DAPI, on the other hand, was used for the remaining microbial samples. After counterstaining, a drop of Fluoromount™ Aqueous Mounting Medium (Sigma) was added to each sample (including negative controls) to increase the preservation period of the fluorescence to at least one week. In these cases, samples were kept at 4°C before visualisation.

3.2.5. Sample Visualization

For sample visualisation, an Olympus BX51 fluorescence microscope (Japan) was used. The fluorescence microscope was equipped with filters sensitive to the fluorochromes attached to the PNA oligonucleotides under study: BP 360-370 nm, LP 420 nm (DAPI, blue), BP 470-490 nm, LP 520 nm (Fluorescein Isothiocyanate, FITC, green); and BP 530-550 nm, LP 590 nm (Tetramethylrhodamine isothiocyanate, TRITC, red). Image acquisition and processing were done on CellSens software (Olympus). At least five images were captured per sample.

3.3. Biofilm Assay

In this study, the species *P. aeruginosa*, *S. aureus*, and *C. albicans* were used to develop single-, dual-, and triple-species biofilms. These biofilms were formed on 96-well microtiter plates and compared to biofilms formed on PVC, either uncoated or coated with a previously established antimicrobial coating.

3.3.1. Biofilm Formation on 96-well Microtiter Plates

To prepare bacterial suspensions, a few colonies were transferred from the previously prepared solid microbial subcultures to an Erlenmeyer containing 20 mL of TSB or SDB for bacterial and fungal species, respectively. Afterward, the Erlenmeyer was incubated overnight on an orbital shaker incubator (ES-20/60; Biosan; Latvia) at 37°C and 120 rpm.

Afterward, 1 mL of the overnight liquid microbial cultures were centrifuged for 10 min at 9000 g (bacteria) or 3000 g (fungal species). After supernatant removal, the pellet was resuspended in liquid broth medium, TSB (*P. aeruginosa* and *S. aureus*), or Roswell Park Memorial Institute (RPMI) 1640 for fungal suspensions.

The optical density (OD) of each bacterial suspension was then measured at 620 nm ($OD_{620\ nm}$) on a microtiter plate reader (EZ Read 800 Plus; Biochrom; USA), integrating the Galapagos software (Biochrom). In order to achieve a final concentration of 1×10^7 CFU/mL in the biofilm inoculum, previously established calibration curves specific for *P. aeruginosa* (**Equation 1**) and *S. aureus* (**Equation 2**) were used. Regarding the fungal culture, the number of cells within the liquid cultures was estimated in a Neubauer counting chamber and diluted to reach the desired concentration.

$$CFU/mL = 9 \times 10^8 OD_{620\ nm} - 1 \times 10^8 \qquad \textbf{Equation 1}$$

$$CFU/mL = 1 \times 10^9 OD_{620\ nm} - 3 \times 10^7 \qquad \textbf{Equation 2}$$

To promote biofilm formation, 200 µL of each bacterial or fungal suspension were paced per well in a 96-well flat microtiter plate (polystyrene; Orange Scientific; USA). For dual and triple-species biofilms, cell suspensions were mixed equally at 50% and 33.3%, respectively, with a final volume of 200 µL per well. Subsequently, the microtiter plates were incubated at 37°C and 120 rpm for 24h.

3.3.2. Biofilm Analysis

After biofilm formation, the planktonic fraction (supernatant) was removed, and the wells were washed twice with sterile distilled water. Biofilms were then analysed regarding the number of cultivable cells and biomass through CFU counting and the crystal violet (CV) staining method, respectively.

3.3.2.1. Determination of Cultivable Cells

To determine the number of cultivable cells in the biofilms, 200 µL of sterile distilled water was added to each well, and the plate was sonicated for 10 min in an ultrasonic bath. Then, the biofilm suspension in the wells was homogenised by pipetting, and a total volume of 1 mL of each biofilm cell suspension was further collected and serially diluted (10-fold) in sterile distilled water. Subsequently, a 10 µL drop of each diluted biofilm sample was plated in duplicate on unspecific or specific solid agar media. For this, TSA and SDA were used for the unspecific growth of bacteria and fungi, respectively. Concerning selective agar media, cetrimide agar (Liofilchem) was used for *P. aeruginosa* isolation;

Mannitol Salt Agar (MSA; Liofilchem) for *S. aureus*; and SDA supplemented with 60 mg/L gentamicin (NZYTech; Portugal) was applied for *C. albicans* isolation. The plates were incubated at 37°C for 16 to 24h before CFU counting.

3.3.2.2. Biomass Quantification

Subsequent to biofilm washing, 200 µL of pure methanol was added to each well to allow cell fixation. After 15 min, the methanol was removed, and the plates were allowed to air dry. Then, 200 µL of 1% (v/v) CV dye solution (Pro-Labs Diagnostics Inc.; Canada) was applied to each well for 5 min. Subsequently, CV was removed, and the samples were washed twice with distilled water to remove the excess CV stain. Then, 200 µL of 33% (v/v) acetic acid (Thermo Scientific Chemicals) was added to each well to resuspend the stained biofilm. After homogenising by pipetting, the OD of the biofilm samples was measured at 570 nm in a Multiskan™ FC Microplate Photometer (Thermo Fisher Scientific; EUA), and the final $OD_{570\,nm}$ values were recorded.

3.3.3. Biofilm Formation on PVC

To investigate the ability of the aforementioned bacterial and fungal species to develop triple-species biofilms on ETTs, PVC surfaces were employed in this study. Furthermore, the effectiveness of a new PVC antimicrobial coating previously developed was also evaluated to prevent the formation of triple-species consortia formed by *P. aeruginosa*, *S. aureus*, and *C. albicans*.

3.3.3.1. PVC preparation and functionalization

In this study, immobilisation of CIP and CHX on PVC coupons followed an in-group, well-established procedure using a pDA-based functionalization strategy [74], [78].

Before PVC modification, 1 mm-thickness unplasticized sheets of PVC (purchased from Goodfellow Cambridge Ltd, Cambridgeshire, UK) were cut into 1x1 cm-squared coupons, subjected to an ultrasonic cleaning treatment in commercial detergent (Sonasol, Henkel Ibérica, Portugal), sterilised with 70% (v/v) ethanol, thoroughly rinsed with ultrapure sterile water, and subjected to 1h of irradiation with UV light. Cleaned PVC and sterilised PVC surfaces were further functionalized and immobilised with CIP and/or CHX using a previously reported one-step approach for the immobilisation of CHX on stainless steel [74], the so-called mussel-inspired coating strategy. For this, the PVC coupons were simply immersed in a 2 mg/mL solution of dopamine (Sigma) added to CHX and CIP solutions combined at a final concentration of 0.5 mg/mL, which were freshly prepared together in 10 mM bicine buffer pH 8.5 (Sigma) for 18h at

room temperature under agitation (70 rpm). This one-step approach allowed the deposition of a pDA film/coating on the PVC surface and the concomitant immobilisation of the combined antimicrobial solution (CIP/CHX). Modified PVC surfaces were then rinsed with sterile ultrapure water and air-dried for further application in biofilm studies. For comparison purposes, unmodified PVC (before pDA coating or antimicrobial immobilisation) were used in further biofilm assays.

3.3.3.2. Biofilm Formation on PVC surfaces

To investigate the ability of *P. aeruginosa*, *S. aureus* and *C. albicans* to develop triple-species biofilms on PVC, bacterial and fungal liquid cultures at $1x10^7$ CFU/mL were then prepared as described before. Then, 1 mL of the triple-species microbial suspension was transferred to the 24-well plates containing unmodified and CIP/CHX-modified PVC coupons. The plates were further incubated at 37°C and 120 rpm for 24h to promote biofilm formation. After this, their number of cultivable cells was determined using the method described in **Section 3.3.2.1.**. It is important to emphasise that this analysis was based on a single experiment.

3.3.3.3. Biofilm Formation on PVC surfaces

To assess the presence of *P. aeruginosa*, *S. aureus*, and *C. albicans* in the triple-species biofilms that developed on PVC and PVC functionalized with pDA to immobilise CIP and CHX, the FISH technique was carried out. This technique used an FV3000 confocal microscope with 40x amplification. It should be noted that this test was carried out by the group, and therefore its results have been provided to complement the results obtained with the CFU technique.

3.4. Data analysis and Statistics

To ensure the reproducibility of the outcomes, a minimum of three independent replicates were conducted for almost all experiments. The only exception where reproducibility was not ensured was in the analysis of biofilms formed in the assay involving PVC and functionalized PVC. Additionally, the results were reported as the mean value along with their corresponding standard deviation (SD).

Data analysis and statistical tests were made on Microsoft Excel (Microsoft; EUA) and GraphPad Prism 8.4.2. (Dotmatics; Bishop's Stortford; UK), respectively. Outliers were detected by using the interquartile range method.

Statistical analyses encompassed an assessment of data normality, followed by the application of non-parametric tests, specifically Kruskal-Wallis multiple comparison tests with a significance level set at 0.05. Additionally, Dunn's multiple post hoc comparison test was performed. $P < 0.05$ was considered statistically significant.

CHAPTER 4: RESULTS AND DISCUSSION

4.1. PNA-FISH Experimental Specificity Testing

The first goal was to evaluate the specificity of several previously designed PNA probes so that they could be validated in multiplex. Therefore, with these PNA probes, it will be possible to detect several VAP-related microorganisms simultaneously in one sample.

Because PNA probes were designed to specifically target the 16S or 18S rRNA regions of the genetic codes of bacteria and fungi, respectively, this targeted approach ensures specificity for each PNA probe. This specificity in PNA probe binding is due to these probes targeting regions of the genetic code known as 16S rRNA, a region known for its conservation in prokaryotic species [56], [79].

A number of factors have an impact on the probe binding and specificity, namely the type of fixative agent, the duration of hybridization, the temperature, the pH, the concentration of the probe, and the components in the HS (e.g., dextran sulphate, formamide) [80], [81]. The hybridization temperature influences the probe's affinity for the target sequence, while the hybridization duration is critical for probe penetration through the cell membrane/envelope, binding to the complementary sequence, and the unravelling of secondary and tertiary structures within rRNA, as well as any folded regions within the probe. The amount of formamide in the HS also plays a critical role by facilitating the hybridization at lower temperatures and acting as a denaturing agent that reduces the thermal stability of double-stranded polynucleotides. This, in turn, enhances accessibility to the rRNA target and competes for hydrogen bonds, contributing to the effectiveness of the hybridization process [82]–[84].

In this work, certain conditions were investigated to address the specificity of PNA probes previously designed for the VAP-related species *P. aeruginosa*, *S. aureus*, *K. pneumoniae*, *S. epidermidis*, and *A. baumannii*. Specifically, a range of different temperatures was used: 52°C, 58°C, 60°C, 62°C, and 65°C, and the percentage of formamide in the HS varied from 30% (v/v) (HS1) to 5% (v/v) (HS2). Regarding the hybridization time, 90 min were used. **Figure 5** presents the outcomes achieved following the application of the PNA-FISH methodology under the specified conditions for *P. aeruginosa* ATCC 27853.

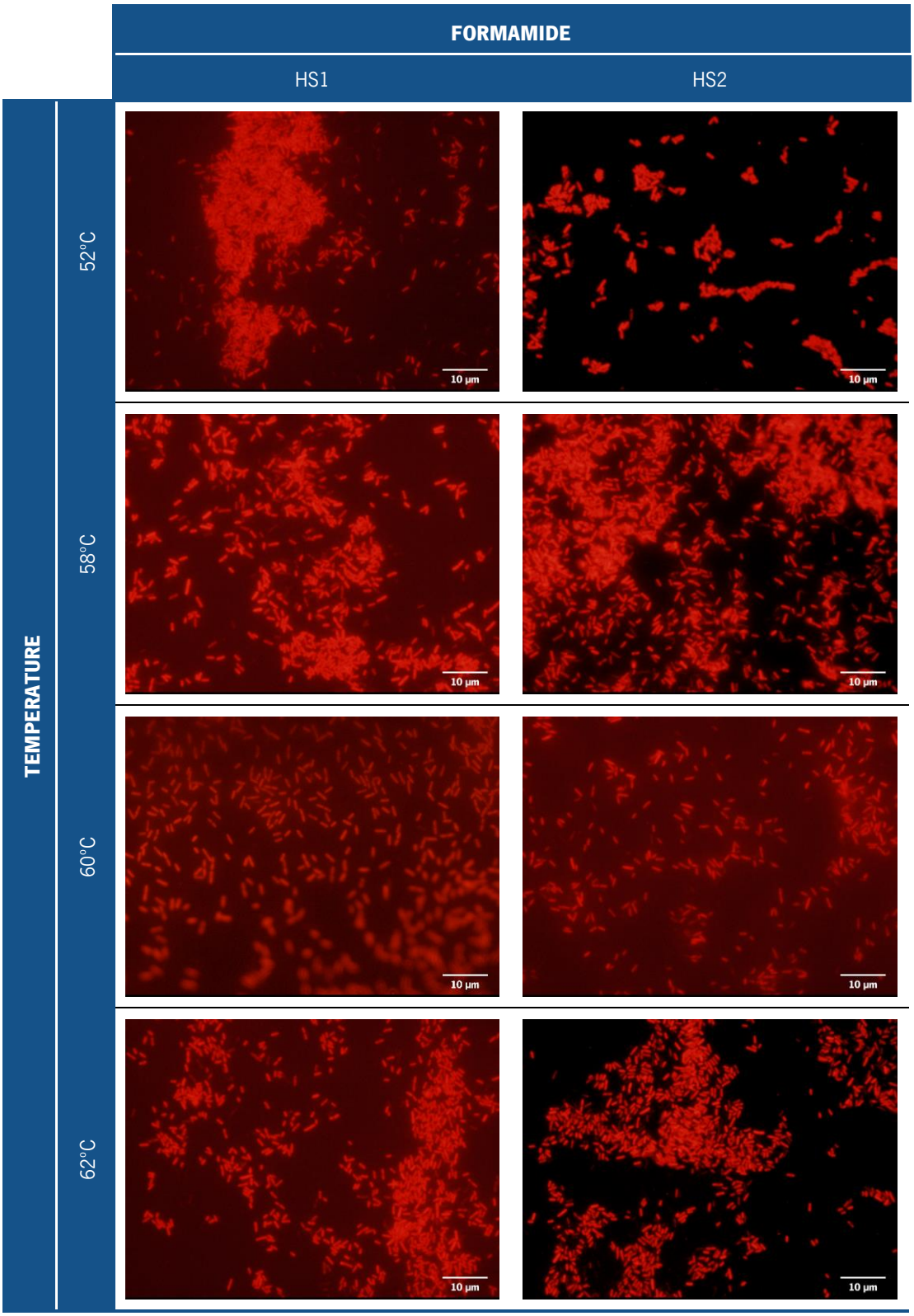
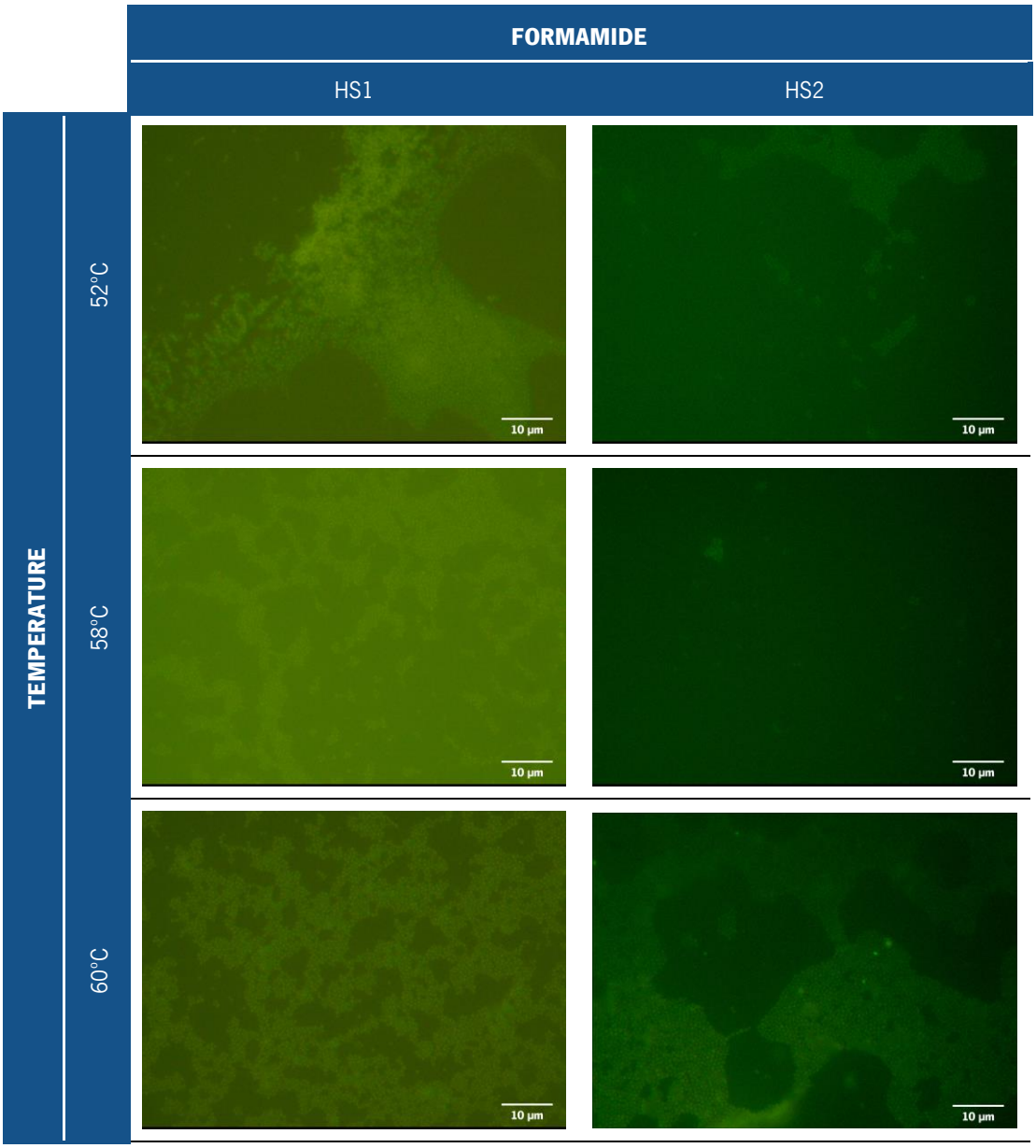


Figure 5: Detection of *P. aeruginosa* ATCC 27853 by the red fluorescent probe Paer565 in a pure smear of the organism under different hybridization temperatures (52°C, 58°C, 60°C, and 62°C) and using HSs with distinct percentages of formamide (30% (v/v) (HS1) and 5% (v/v) (HS2)).

Regardless of variations in the hybridization temperature and formamide concentration in the HS, the PNA probe Paer565 consistently exhibited hybridization in the target species, *P. aeruginosa*. For all conditions, an abundant number of cells were detected, whether in clustered or dispersed forms. Additionally, among the tested temperatures, it was noteworthy that 62°C appears to yield a higher hybridization signal, particularly when the probe was prepared with HS2. This outcome was not anticipated since lower concentrations of formamide are generally used at higher temperatures to maintain high stringency, which favours specific hybridization [83]. However, as the exposure times of the images are not the same, it is not possible to be certain about this observation.

Figure 6 shows the results obtained by using the PNA-FISH technique with the given parameters for *S. aureus* ATCC 25923.



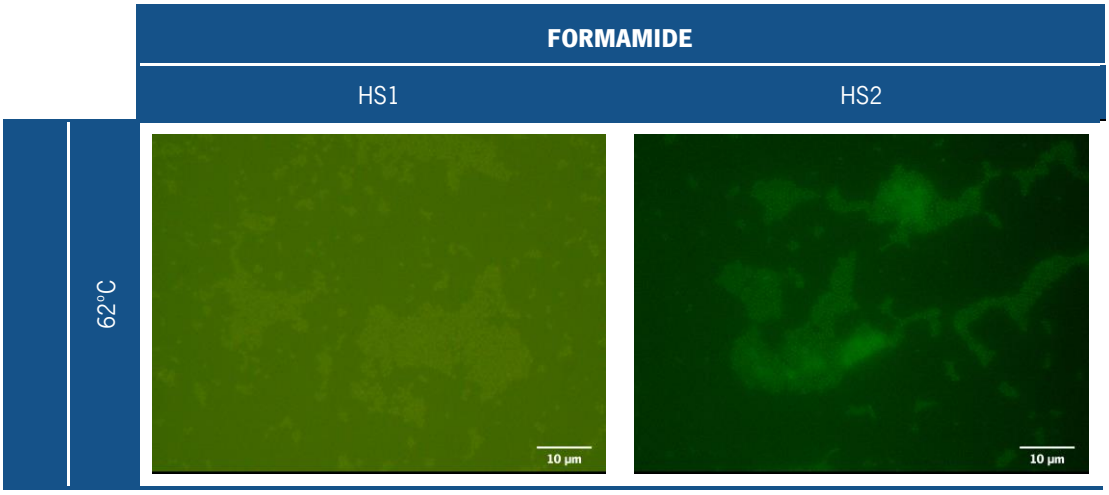


Figure 6: Detection of *S. aureus* ATCC 25923 by the green fluorescent probe Saur1 in a pure smear of the organism under different hybridization temperatures (52°C, 58°C, 60°C, and 62°C) and using HSs with distinct percentages of formamide (30% (v/v) (HS1) and 5% (v/v) (HS2)).

Figure 6 showed that *S. aureus* did not undergo hybridization with the Saur1 PNA probe, independently of the condition used. Some hybridised cells were only observed at 60°C when HS2 was used. This lack of success in the *S. aureus* hybridization by the green fluorescent Saur1 probe led to speculation about the malfunctioning of the Saur1 or eventually any problems related to the probe synthesis. This conclusion is not consistent with previous research conducted by Hartmann et al., Oliveira et al., and González et al., all of which demonstrated that hybridization could occur between the same *S. aureus* strain and different PNA probes [79], [85], [86]. It should be emphasised that all these aforementioned studies employed a hybridization temperature of 55°C.

In **Figure 7**, the outcomes acquired by utilising the PNA-FISH methodology with the different temperatures (52°C, 58°C, 60°C, and 62°C) and formamide concentrations (5% (v/v) and 30% (v/v)) for *K. pneumoniae* ATCC 11296 are presented.

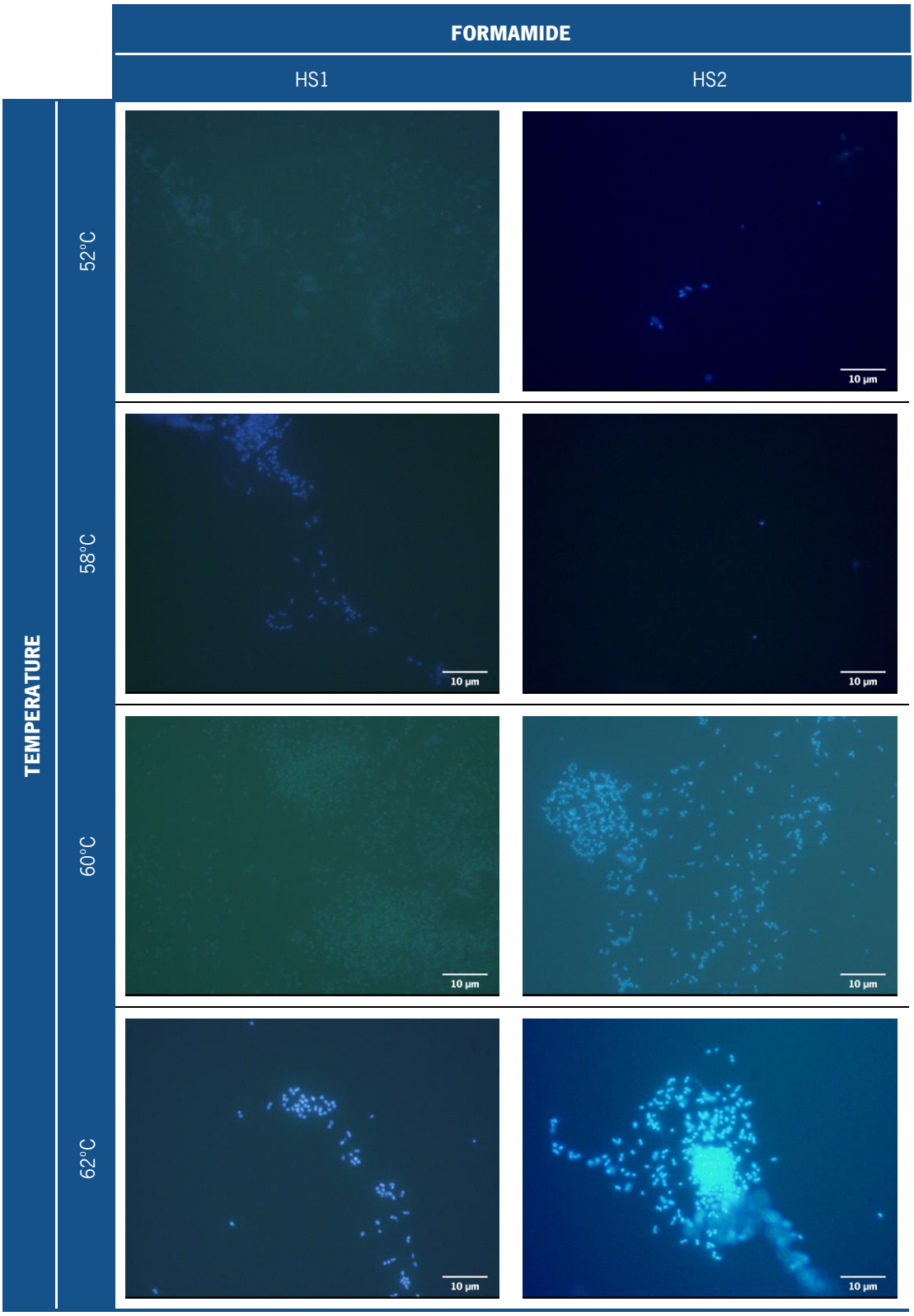
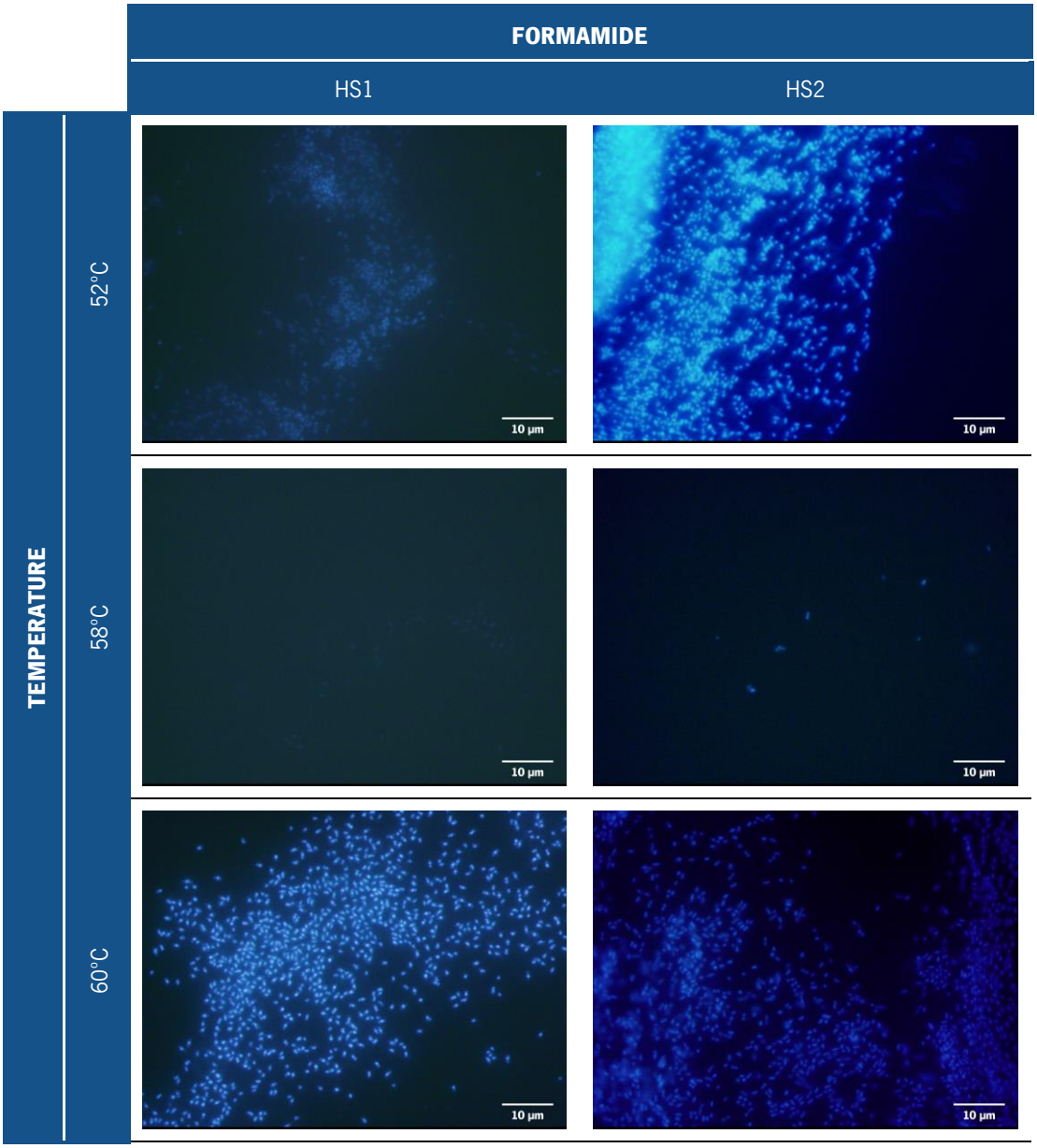


Figure 7: Detection of *K. pneumoniae* ATCC 11296 by the blue fluorescent probe Kpneu1 in a pure smear of the organism under different hybridization temperatures (52°C, 58°C, 60°C, and 62°C) and using HSs with distinct percentages of formamide (30% (v/v) (HS1) and 5% (v/v) (HS2)).

According to **Figure 7**, it appears that the blue-labelled Kpneu1 probe could detect *K. pneumoniae* ATCC 11296 cells, specifically using HSs with formamide concentrations of 5% (v/v) and 30% (v/v) and

under temperatures of 52°C, 58°C, and 62°C. A closer examination of the images reveals that, as the formamide concentration decreases, *K. pneumoniae* ATCC 11296 indeed exhibits a better hybridization signal with the Kpneu1 probe when using the HS with a lower concentration of formamide. This observation is supported by the fact that none of the bacteria hybridised when exposed to HS1, except for hybridization at 58°C and 62°C, whereas most of the bacteria exhibited hybridization in the presence of HS2. Nevertheless, it should be noted that the exposure time of the images was not recorded, which made it difficult to compare the fluorescence signals in the images.



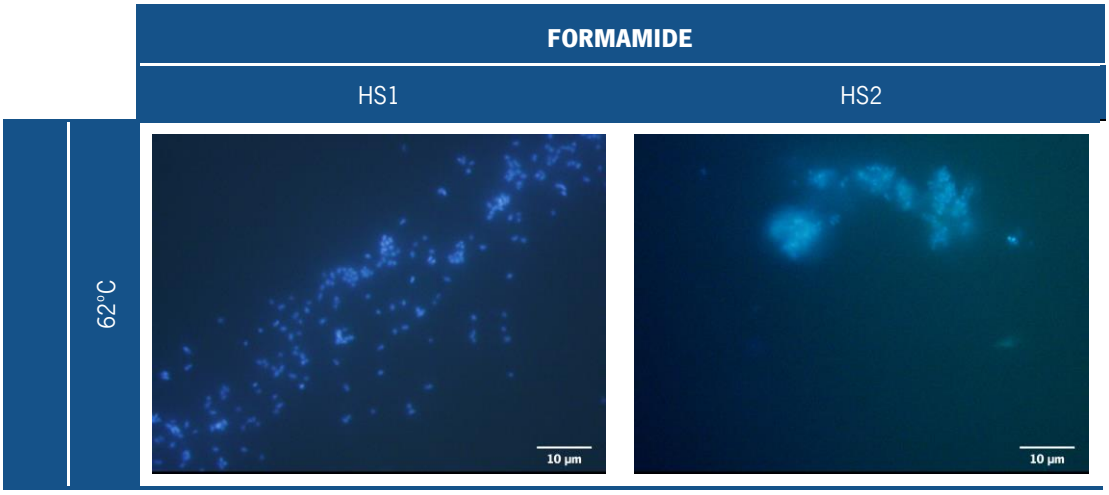
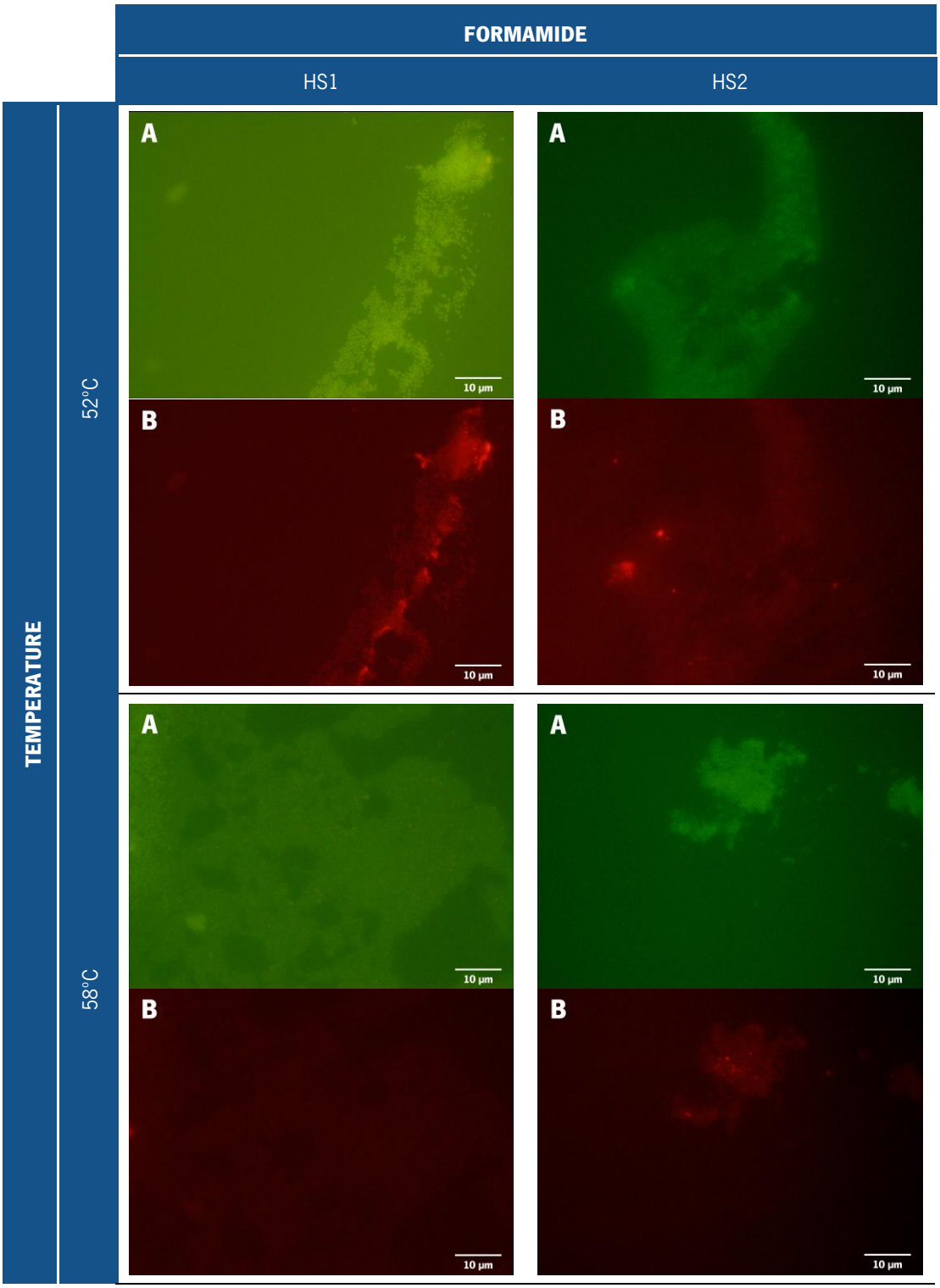


Figure 8: Detection of *K. pneumoniae* ATCC 43216 by the blue fluorescent probe Kpneu1 in a pure smear of the organism under different hybridization temperatures (52°C, 58°C, 60°C, and 62°C) and using HSs with distinct percentages of formamide (30% (v/v) (HS1) and 5% (v/v) (HS2)).

The Kpneu1 probe was also tested in another *K. pneumoniae* strain, namely *K. pneumoniae* ATCC 43216. **Figure 8** demonstrated that, at 58°C, Kpneu1 showed lower efficacy compared to the remaining hybridization temperatures. In contrast, at 52°C, 60°C, and 62°C, the hybridization was successful. Furthermore, it is evident that, in general, Kpneu1 worked better with the strain of *K. pneumoniae* ATCC 43216 than with ATCC 11296.

No significant differences in the hybridization signals were observed for different concentrations of formamide in the HS, apart from the temperature of 52°C. In this specific case, the hybridization signal obtained by probes prepared in the HS1 was apparently lower than that obtained for probes prepared in the HS2. This result was unexpected, given that higher concentrations of formamide are typically used at lower temperatures [83].

Figure 9 presents the outcomes obtained for the orange-labelled Sepi1 probe, specifically designed for *S. epidermidis* detection. As the fluorescence microscope used in this work lacks the filter with the required wavelength for specific detection of the ATTO 550-labelled Sepid1 probe, the images were acquired using the green and red filters. These two filters were selected because the fluorescence emission signal of the orange colour is within the spectral range encompassed by the green and red filters. As a result, owing to the spectral characteristics of the fluorescent molecule within these PNA probes, spanning from the green to the red spectrum, the use of both filters was essential to effectively visualising the obtained results. It should be noted that although these are not suitable filters, it is possible to observe a fluorescence signal if hybridization occurs.


FORMAMIDE
HS1
HS2
TEMPERATURE
52°C
58°C
A
B
10 µm

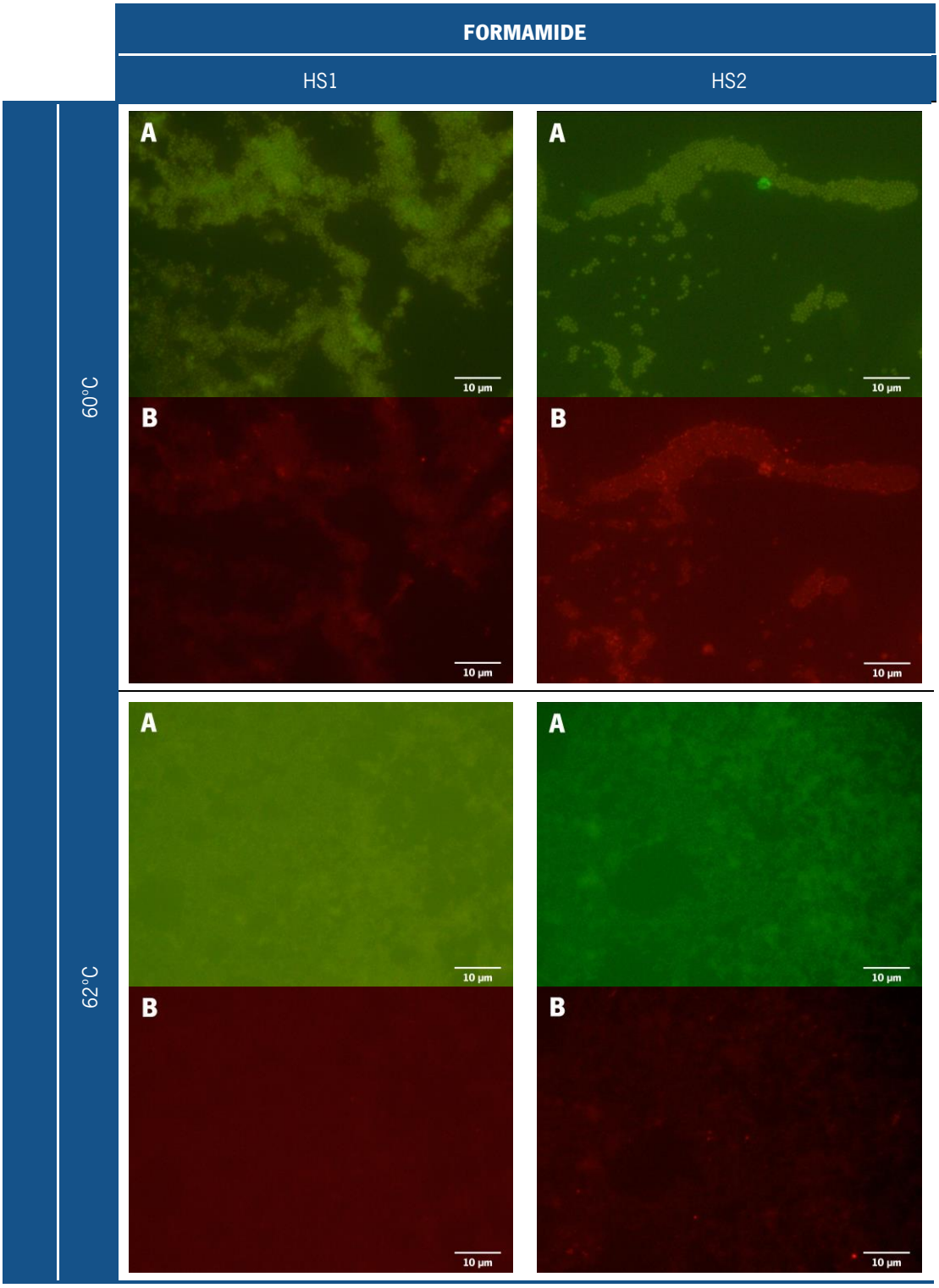
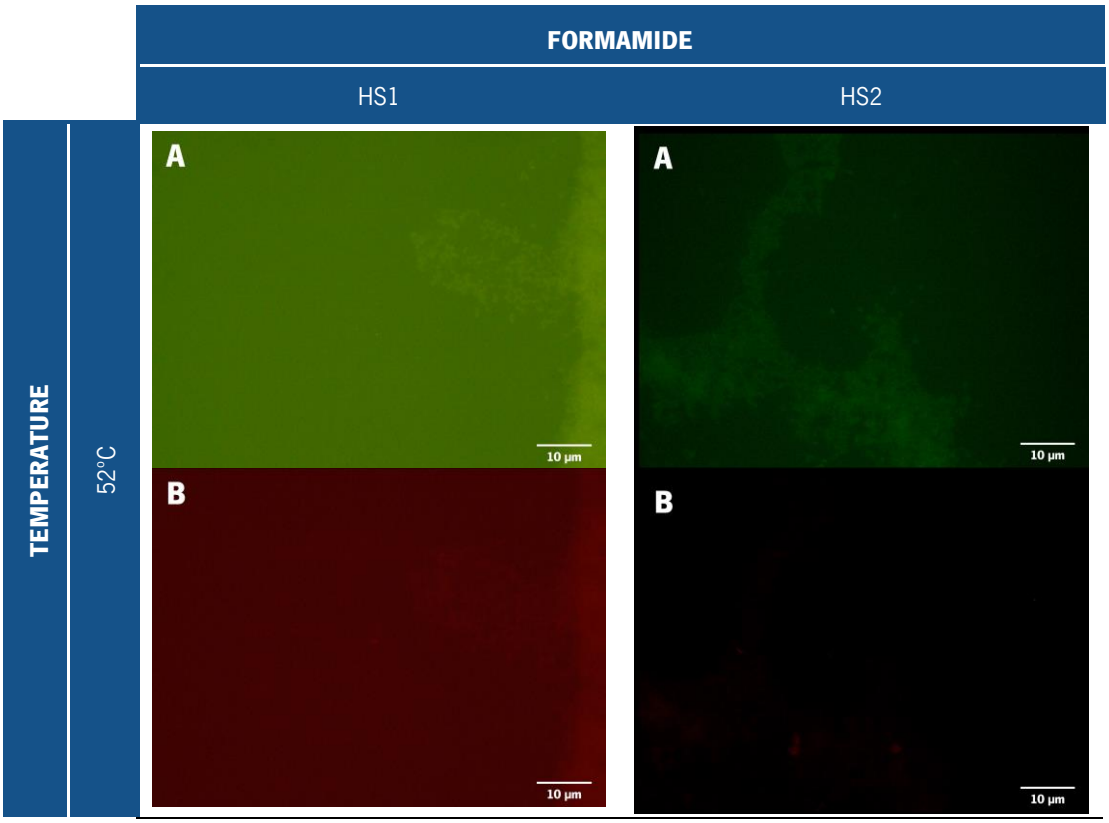


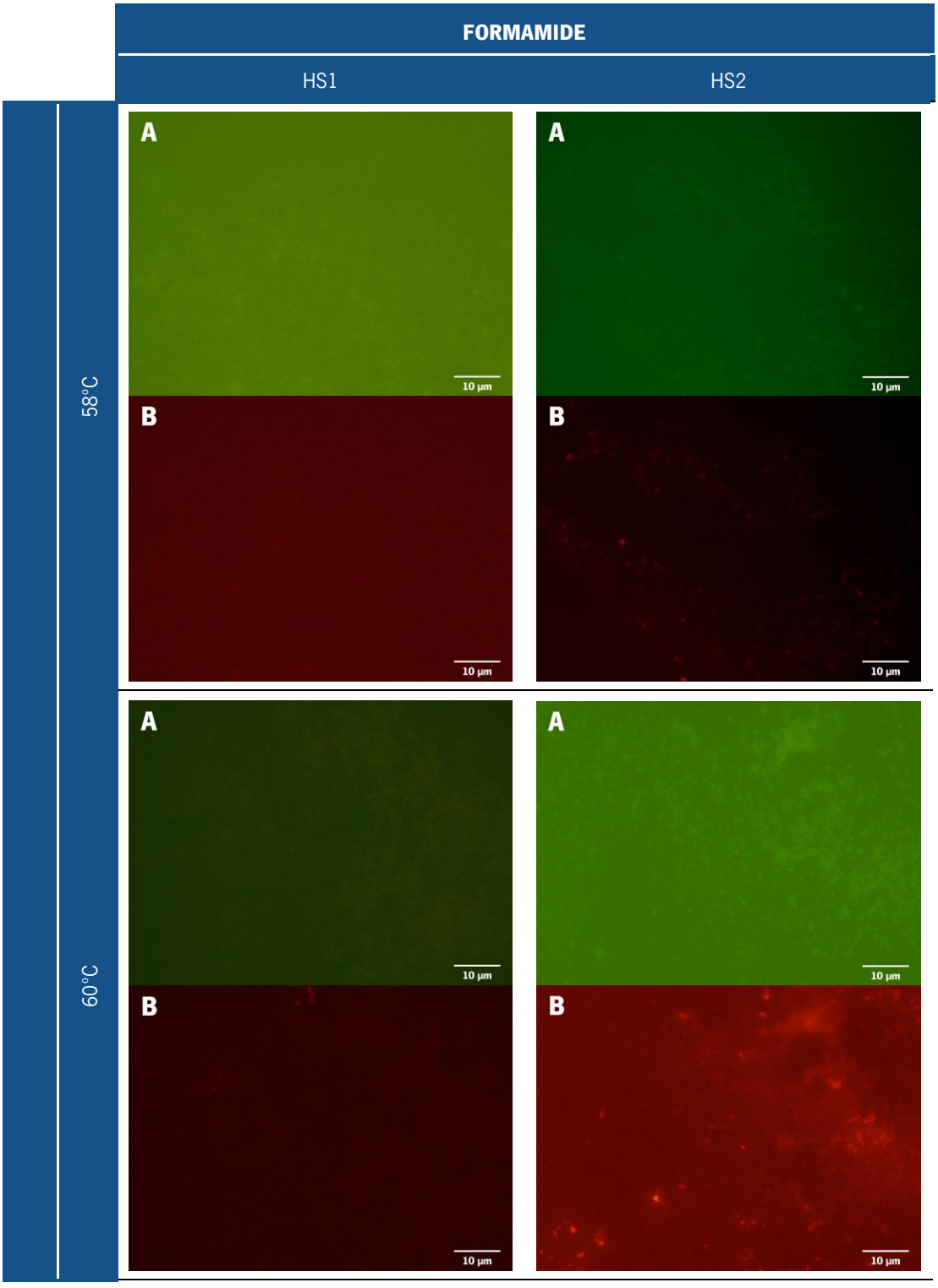
Figure 9: Detection of *S. epidermidis* CECT 4183 by the orange fluorescent probe Sepi1 in a pure smear of the organism under different hybridization temperatures (52°C, 58°C, 60°C, and 62°C) and using HSs with distinct percentages of formamide (30% (v/v) (HS1) and 5% (v/v) (HS2)). **A** shows the image in the green filter depicted, while image **B** portrays the red filter.

Figure 9 demonstrates that the Sepi1 PNA probe does not exhibit effective hybridization against *S. epidermidis*, as denoted by the low number of hybridised bacterial cells in the samples. In general, probes prepared in HSs containing the lowest formamide concentration (HS2) apparently displayed less

variability at all temperature conditions. In the red filter, some hybridised cells were detected at all temperatures. Conversely, in the experiments employing a higher formamide concentration (referred to as HS1), only a very small number of hybridised cells were sparsely observed, specifically at 52°C, 60°C, and 62°C, while no hybridization was detected at 58°C.

Figure 10 presents the outcomes obtained for the use of the Abau1 probe against *A. baumannii* under different temperature and formamide conditions. As occurred for the Sepi1 probe, images were acquired under the red and green channels, which present wavelengths close to the fluorophore molecule coupled with the Abau1 probe, ATTO 532. The use of green and red filters was employed because the fluorescence emission colour from Abau1 falls within the spectrum covered by these filters.




FORMAMIDE
HS1
HS2
58°C
60°C
A
B
10 µm

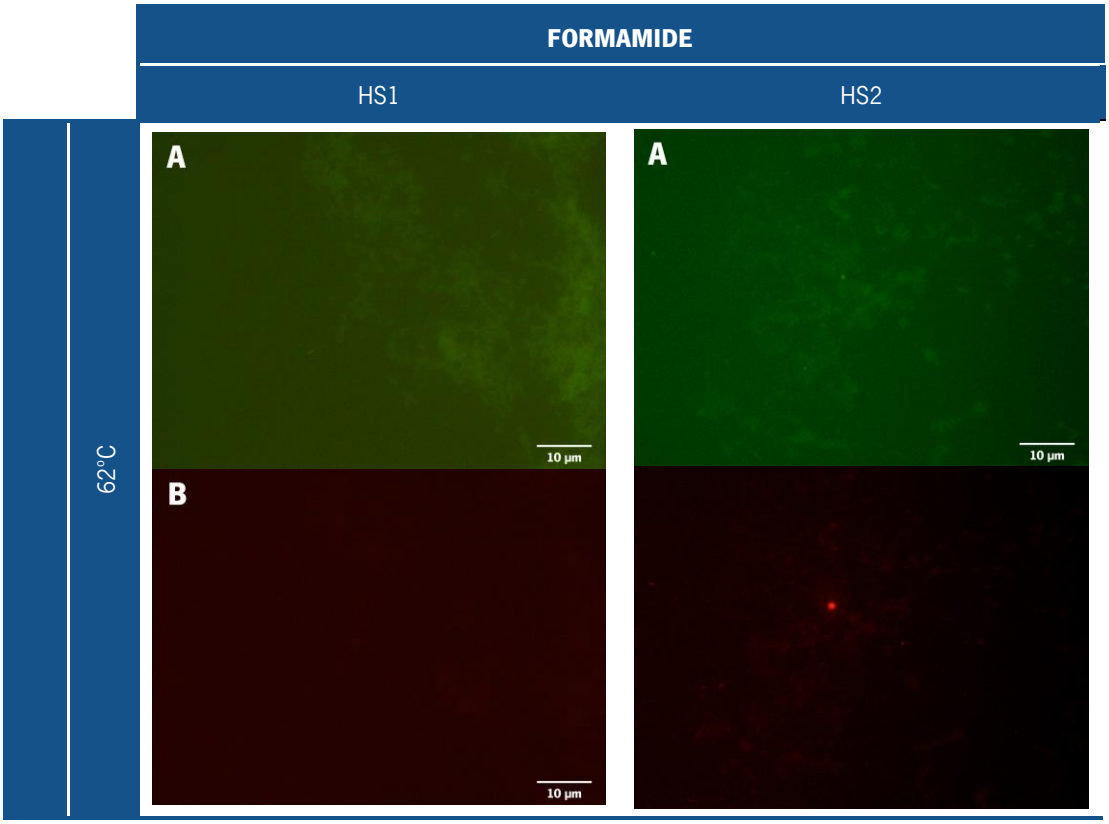
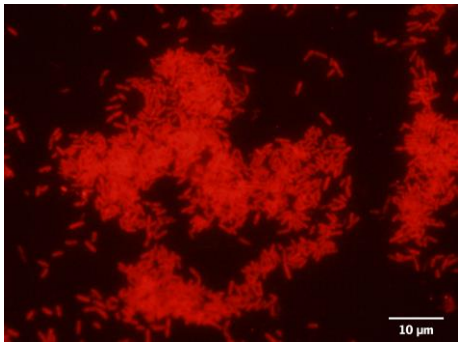


Figure 10: Detection of *A. baumannii* ATCC 19106 by the green fluorescent probe Abau1 in a pure smear of the organism under different hybridization temperatures (52°C, 58°C, 60°C, and 62°C) and using HSs with distinct percentages of formamide (30% (v/v) (HS1) and 5% (v/v) (HS2)). **A** shows the image in the green filter depicted, while image **B** portrays the red filter.

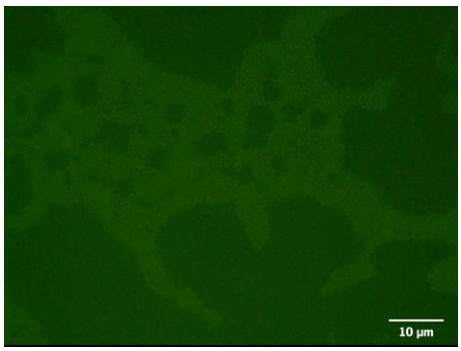
The analysis of the images presented in **Figure 10** indicates that the hybridization specificity of the Abau1 probe with *A. baumannii* is low. In experiments where the probes were prepared with HS1 (30% (v/v) formamide) at a temperature of 60°C, there appears to be some hybridization, i.e., some cells appear brighter than others. Conversely, in experiments conducted with HS2, denoting the HS with the lowest formamide concentration, all results exhibited a consistent pattern characterised by the apparent hybridization of some cells. It is worth noting that at a temperature of 60°C, a higher number of hybridised bacteria were apparently detected, specifically by the red channel. Therefore, these experiments underscore the influence of formamide concentration and temperature on the hybridization process.

Overall, it was observed that the best hybridization outcomes were apparently shown with the probes prepared in HS2. As previously mentioned, lower formamide concentrations typically require the use of higher hybridization temperatures to facilitate stronger binding between the PNA probes and the bacteria, consequently resulting in an elevated hybridization rate [83]. Therefore, the FISH experiments were further conducted for all the abovementioned species at a higher temperature of 65°C, with probes prepared in HS2 (5% (v/v) formamide) (**Figure 11**).

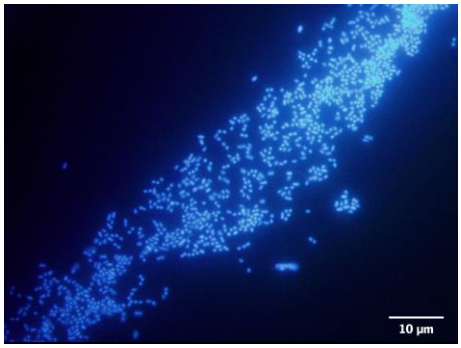
P. aeruginosa ATCC 27853



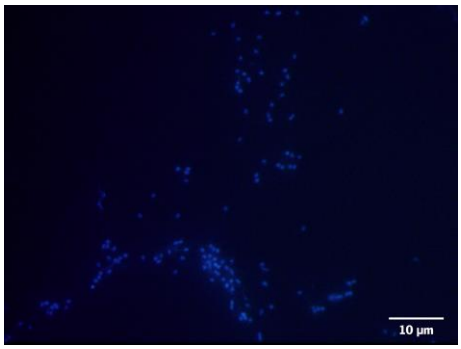
S. aureus ATCC 25923



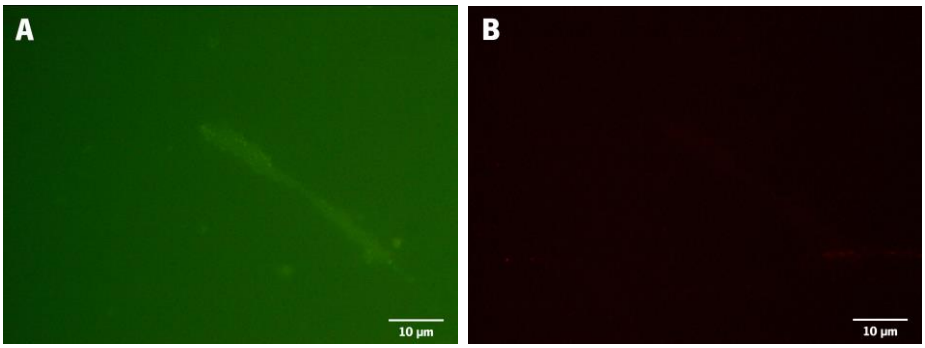
K. pneumoniae ATCC 11296



K. pneumoniae ATCC 43216



S. epidermidis CECT 4183



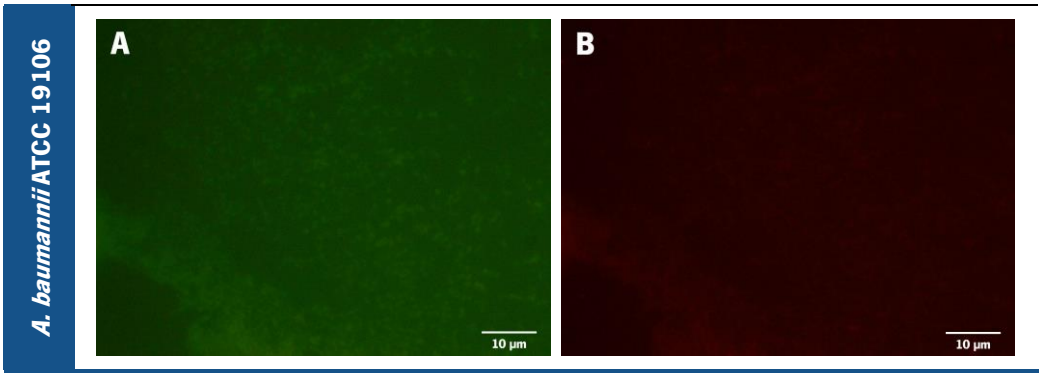


Figure 11: PNA-FISH results, made at a hybridization temperature of 65°C and involving the PNA probes Paer565, Saur1, Kpneu1, Sepi1, and Abau1, that were designed for the specific targeting of *P. aeruginosa* ATCC 27853, *S. aureus* ATCC 25923, *K. pneumoniae* ATCC 11296, *K. pneumoniae* ATCC 43216, *S. epidermidis* CECT 4183, and *A. baumannii* ATCC 19106, respectively. In the case of *S. epidermidis* and *A. baumanniil*, Image **A** illustrates the results in the green filter, while Image **B** presents the results in the red filter.

Analysing **Figure 11**, it becomes evident that hybridization was effective at 65°C for *P. aeruginosa* and both strains of *K. pneumoniae*. On the other hand, no hybridization was found for *S. aureus*, *S. epidermidis*, or *A. baumannii* under these conditions.

In summary, it is evident that the experimental specificity of the PNA probes yielded successful outcomes exclusively for *P. aeruginosa* and *K. pneumoniae*. To confirm specificity for *S. epidermidis* and *A. baumannii*, further validation would be necessary using a microscope equipped with the appropriate filter for Sepi1 and Abau1 fluorescence emissions. In the case of *S. aureus*, as Saur1 did not yield fluorescence under any of the tested conditions, it would be ideal to consider the selection of a new oligonucleotide and its subsequent testing for specificity.

It is important to emphasise that conducting tests of this nature is challenging due to the requirement that all the probes must be functioning under identical conditions and not cross-react with non-target microorganisms in multiplex tests. This is the reason behind the time-consuming and demanding process, but it is critical for obtaining accurate and reliable results in microbial identification and detection.

4.2. Assessment of Biofilm Formation

P. aeruginosa, *S. aureus*, and *C. albicans* are among the most common pathogenic microorganisms found in ETT-associated infections, including VAP. These pathogens can contribute to respiratory infections when they co-colonise or infect the airway through the ETT.

Conventional ETTs are generally made of flexible materials such as PVC, which possesses hydrophobic properties, rendering the ETT surface susceptible to the attachment of pathogenic

microorganisms and subsequent biofilm development [9], [68], [69]. During the latest years, technological developments on materials able to endow the ETT surface with active antimicrobial properties have been emerging, aiming at reducing the ETT bioburden and the risk of VAP while retaining/improving the safety of use. As such, a new ETT coating was developed in group, consisting of the immobilisation of CIP and CHX through a pDA functionalization-based approach.

Hence, in this work, it was aimed to evaluate the ability of *P. aeruginosa*, *S. aureus*, and *C. albicans* to develop single-, dual-, and triple-species biofilms on 96-well polystyrene plates and further compare their biofilm formation on PVC surfaces, uncoated and immobilised with CIP and CHX.

1.4.1. Biofilm Formation on Polystyrene 96-Well Microtiter Plates

Two distinct techniques were employed to evaluate the biofilms formed on polystyrene 96-well plates over 24h: one for ascertaining the count of viable microorganisms within the developed biofilms, known as CFU counting, and the other for measuring the biomass of the biofilms, known as the crystal violet method [87]. **Figure 12** shows the outcomes following the counting of viable microorganisms in the single-species, dual-species, and triple-species biofilms, respectively.

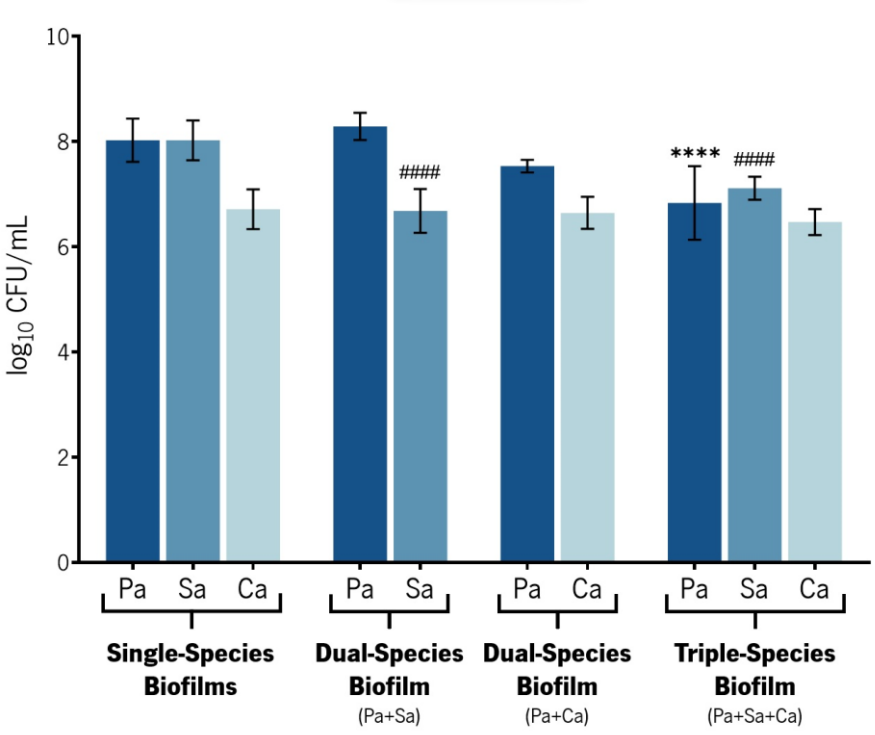


Figure 12: Quantification of cultivable cells by CFU counting, expressed in log10 CFU/mL, within single-, dual-, and triple-species biofilms of *P. aeruginosa* ATCC 27853 (Pa), *S. aureus* ATCC 25923 (Sa), and *C. albicans* SC 5314 (Ca) for 24h at 37°C. The results are presented as mean±SD from three independent assays. Statistical analysis was conducted using ANOVA followed by a Kruskal-Wallis multiple comparisons test, comparing (*) significant differences between single-species *P. aeruginosa* biofilms and other *P. aeruginosa* biofilm types ($p<0.05$) and (#) significant differences between single-species *S. aureus* biofilms and other *S.*

aureus biofilm types (#<0.05). No significant differences were observed between single-species *C. albicans* biofilms and other *C. albicans* biofilm types.

Regarding single-species biofilms, both bacterial populations showed the highest ability to develop biofilms on polystyrene surfaces. In contrast, the fungal species *C. albicans* showed less ability compared to the others (a difference of about 1.3 $\log_{10}$ CFU/mL). Specifically, the average count of *P. aeruginosa* and *S. aureus* cultivable biofilm cells was 8.0 $\log_{10}$ CFU/mL, and 6.7 $\log_{10}$ CFU/mL cells for *C. albicans* biofilms.

When grown with *P. aeruginosa* in dual-species biofilms, *S. aureus* biofilms decreased the number of cultivable cells by 1.4 $\log_{10}$ CFU/mL, whereas no significant reduction was observed for *P. aeruginosa* cells in the presence of staphylococcal cells. This finding corroborates other studies, which have demonstrated that the presence of *P. aeruginosa* often leads to a competitive dominance over *S. aureus* [88], [89]. This competitive advantage for *P. aeruginosa* over *S. aureus* may be due to several factors, including resource competition, such as iron acquisition, as well as the impact of *P. aeruginosa*'s secreted products and exoproducts on staphylococcal cells. These compounds are known to inhibit *S. aureus* growth and even cause its lysis, as previously reported [90]–[93]. Additionally, the exposure of *S. aureus* to the planktonic phase (supernatant) of the *P. aeruginosa* and *S. aureus* biofilms has a detrimental effect on the growth of *S. aureus* [93]. Collectively, these factors may explain the reduction in the growth of *S. aureus* in the presence of *P. aeruginosa*.

In the case of dual-species encompassing the bacterial species *P. aeruginosa* and the fungal species *C. albicans*, their coexistence in the consortia led to a slight reduction in the number of cultivable cells of both populations (< 1 $\log_{10}$ CFU/mL). Despite this reduction, *P. aeruginosa* was still the prevalent population, presenting, on average, 7.5 $\log_{10}$ CFU/mL, while *C. albicans* was reduced to 6.6 $\log_{10}$ CFU/mL.

P. aeruginosa and *C. albicans* are known to engage in antagonistic interactions [94]–[97]. During the colonisation of surfaces, both microorganisms appear to compete for available binding sites, which may justify, in part, the reduction in the number of cells for both species within the consortia as compared to their respective cells in single biofilms. Another explanation for the prevalence of *P. aeruginosa* over *C. albicans* is the phenomenon wherein *P. aeruginosa* forms a dense biofilm on the fungal filaments, which can ultimately lead to *C. albicans* death, which may result from the virulence factors of *P. aeruginosa*, including pili and secreted molecules. Also, a specific *P. aeruginosa* quorum sensing molecule, N-(3-oxo-dodecanoyl)-L-homoserine lactone, is responsible for repressing filamentation and promoting yeast growth by changing the gene expression in *C. albicans* biofilms [94]–[96], [98]–[100].

Another potential explanation for the reduction in *P. aeruginosa* culturable cells in the dual-species biofilm with *C. albicans* could be associated with the secretion of farnesol, a 12-carbon sesquiterpene, by the fungal species. Farnesol serves as a virulence factor and functions as a repressor of the transition from yeast to hyphal growth in *C. albicans*. Additionally, the farnesol molecule inhibits the production of pyocyanin by *P. aeruginosa*, which is toxic to *C. albicans*, and it also impedes swarming motility in *P. aeruginosa* [94]–[96], [98]–[100].

Regarding the triple-species biofilm, composed of *P. aeruginosa*, *S. aureus*, and *C. albicans*, a 1.2 $\log_{10}$ CFU/mL decrease in the average number of cultivable cells of *P. aeruginosa* cells was noticed as compared to single biofilms of the respective species (6.8 $\log_{10}$ CFU/mL vs. 8.0 $\log_{10}$ CFU/mL). *S. aureus* demonstrates an increase in its average count of culturable cells, rising to 7.11 $\log_{10}$ CFU/cm^3 when compared to its dual-species biofilm. On the other hand, *C. albicans* showed a decrease, albeit slight, in its CFU count compared to its single-species biofilm (6.5 $\log_{10}$ CFU/mL vs. 6.7 $\log_{10}$ CFU/mL).

As for *P. aeruginosa* and *C. albicans* dual-species biofilm, the reduction of *P. aeruginosa* in the triple-species biofilm can be attributed to the presence of *C. albicans*, which secretes farnesol, thereby increasing the vulnerability of *P. aeruginosa* [94]–[96], [98]–[100]. In contrast, the decrease in *C. albicans* may be due to the presence of *P. aeruginosa*, as this Gram-negative bacterium has the capability to eliminate hyphal strains of *C. albicans*.

On the other hand, *S. aureus* has been shown to exhibit a preference for adhering to the filaments of *C. albicans* rather than its yeast cells, facilitated by specific protein-protein interactions on the filament surface [101]–[103]. This interaction is apparently like what occurs in *P. aeruginosa* and *C. albicans* and may reveal a synergistic interaction between *S. aureus* and *C. albicans*. Furthermore, studies have demonstrated that the filamentous form of the fungus supports the survival of *S. aureus*, and in turn, the bacteria stimulate the germination of the fungus [102], [103]. The survival of *S. aureus* is further promoted by fungal proteases that enable bacterial growth through the degradation of serum proteins, which typically inhibit bacterial proliferation. Consequently, *C. albicans* creates a growth-conducive environment by aligning it with the bacteria's requirements and offering a substrate for their proliferation [102], [103].

It is important to note that no prior studies have provided an explanation for the interactions occurring within triple-species biofilms composed of *P. aeruginosa*, *S. aureus*, and *C. albicans*. However, investigating these interactions is crucial due to their potential negative impact on infections like VAP because polymicrobial biofilms may have the capacity to exacerbate the severity and complexity of treating this disease. For instance, there is a possibility that *C. albicans* might inflict physical damage on organ walls, facilitating the ingress of other microorganisms, notably *P. aeruginosa* and *S. aureus*.

Furthermore, *C. albicans*' antagonistic relationship with *P. aeruginosa* and synergistic interaction with *S. aureus* may contribute to the evolution of genes related to pathogenesis (including an increase in its AMR) and the perpetuation of these genes. Moreover, these interactions might amplify the virulence of these microorganisms [95]. Furthermore, it has been demonstrated that exoproteins from *S. aureus* trigger the formation of small colony variants in *P. aeruginosa*. Similarly, the synthesis of 4-hydroxy-2-heptylquinoline-N-oxide by *P. aeruginosa* prompts the emergence of small colony variants in *S. aureus*. These interactions between the two microorganisms not only strengthen their resistance to antibiotics but also facilitate evasion of the host's immune response [104].

Figure 13 shows the outcomes following the biomass of the single-species, dual-species, and triple-species biofilms.

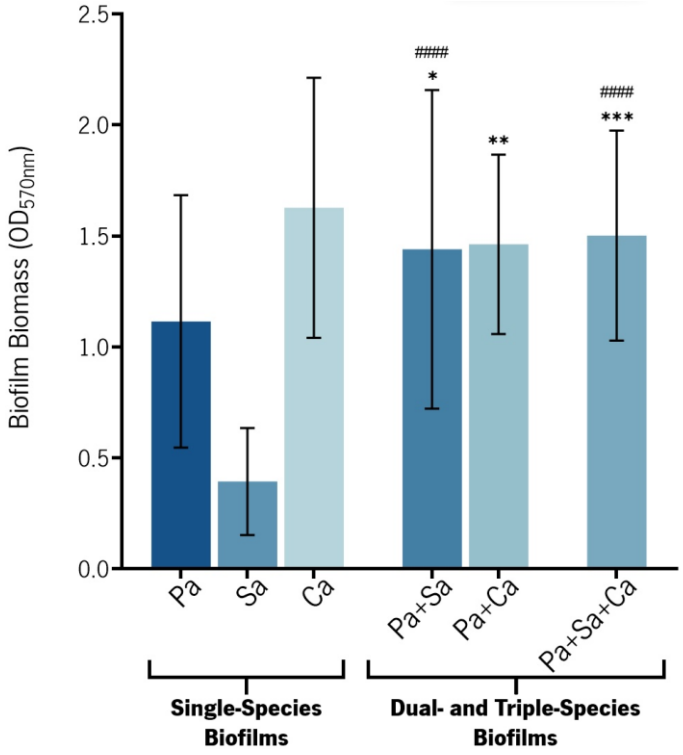


Figure 13: Biofilm biomass, expressed as OD 570 nm values, obtained for single-, dual-, and triple-species of biofims developed by *P. aeruginosa* ATCC 27853 (Pa), *S. aureus* ATCC 25923 (Sa), and *C. albicans* SC 5314 (Sa) for 24h at 37°C. The results are presented as mean±SD from three independent assays. Statistical analysis was conducted using ANOVA followed by a Kruskal-Wallis multiple comparisons test, comparing (*) significant differences between single-species *P. aeruginosa* biofilms and other *P. aeruginosa* biofilm types ($p<0.05$) and (#) significant differences between single-species *S. aureus* biofilms and other *S. aureus* biofilm types (#<0.05). No significant differences were observed between single-species *C. albicans* biofilms and other *C. albicans* biofilm types.

Figure 13 shows that, for single-species biofilms, a higher biomass was obtained for *P. aeruginosa* and *C. albicans* when compared to *S. aureus* biofilms. Concerning the dual-species biofilm formed by *P. aeruginosa* and *S. aureus*, a significant increase in the production of the biofilm matrix was

observed when compared to biofilms formed by each species individually. This increase in biomass can be attributed to the competitive interactions between *P. aeruginosa* and *S. aureus*.

P. aeruginosa produces heptyl-4-hydroxyquinoline N-oxide, which inhibits the electron transport chain of *S. aureus*. Consequently, *S. aureus* undergoes a shift towards a fermentative growth mode, ultimately resulting in a reduction in its viability. This shift prompts an increase in *S. aureus* biofilm formation and triggers the transition of *S. aureus* into small-colony variants. This phenotypic change enables *S. aureus* to endure unfavourable conditions as it acquires mutations in the electron transport chain, thus enhancing its resistance to *P. aeruginosa*-induced damage [105], [106].

Furthermore, *P. aeruginosa* expresses three exopolysaccharides, namely alginate, Pel, and Psl, within its biofilm extracellular matrix, serving structural and protective roles. In dual-species biofilms of *P. aeruginosa* and *S. aureus*, the expression of Psl results in *P. aeruginosa* predominantly occupying the upper layer of the biofilms, whereas the expression of Pel appears to promote the coexistence of *P. aeruginosa* and *S. aureus*. Moreover, Pel is often associated with the formation of floating biofilms (pellicles). Thus, these quorum sensing protection mechanisms utilised by these microorganisms collectively contribute to an amplified production of the biofilm matrix [105].

Concerning the dual-species biofilm comprising *P. aeruginosa* and *C. albicans*, a substantial increase in the average biomass was evident when compared with the biofilm mass from *P. aeruginosa* alone. However, in comparison to the single-species biofilm of *C. albicans*, there is a slight decrease in the average biomass.

As previously mentioned, *P. aeruginosa* exhibits a preference for attaching to *C. albicans* hyphae, ultimately leading to their death. Moreover, *P. aeruginosa* exerts an inhibitory effect on the transition of *C. albicans* from yeast to hyphal forms, thereby promoting the survival of *C. albicans*. In contrast, *C. albicans* engages in the production of ethanol, which serves to enhance biofilm formation, suppress swarming motility, and elevate the production of antifungal phenazines by *P. aeruginosa*. These phenotypic characteristics, in turn, result in the disruption of the central pathway responsible for inducing hyphal growth alongside the inhibition of mitochondrial activity, consequently stimulating ethanol production by *C. albicans*. These complex interactions have a collective impact on the availability of environmental factors such as iron levels, pH, and oxygen tension, thus culminating in an antagonistic relationship between *P. aeruginosa* and *C. albicans* [107], [108]. Consequently, the observed variations in biomass may be attributed to the competition that unfolds within this context. In the presence of *P. aeruginosa*, *C. albicans* may experience resource competition, leading to a reduction in its biomass compared to that of a single-species *C. albicans* biofilm. Conversely, *P. aeruginosa*'s adaptive

mechanisms enable it to thrive within the dual-species biofilm, potentially resulting in an increase in its biomass when compared to a single-species *P. aeruginosa* biofilm.

In the case of the triple-species biofilm, a similarity was noted in the outcomes regarding biomass formation compared to the dual-species biofilms. When comparing the biomass of the triple-species biofilm to that of the single-species biofilms of each microorganism, it becomes evident that there was an increase in the biomass of the triple-species biofilm when contrasted with the bacterial biofilms. However, there is a reduction in biomass when compared to the individual fungal biofilms.

As previously discussed, this variability in the production of the matrix may be attributed to the intricate interplay of competition and cooperation among the three microorganisms. On one hand, *P. aeruginosa*'s defence mechanisms hinder *S. aureus* and eliminate *C. albicans* when it assumes its hyphal form. Conversely, a synergistic relationship emerges as *S. aureus* binds to the hyphal form of *C. albicans*, granting survival to *S. aureus* and facilitating germination for *C. albicans* [94], [98], [102], [103]. Consequently, these interactions establish a dynamic environment in which resource competition influences the biomass of *C. albicans*, while the adaptive mechanisms of *P. aeruginosa* and *S. aureus* enable their thriving and the generation of enhanced biomass in the triple-species biofilm.

Additionally, when comparing the production of the matrix in the triple-species biofilm to that in the dual-species biofilms, it was evident that the increase in biomass was not significant. One of the contributing factors to this result could be the competitive interactions among the three microorganisms, which may have resulted in a reduction of the biofilm matrix. As depicted in **Figure 13**, all three populations coexist within the biofilm, potentially influencing this outcome.

1.4.2. Biofilm Formation on PVC

In this work, *P. aeruginosa*, *S. aureus*, and *C. albicans* were also evaluated in terms of biofilm formation on PVC surfaces. To evaluate the efficacy of PVC surfaces that had been previously functionalized with pDA to immobilise CIP and CHX in preventing microbial adhesion, specifically in inhibiting biofilm development by microorganisms typically associated with VAP, namely *P. aeruginosa*, *S. aureus*, and *C. albicans*, an examination was conducted in which cultivable cells were determined through CFU counting. This test involved a comparison of the count of viable cells within biofilms established on both PVC and the functionalized PVC surfaces (**Figure 14**).

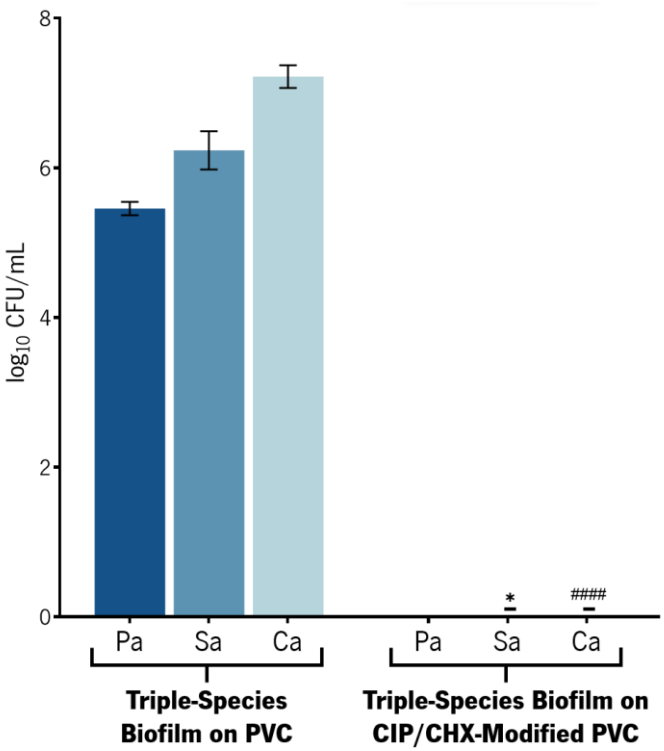


Figure 14: Biofilm quantification by plate count of triple-species 24h biofilms of *P. aeruginosa* ATCC 27853 (Pa), *S. aureus* ATCC 25923 (Sa), and *C. albicans* SC 5314 (Ca) formed in PVC and PVC that had been previously functionalized with pDA to immobilise CIP and CHX. The results are presented as mean±SD from two independent assays. Statistical analysis was conducted using ANOVA followed by a Kruskal-Wallis multiple comparisons test, comparing (*) significant differences between *S. aureus* biofilms ($p<0.05$) and (#) significant differences between *C. albicans* biofilms (#<0.05). No significant differences were observed between *P. aeruginosa* biofilms.

When comparing the count of viable cells within the triple-species biofilms of *P. aeruginosa*, *S. aureus*, and *C. albicans* that formed on the PVC surface (**Figure 14**) to those of the triple-species biofilms on polystyrene surfaces (**Figure 12**), it becomes evident that there was a reduction in the average count of viable cells for both *P. aeruginosa* (a difference of 1.4 $\log_{10}$ CFU/mL) and *S. aureus* (a difference of 0.9 $\log_{10}$ CFU/mL). However, this pattern was not shown for *C. albicans*, as the PVC surface induced an increase in the count of its cultivable cells, with a difference of 0.8 $\log_{10}$ CFU/mL. The differences in the count of viable cells within the triple-species biofilms on PVC and polystyrene surfaces can be attributed to the distinct physical and chemical characteristics of these materials. These properties may influence the adherence and growth of microorganisms. For instance, it is recognised that microorganisms generally exhibit greater adherence to hydrophilic surfaces. However, both PVC and polystyrene are classified as hydrophobic materials, with PVC being characterised as particularly hydrophobic[109], [110]. Consequently, a plausible explanation for the decrease in *P. aeruginosa* and *S. aureus* adherence may be attributed to this inherent hydrophobic property. In the case of *C. albicans*, the PVC surface may have offered a more favourable environment for the proliferation of *C. albicans*, resulting in

an increase in the number of culturable cells. Furthermore, this behaviour was also reported by Shinde et al [111].

Figure 14 demonstrates the significant impact of the CIP/CHX-modified PVC surfaces in inhibiting the formation of triple-species biofilms by the *P. aeruginosa*, *S. aureus*, and *C. albicans* consortium. These preliminary tests showed that a substantial reduction in the presence of these microorganisms was evident when comparing the number of cultivable cells on PVC and the modified PVC, with *P. aeruginosa* showing a decrease of 5.5 $\log_{10}$ CFU/mL, *S. aureus* exhibiting a decrease of 6.2 $\log_{10}$ CFU/mL, and *C. albicans* experiencing a decline of 7.2 $\log_{10}$ CFU/mL. Hence, the combination of CHX, acknowledged for its antiseptic properties against both Gram-positive and Gram-negative bacteria, and CIP, a well-established broad-spectrum antimicrobial agent against Gram-positive and Gram-negative bacteria, ensures the efficacy of this coating strategy in preventing microbial colonisation and the development of biofilms by *P. aeruginosa, S. aureus, and C. albicans* [63], [74].

To validate the results obtained through the CFU counting method, an additional assessment was conducted using the FISH technique to confirm the presence of *P. aeruginosa*, *S. aureus*, and *C. albicans* on both the PVC surfaces and the PVC surfaces functionalized with pDA for the immobilisation of CIP and CHX (**Figure 15**). It is important to emphasise that **Figure 15** was captured using an FV3000 confocal microscope and was supplied by the research group to complement the analysis conducted in this master's thesis of the triple-species biofilm that developed on these two PVC surfaces.

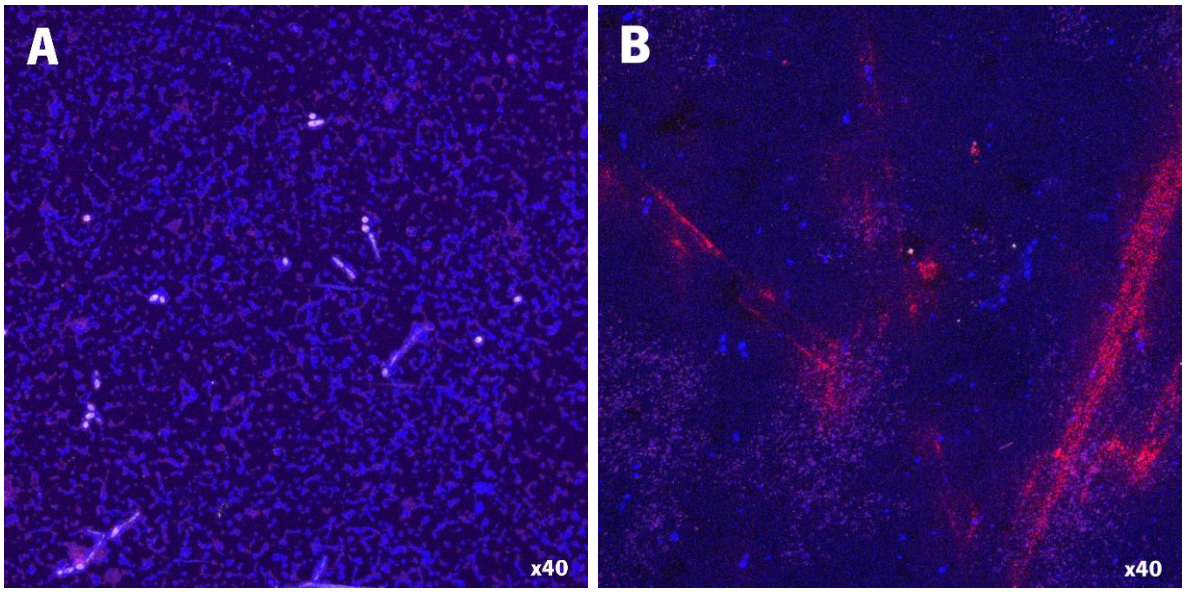


Figure 15: Detection of *P. aeruginosa* ATCC 27853 (Red), *S. aureus* ATCC 25923 (Blue), and *C. albicans* SC 5314 (White) in 24h triple-species biofilms formed in PVC (**A**) and PVC that had been previously functionalized with pDA to immobilise CIP and CHX (**B**), by using FISH technique.

Figure 15 illustrates the presence of *P. aeruginosa*, *S. aureus*, and *C. albicans* on the PVC surface. In contrast, when PVC surfaces are modified with pDA for the immobilisation of CIP and CHX, only *P. aeruginosa* and *S. aureus* are observed. This indicates a decreased colonisation of microorganisms on the modified PVC surface.

These findings contradict the outcomes in **Figure 14**, in which no cultivable cells of these pathogens were identified in the CFU counting method. One possible explanation for this discrepancy is that *P. aeruginosa*, *S. aureus*, and *C. albicans* entered in a non-cultivable state. Thus, these microorganisms can remain alive and metabolically active but not form colonies on traditional culture media [112]. However, they are not cultivable when in contact with PVC surfaces modified with pDA for the immobilisation of CIP and CHX.

Therefore, this coating strategy may not entirely prevent the formation of biofilms by this consortium, but it does make *P. aeruginosa* and *S. aureus* non-culturable.

CHAPTER 5: CONCLUSION AND FUTURE PERSPECTIVES

The first goal was to optimise a PNA-FISH methodology to be further used to diagnose VAP-related pathogens. Hence, factors like the hybridization temperature and the concentration of formamide in the HS were evaluated to address the specificity of PNA probes designed for *P. aeruginosa* (Paer565), *S. aureus* (Saur1), *K. pneumoniae* (Kpneu1), *S. epidermidis* (Sepi1), and *A. baumannii* (Abau1). Results showed that for the PNA probes Paer565, Saur1, Kpneu1, Sepi1, and Abau1, it was not feasible to determine a similar optimal hybridization temperature for these microorganisms. Although Paer565 exhibited effective performance across the temperature range under investigation, the other PNA probes did not display consistent behaviour. Specifically, Saur1, Sepi1, and Abau1 displayed a slight hybridization signal, while the two strains of *K. pneumoniae* hybridised with Kpneu1. *K. pneumoniae* ATCC 11296 showed hybridization at 52°C, 58°C, and 62°C, and *K. pneumoniae* ATCC 43216 at 52°C, 60°C, and 62°C. Consequently, even though determining the optimal hybridization temperature for all microorganisms using these specific PNA probes proved challenging, it was possible to confirm that the Paer565 and Kpneu1 probes can be employed in multiplex assays at hybridization temperatures of 52°C and 62°C.

In the case of formamide concentration in the HS, it was determined that lower concentrations, specifically 5% (v/v), yielded better hybridization results. Despite the variations observed in this hybridization parameter, it is noteworthy that both Paer565 and Kpneu1 exhibited successful hybridization at both concentrations. In contrast, the Saur1, Sepi1, and Abau1 probes failed to yield consistent outcomes. It is essential to acknowledge that the results for Sepi1 and Abau1 may have been influenced by inappropriate fluorescence filters. Therefore, it is recommended that future studies involving these PNA probes use filters within the appropriate wavelength range. As for Saur1, the minimal hybridization signal suggests a deficiency in its performance. Consequently, to incorporate a PNA probe targeting *S. aureus* into forthcoming multiplex assays, the development of a new PNA probe is suggested. For future studies involving these probes, it is also desirable to assess and validate their sensitivity to their specific target species and to validate the procedure either in clinical samples or in biofilms.

Regarding the biofilm assays conducted on polystyrene 96-well plates, it became evident that *P. aeruginosa* showed the highest ability to develop single-species biofilms, followed by *S. aureus* and *C. albicans.* Similar observations were found for dual-species biofilms involving *P. aeruginosa*, with this species prevailing over *S. aureus* or *C. albicans.* However, in the context of triple-species biofilms, *S. aureus* became the dominant species within the consortia, followed by *P. aeruginosa*, with *C. albicans* being the less predominant population.

Concerning biofilm formation on PVC, a notable difference from the triple-species biofilms on polystyrene was observed. In this context, *C. albicans* emerged as the primary microorganism, followed by *P. aeruginosa*, and *S. aureus* was the less dominant species. However, on functionalized PVC surfaces, no culturable cells were identified within the consortia. The application of FISH evidenced the presence of all bacterial and fungal species on the uncoated PVC surfaces and revealed a reduction in the presence of these microorganisms when PVC surfaces were immobilised with CIP and CHX, particularly *C. albicans*. Consequently, in the assessment where the CFU method was employed, *P. aeruginosa*, *S. aureus*, and *C. albicans* existed in a non-cultivable state.

Therefore, the immobilization of PVC surfaces with CIP and CHX has demonstrated its effectiveness in reducing the number of culturable cells within triple-species biofilms of *P. aeruginosa*, *S. aureus*, and *C. albicans*. However, further exploration with alternative techniques, such as quantitative PCR, and methodologies, such as Live/Dead staining, will be valuable in confirming the viability of these cells.

CHAPTER 6: BIBLIOGRAPHY

[1] B. Ozcelik *et al.*, "Evaluation of the Novel Antimicrobial BCP3 in a Coating for Endotracheal Tubes," *ACS Omega*, vol. 5, no. 18, pp. 10288–10296, May 2020, doi: 10.1021/acsomega.9b04178.

[2] I. Vandecandelaere *et al.*, "Assessment of microbial diversity in biofilms recovered from endotracheal tubes using culture dependent and independent approaches," *PLoS One*, vol. 7, no. 6, Jun. 2012, doi: 10.1371/journal.pone.0038401.

[3] L. Fernández-Barat and A. Torres, "Biofilms in ventilator-associated pneumonia," *Future Microbiology*, vol. 11, no. 12. Future Medicine Ltd., pp. 1599–1610, Dec. 01, 2016. doi: 10.2217/fmb-2016-0040.

[4] Ecdc, "Healthcare-associated infections acquired in intensive care units Annual Epidemiological Report 2019," 2019.

[5] R. Dsouza *et al.*, "*In vivo* detection of endotracheal tube biofilms in intubated critical care patients using catheter-based optical coherence tomography," *J Biophotonics*, vol. 12, no. 5, May 2019, doi: 10.1002/jbio.201800307.

[6] S. Gil-Perotin *et al.*, "Implications of endotracheal tube biofilm in ventilator-associated pneumonia response: A state of concept," *Crit Care*, vol. 16, no. 3, May 2012, doi: 10.1186/cc11357.

[7] O. C. Tablan, L. J. Anderson, R. Besser, C. Bridges, and R. Hajjeh, "Guideline for Preventing Healthcare-Associated Pneumonia (2003)," Mar. 2004.

[8] S. Y. Chi *et al.*, "Bacterial pathogens of ventilator associated pneumonia in a tertiary referral hospital," *Tuberc Respir Dis (Seoul)*, vol. 73, no. 1, pp. 32–37, Jul. 2012, doi: 10.4046/trd.2012.73.1.32.

[9] D. Alves, T. Grainha, M. O. Pereira, and S. P. Lopes, "Antimicrobial materials for endotracheal tubes: A review on the last two decades of technological progress," *Acta Biomaterialia*, vol. 158. Acta Materialia Inc, pp. 32–55, Mar. 01, 2023. doi: 10.1016/j.actbio.2023.01.001.

[10] M. Mirkarimi, M. Alisamir, S. Saraf, S. Heidari, S. Barouti, and S. Mohammadi, "Clinical and Epidemiological Determinants of Lower Respiratory Tract Infections in Hospitalized Pediatric Patients," *Int J Pediatr*, vol. 2020, pp. 1–7, Nov. 2020, doi: 10.1155/2020/8844420.

[11] B. Santella *et al.*, "Lower Respiratory Tract Pathogens and Their Antimicrobial Susceptibility Pattern: A 5-Year Study," *Antibiotics*, vol. 10, no. 7, p. 851, Jul. 2021, doi: 10.3390/antibiotics10070851.

[12] A. Mahashur, "Management of lower respiratory tract infection in outpatient settings: Focus on clarithromycin," *Lung India*, vol. 35, no. 2, pp. 143–149, Mar. 2018, doi: 10.4103/lungindia.lungindia_262_17.

[13] R. Klekotka, E. Mizgała, and W. Król, "The Etiology of Lower Respiratory Tract Infections in People with Diabetes," *Adv Respir Med*, vol. 83, no. 5, pp. 401–408, Sep. 2015, doi: 10.5603/PiAP.2015.0065.

[14] J.-F. Timsit, W. Esaied, M. Neuville, L. Bouadma, and B. Mourvillier, "Update on ventilator-associated pneumonia," *F1000 Research*, vol. 6, Nov. 2017, doi: 10.12688/f1000research.12222.1.

[15] L. Papazian, M. Klompas, and C.-E. Luyt, "Ventilator-associated pneumonia in adults: a narrative review," *Intensive Care Med*, vol. 46, no. 5, pp. 888–906, May 2020, doi: 10.1007/s00134-020-05980-0.

[16] P. Gunasekera and A. Gratrix, "Ventilator-associated pneumonia," *BJA Educ*, vol. 16, no. 6, pp. 198–202, Jun. 2016, doi: 10.1093/bjaed/mkv046.

[17] P. M. Charles *et al.*, "Ventilator-associated pneumonia," *Australasian Medical Journal*, vol. 7, no. 8, pp. 334–344, Aug. 2014, doi: 10.4066/AMJ.2014.2105.

[18] M. I. Restrepo, J. Peterson, J. F. Fernandez, Z. Qin, A. C. Fisher, and S. C. Nicholson, "Comparison of the Bacterial Etiology of Early-Onset and Late-Onset Ventilator-Associated Pneumonia in Subjects Enrolled in 2 Large Clinical Studies," *Respir Care*, vol. 58, no. 7, pp. 1220–1225, Jul. 2013, doi: 10.4187/respcare.02173.

[19] A. Rouzé, I. Martin-Loeches, and S. Nseir, "Airway Devices in Ventilator-Associated Pneumonia Pathogenesis and Prevention," *Clin Chest Med*, vol. 39, no. 4, pp. 775–783, Dec. 2018, doi: 10.1016/j.ccm.2018.08.001.

[20] V. Monteiro-Neto, L. G. Lima-Neto, A. G. Abreu, and C. R. A. V. Monteiro, "Microbiology of Ventilator-Associated Pneumonia," in *Contemporary Topics of Pneumonia*, Z. Chroneos, Ed., InTechIntechOpen, 2017, pp. 105–124. doi: 10.5772/intechopen.69430.

[21] V. I. Enne, Y. Personne, L. Grgic, V. Gant, and A. Zumla, "Aetiology of hospital-acquired pneumonia and trends in antimicrobial resistance," *Curr Opin Pulm Med*, vol. 20, no. 3, pp. 252–258, May 2014, doi: 10.1097/MCP.0000000000000042.

[22] A. Alnimr, "Antimicrobial Resistance in Ventilator-Associated Pneumonia: Predictive Microbiology and Evidence-Based Therapy," *Infect Dis Ther*, vol. 12, no. 6, pp. 1527–1552, Jun. 2023, doi: 10.1007/s40121-023-00820-2.

[23] M. Bassetti, L. Taramasso, D. R. Giacobbe, and P. Pelosi, "Management of ventilator-associated pneumonia: epidemiology, diagnosis and antimicrobial therapy," *Expert Rev Anti Infect Ther*, vol. 10, no. 5, pp. 585–596, May 2012, doi: 10.1586/eri.12.36.

[24] I. Erdem *et al.*, "A 5-year surveillance of healthcare-associated infections in a university hospital: A retrospective analysis," *SAGE Open Med*, vol. 10, p. 205031212210917, Jan. 2022, doi: 10.1177/20503121221091789.

[25] L. M. Weiner *et al.*, "Antimicrobial-Resistant Pathogens Associated With Healthcare-Associated Infections: Summary of Data Reported to the National Healthcare Safety Network at the Centers for Disease Control and Prevention, 2011–2014," *Infect Control Hosp Epidemiol*, vol. 37, no. 11, pp. 1288–1301, Nov. 2016, doi: 10.1017/ice.2016.174.

[26] M. F. Moradali, S. Ghods, and B. H. A. Rehm, "*Pseudomonas aeruginosa* Lifestyle: A Paradigm for Adaptation, Survival, and Persistence," *Front Cell Infect Microbiol*, vol. 7, Feb. 2017, doi: 10.3389/fcimb.2017.00039.

[27] M. W. Azam and A. U. Khan, "Updates on the pathogenicity status of *Pseudomonas aeruginosa*," *Drug Discov Today*, vol. 24, no. 1, pp. 350–359, Jan. 2019, doi: 10.1016/j.drudis.2018.07.003.

[28] C. Liu *et al.*, "Clinical Practice Guidelines by the Infectious Diseases Society of America for the Treatment of Methicillin-Resistant *Staphylococcus aureus* Infections in Adults and Children: Executive Summary," *Clinical Infectious Diseases*, vol. 52, no. 3, pp. 285–292, Feb. 2011, doi: 10.1093/cid/cir034.

[29] M. Otto, "*Staphylococcus epidermidis* — the 'accidental' pathogen," *Nat Rev Microbiol*, vol. 7, no. 8, pp. 555–567, Aug. 2009, doi: 10.1038/nrmicro2182.

[30] K. Y. Le, M. D. Park, and M. Otto, "Immune Evasion Mechanisms of *Staphylococcus epidermidis* Biofilm Infection," *Front Microbiol*, vol. 9, Feb. 2018, doi: 10.3389/fmicb.2018.00359.

[31] L. C. S. Antunes, P. Visca, and K. J. Towner, "*Acinetobacter baumannii*: evolution of a global pathogen," *Pathog Dis*, vol. 71, no. 3, pp. 292–301, Aug. 2014, doi: 10.1111/2049-632X.12125.

[32] I. Kyriakidis, E. Vasileiou, Z. D. Pana, and A. Tragiannidis, "*Acinetobacter baumannii* Antibiotic Resistance Mechanisms," *Pathogens*, vol. 10, no. 3, p. 373, Mar. 2021, doi: 10.3390/pathogens10030373.

[33] J. J. Champoux, F. C. Neidhardt, W. L. Drew, and J. J. Plorde, *Sherris Medical Microbiology: An Introduction to Infectious Diseases*, 4th ed. New York: The McGraw-Hill Companies, Inc., 2004.

[34] N. A. R. Gow and B. Yadav, "Microbe Profile: Candida albicans: a shape-changing, opportunistic pathogenic fungus of humans," *Microbiology (N Y)*, vol. 163, no. 8, pp. 1145–1147, Aug. 2017, doi: 10.1099/mic.0.000499.

[35] D. Kart, S. Tavernier, H. Van Acker, H. J. Nelis, and T. Coenye, "Activity of disinfectants against multispecies biofilms formed by *Staphylococcus aureus*, *Candida albicans* and *Pseudomonas aeruginosa*," *Biofouling*, vol. 30, no. 3, pp. 377–383, Mar. 2014, doi: 10.1080/08927014.2013.878333.

[36] D. Bensasson *et al.*, "Diverse Lineages of *Candida albicans* Live on Old Oaks," *Genetics*, vol. 211, no. 1, pp. 277–288, Jan. 2019, doi: 10.1534/genetics.118.301482.

[37] J.-B. Méar *et al.*, "*Candida albicans* and *Pseudomonas aeruginosa* interactions: More than an opportunistic criminal association?," *Med Mal Infect*, vol. 43, no. 4, pp. 146–151, Apr. 2013, doi: 10.1016/j.medmal.2013.02.005.

[38] S. P. Saville, A. L. Lazzell, C. Monteagudo, and J. L. Lopez-Ribot, "Engineered Control of Cell Morphology In Vivo Reveals Distinct Roles for Yeast and Filamentous Forms of Candida albicans during Infection," *Eukaryot Cell*, vol. 2, no. 5, pp. 1053–1060, Oct. 2003, doi: 10.1128/EC.2.5.1053-1060.2003.

[39] S. Fanning and A. P. Mitchell, "Fungal Biofilms," *PLoS Pathog*, vol. 8, no. 4, p. e1002585, Apr. 2012, doi: 10.1371/journal.ppat.1002585.

[40] M.-S. Delisle *et al.*, "Impact of *Candida* Species on Clinical Outcomes in Patients with Suspected Ventilator-Associated Pneumonia," *Can Respir J*, vol. 18, no. 3, pp. 131–136, May 2011, doi: 10.1155/2011/827692.

[41] S. M. Fernando *et al.*, "Diagnosis of ventilator-associated pneumonia in critically ill adult patients—a systematic review and meta-analysis," *Intensive Care Med*, vol. 46, no. 6, pp. 1170–1179, Jun. 2020, doi: 10.1007/s00134-020-06036-z.

[42] A.-M. Bălan, C. Bodolea, S. D. Trancă, and N. Hagău, "Trends in Molecular Diagnosis of Nosocomial Pneumonia Classic PCR vs. Point-of-Care PCR: A Narrative Review," *Healthcare*, vol. 11, no. 9, p. 1345, May 2023, doi: 10.3390/healthcare11091345.

[43] P. Póvoa *et al.*, "Biomarker kinetics in the prediction of VAP diagnosis: results from the BioVAP study," *Ann Intensive Care*, vol. 6, no. 1, p. 32, Dec. 2016, doi: 10.1186/s13613-016-0134-8.

[44] R. H. Kallet, "The Vexing Problem of Ventilator-Associated Pneumonia: Observations on Pathophysiology, Public Policy, and Clinical Science," *Respir Care*, vol. 60, no. 10, pp. 1495–1508, Oct. 2015, doi: 10.4187/respcare.03774.

[45] G. B. Nair and M. S. Niederman, "Ventilator-associated pneumonia: present understanding and ongoing debates," *Intensive Care Med*, vol. 41, no. 1, pp. 34–48, Jan. 2015, doi: 10.1007/s00134-014-3564-5.

[46] B. Bouhemad, O. Dransart-Rayé, F. Mojoli, and S. Mongodi, “Lung ultrasound for diagnosis and monitoring of ventilator-associated pneumonia,” *Ann Transl Med*, vol. 6, no. 20, pp. 418–418, Oct. 2018, doi: 10.21037/atm.2018.10.46.

[47] L. Kreitmann, A. Gaudet, and S. Nseir, “Ventilator-Associated Pneumonia in Immunosuppressed Patients,” *Antibiotics*, vol. 12, no. 2, p. 413, Feb. 2023, doi: 10.3390/antibiotics12020413.

[48] M. Bassetti, L. Taramasso, D. R. Giacobbe, and P. Pelosi, “Management of ventilator-associated pneumonia: epidemiology, diagnosis and antimicrobial therapy,” *Expert Rev Anti Infect Ther*, vol. 10, no. 5, pp. 585–596, May 2012, doi: 10.1586/eri.12.36.

[49] L. J. Staub, R. R. M. Biscaro, and R. Maurici, “Accuracy and Applications of Lung Ultrasound to Diagnose Ventilator-Associated Pneumonia: A Systematic Review,” *J Intensive Care Med*, vol. 33, no. 8, pp. 447–455, Aug. 2018, doi: 10.1177/0885066617737756.

[50] L. J. Staub, R. R. M. Biscaro, and R. Maurici, “Emergence of Alveolar Consolidations in Serial Lung Ultrasound and Diagnosis of Ventilator-Associated Pneumonia,” *J Intensive Care Med*, vol. 36, no. 3, pp. 304–312, Mar. 2021, doi: 10.1177/0885066619894279.

[51] J.-Y. Fagon, “Biological markers and diagnosis of ventilator-associated pneumonia,” *Crit Care*, vol. 15, no. 2, p. 130, Mar. 2011, doi: 10.1186/cc10050.

[52] J. I. F. Salluh, V. C. Souza-Dantas, and P. Póvoa, “The current status of biomarkers for the diagnosis of nosocomial pneumonias,” *Curr Opin Crit Care*, vol. 23, no. 5, pp. 391–397, Oct. 2017, doi: 10.1097/MCC.0000000000000442.

[53] M. Lung and G. Codina, “Molecular diagnosis in HAP/VAP,” *Curr Opin Crit Care*, vol. 18, no. 5, pp. 487–494, Oct. 2012, doi: 10.1097/MCC.0b013e3283577d37.

[54] M. C. V. Guillamet, J. P. Burnham, and M. H. Kollef, “Novel Approaches to Hasten Detection of Pathogens and Antimicrobial Resistance in the Intensive Care Unit,” *Semin Respir Crit Care Med*, vol. 40, no. 04, pp. 454–464, Aug. 2019, doi: 10.1055/s-0039-1693160.

[55] N. Singhal, M. Kumar, P. K. Kanaujia, and J. S. Virdi, "MALDI-TOF mass spectrometry: an emerging technology for microbial identification and diagnosis," *Front Microbiol*, vol. 6, Aug. 2015, doi: 10.3389/fmicb.2015.00791.

[56] S. P. Lopes, D. T. Carvalho, M. O. Pereira, and N. F. Azevedo, "Discriminating typical and atypical cystic fibrosis-related bacteria by multiplex PNA-FISH," *Biotechnol Bioeng*, vol. 114, no. 2, pp. 355–367, Feb. 2017, doi: 10.1002/bit.26085.

[57] R. Koncan *et al.*, "Direct identification of major Gram-negative pathogens in respiratory specimens by respiFISH® HAP Gram (–) Panel, a beacon-based FISH methodology," *European Journal of Clinical Microbiology & Infectious Diseases*, vol. 34, no. 10, pp. 2097–2102, Oct. 2015, doi: 10.1007/s10096-015-2458-y.

[58] E. C. Jensen, "Types of Imaging, Part 2: An Overview of Fluorescence Microscopy," *Anat Rec*, vol. 295, no. 10, pp. 1621–1627, Oct. 2012, doi: 10.1002/ar.22548.

[59] J. G. White, W. B. Amos, and M. Fordham, "An evaluation of confocal versus conventional imaging of biological structures by fluorescence light microscopy.," *J Cell Biol*, vol. 105, no. 1, pp. 41–48, Jul. 1987, doi: 10.1083/jcb.105.1.41.

[60] M. Ashraf and L. Ostrosky-Zeichner, "Ventilator-Associated Pneumonia: A Review," *Hosp Pract*, vol. 40, no. 1, pp. 93–105, Feb. 2012, doi: 10.3810/hp.2012.02.950.

[61] S. T. Micek and L. P. Skrupky, "Current Concepts in the Prevention and Treatment of Ventilator-Associated Pneumonia," *J Pharm Pract*, vol. 23, no. 1, pp. 25–32, Feb. 2010, doi: 10.1177/0897190009356553.

[62] S.-S. Jean, Y.-C. Chang, W.-C. Lin, W.-S. Lee, P.-R. Hsueh, and C.-W. Hsu, "Epidemiology, Treatment, and Prevention of Nosocomial Bacterial Pneumonia," *J Clin Med*, vol. 9, no. 1, p. 275, Jan. 2020, doi: 10.3390/jcm9010275.

[63] A. Kalanuria, W. Zai, and M. Mirski, "Ventilator-associated pneumonia in the ICU," *Crit Care*, vol. 18, no. 2, p. 208, 2014, doi: 10.1186/cc13775.

[64] O. Diaconu, I. Siriopol, L. I. Poloşanu, and I. Grigoraş, "Endotracheal Tube Biofilm and its Impact on the Pathogenesis of Ventilator-Associated Pneumonia," *The Journal of Critical Care Medicine*, vol. 4, no. 2, pp. 50–55, Apr. 2018, doi: 10.2478/jccm-2018-0011.

[65] T. Webster and M. Machado, "Decreased Pseudomonas aeruginosa biofilm formation on nanomodified endotracheal tubes: a dynamic lung model," *Int J Nanomedicine*, vol. 11, pp. 3825–3831, Aug. 2016, doi: 10.2147/IJN.S108253.

[66] A. C. Zangirolami *et al.*, "Avoiding ventilator-associated pneumonia: Curcumin-functionalized endotracheal tube and photodynamic action," *Proceedings of the National Academy of Sciences*, vol. 117, no. 37, pp. 22967–22973, Sep. 2020, doi: 10.1073/pnas.2006759117.

[67] S. Lethongkam *et al.*, "Prolonged inhibitory effects against planktonic growth, adherence, and biofilm formation of pathogens causing ventilator-associated pneumonia using a novel polyamide/silver nanoparticle composite-coated endotracheal tube," *Biofouling*, vol. 36, no. 3, pp. 292–307, Mar. 2020, doi: 10.1080/08927014.2020.1759041.

[68] M. Palau *et al.*, "Hyperthermia Prevents In Vitro and In Vivo Biofilm Formation on Endotracheal Tubes," *Microbiol Spectr*, vol. 11, no. 1, Feb. 2023, doi: 10.1128/spectrum.02807-22.

[69] H. R. Thorarinsdottir, T. Kander, A. Holmberg, S. Petronis, and B. Klarin, "Biofilm formation on three different endotracheal tubes: a prospective clinical trial," *Crit Care*, vol. 24, no. 1, p. 382, Dec. 2020, doi: 10.1186/s13054-020-03092-1.

[70] Z. Dargahi *et al.*, "The biofilm formation and antibiotic resistance of bacterial profile from endotracheal tube of patients admitted to intensive care unit in southwest of Iran," *PLoS One*, vol. 17, no. 11, p. e0277329, Nov. 2022, doi: 10.1371/journal.pone.0277329.

[71] T. Grainha, P. Jorge, D. Alves, S. P. Lopes, and M. O. Pereira, "Unraveling *Pseudomonas aeruginosa* and *Candida albicans* Communication in Coinfection Scenarios: Insights Through Network Analysis," *Front Cell Infect Microbiol*, vol. 10, Nov. 2020, doi: 10.3389/fcimb.2020.550505.

[72] R. M. May *et al.*, "Micro-patterned surfaces reduce bacterial colonization and biofilm formation *in vitro*: Potential for enhancing endotracheal tube designs," *Clin Transl Med*, vol. 3, no. 1, Dec. 2014, doi: 10.1186/2001-1326-3-8.

[73] P. S. Zolfaghari and D. LA Wyncoll, "The tracheal tube: gateway to ventilator-associated pneumonia," *Crit Care*, vol. 15, no. 5, p. 310, 2011, doi: 10.1186/cc10352.

[74] D. Alves, P. Borges, T. Grainha, C. F. Rodrigues, and M. O. Pereira, "Tailoring the immobilization and release of chlorhexidine using dopamine chemistry to fight infections associated to orthopedic devices," *Materials Science and Engineering: C*, vol. 120, p. 111742, Nov. 2020, doi: 10.1016/j.msec.2020.111742.

[75] C. Hu *et al.*, "Antibacterial endotracheal tube with silver-containing double-network hydrogel coating," *Colloid Interface Sci Commun*, vol. 55, p. 100724, Jun. 2023, doi: 10.1016/j.colcom.2023.100724.

[76] D. Alves, A. Magalhães, D. Grzywacz, D. Neubauer, W. Kamysz, and M. O. Pereira, "Co-immobilization of Palm and DNase I for the development of an effective anti-infective coating for catheter surfaces," *Acta Biomater*, vol. 44, pp. 313–322, Aug. 2016, doi: 10.1016/j.actbio.2016.08.010.

[77] D. Alves, A. T. Vaz, T. Grainha, C. F. Rodrigues, and M. O. Pereira, "Design of an Antifungal Surface Embedding Liposomal Amphotericin B Through a Mussel Adhesive-Inspired Coating Strategy," *Front Chem*, vol. 7, Jun. 2019, doi: 10.3389/fchem.2019.00431.

[78] D. Alves, M. O. Pereira, and S. P. Lopes, "Co-immobilization of ciprofloxacin and chlorhexidine as a long-term, broad-spectrum antimicrobial dual-drug coating for polyvinyl chloride (PVC)-based endotracheal tubes," May 2023, doi: 10.1101/2023.04.13.534541.

[79] H. Perry-O'Keefe *et al.*, "Identification of indicator microorganisms using a standardized PNA FISH method," *J Microbiol Methods*, vol. 47, no. 3, pp. 281–292, Dec. 2001, doi: 10.1016/S0167-7012(01)00303-7.

[80] R. Rocha, C. Almeida, and N. F. Azevedo, "Influence of the fixation/permeabilization step on peptide nucleic acid fluorescence in situ hybridization (PNA-FISH) for the detection of bacteria," *PLoS One*, vol. 13, no. 5, May 2018, doi: 10.1371/journal.pone.0196522.

[81] R. Rocha, R. S. Santos, P. Madureira, C. Almeida, and N. F. Azevedo, "Optimization of peptide nucleic acid fluorescence in situ hybridization (PNA-FISH) for the detection of bacteria: The effect of pH, dextran sulfate and probe concentration," *J Biotechnol*, vol. 226, pp. 1–7, May 2016, doi: 10.1016/j.jbiotec.2016.03.047.

[82] R. S. Santos, C. C. Lima, D. Carvalho, F. Meireles, N. Guimarães, and N. F. Azevedo, "Response surface methodology to optimize peptide nucleic acid fluorescence in situ hybridization (PNA-FISH) in *Saccharomyces cerevisiae*," *LWT - Food Science and Technology*, vol. 80, pp. 27–31, Jan. 2017, doi: 10.1016/j.lwt.2017.01.077.

[83] R. S. Santos, N. Guimarães, P. Madureira, and N. F. Azevedo, "Optimization of a peptide nucleic acid fluorescence in situ hybridization (PNA-FISH) method for the detection of bacteria and disclosure of a formamide effect," *J Biotechnol*, vol. 187, pp. 16–24, Jul. 2014, doi: 10.1016/j.jbiotec.2014.06.023.

[84] E. V. Volpi, "Formamide-Free Fluorescence In Situ Hybridization (FISH)," in *Fluorescence In Situ Hybridization (FISH)*, 2nd ed., T. Liehr, Ed., Berlin: Springer, 2017, pp. 135–139. doi: 10.1007/978-3-662-52959-1_12.

[85] V. González *et al.*, "Rapid diagnosis of Staphylococcus aureus bacteremia using S. aureus PNA FISH," *European Journal of Clinical Microbiology & Infectious Diseases*, vol. 23, no. 5, pp. 396–398, May 2004, doi: 10.1007/s10096-004-1112-x.

[86] H. Hartmann, H. Stender, A. Schäfer, I. B. Autenrieth, and V. A. J. Kempf, "Rapid Identification of *Staphylococcus aureus* in Blood Cultures by a Combination of Fluorescence In Situ Hybridization Using Peptide Nucleic Acid Probes and Flow Cytometry," *J Clin Microbiol*, vol. 43, no. 9, pp. 4855–4857, Sep. 2005, doi: 10.1128/JCM.43.9.4855-4857.2005.

[87] C. Wilson *et al.*, "Quantitative and Qualitative Assessment Methods for Biofilm Growth: A Mini-review.," *Res Rev J Eng Technol*, vol. 6, no. 4, Dec. 2017.

[88] L. M. Filkins *et al.*, "Coculture of *Staphylococcus aureus* with *Pseudomonas aeruginosa* Drives *S. aureus* towards Fermentative Metabolism and Reduced Viability in a Cystic Fibrosis Model," *J Bacteriol*, vol. 197, no. 14, pp. 2252–2264, Jul. 2015, doi: 10.1128/JB.00059-15.

[89] R. Baldan *et al.*, "Adaptation of *Pseudomonas aeruginosa* in Cystic Fibrosis Airways Influences Virulence of *Staphylococcus aureus* In Vitro and Murine Models of Co-Infection," *PLoS One*, vol. 9, no. 3, p. e89614, Mar. 2014, doi: 10.1371/journal.pone.0089614.

[90] H. Wu *et al.*, "*Pseudomonas aeruginosa* mutations in lasI and rhlI quorum sensing systems result in milder chronic lung infection," *Microbiology (N Y)*, vol. 147, no. 5, pp. 1105–1113, May 2001, doi: 10.1099/00221287-147-5-1105.

[91] T. Bjarnsholt *et al.*, "Quorum Sensing and Virulence of *Pseudomonas aeruginosa* during Lung Infection of Cystic Fibrosis Patients," *PLoS One*, vol. 5, no. 4, p. e10115, Apr. 2010, doi: 10.1371/journal.pone.0010115.

[92] C. R. Armbruster *et al.*, "*Staphylococcus aureus* Protein A Mediates Interspecies Interactions at the Cell Surface of *Pseudomonas aeruginosa*," *mBio*, vol. 7, no. 3, Jul. 2016, doi: 10.1128/mBio.00538-16.

[93] A. P. Magalhães, T. Grainha, A. M. Sousa, Â. França, N. Cerca, and M. O. Pereira, "Viable but non-cultivable state: a strategy for *Staphylococcus aureus* survivable in dual-species biofilms with *Pseudomonas aeruginosa*?," *Environ Microbiol*, vol. 23, no. 9, pp. 5639–5649, Sep. 2021, doi: 10.1111/1462-2920.15734.

[94] R. Fourie, R. Ells, C. W. Swart, O. M. Sebolai, J. Albertyn, and C. H. Pohl, "*Candida albicans* and *Pseudomonas aeruginosa* Interaction, with Focus on the Role of Eicosanoids," *Front Physiol*, vol. 7, Feb. 2016, doi: 10.3389/fphys.2016.00064.

[95] M. E. Shirtliff, B. M. Peters, and M. A. Jabra-Rizk, "Cross-kingdom interactions: *Candida albicans* and bacteria," *FEMS Microbiol Lett*, vol. 299, no. 1, pp. 1–8, Oct. 2009, doi: 10.1111/j.1574-6968.2009.01668.x.

[96] G. McAlester, F. O'Gara, and J. P. Morrissey, "Signal-mediated interactions between *Pseudomonas aeruginosa* and *Candida albicans*," *J Med Microbiol*, vol. 57, no. 5, pp. 563–569, May 2008, doi: 10.1099/jmm.0.47705-0.

[97] S. Kasetty, D. L. Mould, D. A. Hogan, and C. D. Nadell, "Both *Pseudomonas aeruginosa* and *Candida albicans* Accumulate Greater Biomass in Dual-Species Biofilms under Flow," *mSphere*, vol. 6, no. 3, Jun. 2021, doi: 10.1128/mSphere.00416-21.

[98] L. J. Holcombe *et al.*, "*Pseudomonas aeruginosa* secreted factors impair biofilm development in *Candida albicans*," *Microbiology (N Y)*, vol. 156, no. 5, pp. 1476–1486, May 2010, doi: 10.1099/mic.0.037549-0.

[99] J.-B. Méar *et al.*, "*Candida albicans* and *Pseudomonas aeruginosa* interactions: More than an opportunistic criminal association?," *Med Mal Infect*, vol. 43, no. 4, pp. 146–151, Apr. 2013, doi: 10.1016/j.medmal.2013.02.005.

[100] F. G. Purschke, E. Hiller, I. Trick, and S. Rupp, "Flexible Survival Strategies of *Pseudomonas aeruginosa* in Biofilms Result in Increased Fitness Compared with *Candida albicans*," *Molecular & Cellular Proteomics*, vol. 11, no. 12, pp. 1652–1669, Dec. 2012, doi: 10.1074/mcp.M112.017673.

[101] E. S. Ovchinnikova, B. P. Krom, H. C. van der Mei, and H. J. Busscher, "Force microscopic and thermodynamic analysis of the adhesion between *Pseudomonas aeruginosa* and *Candida albicans*," *Soft Matter*, vol. 8, no. 24, p. 6454, 2012, doi: 10.1039/c2sm25100k.

[102] Y. J. Lin *et al.*, "Interactions between *Candida albicans* and *Staphylococcus aureus* within mixed species biofilms," *Bios*, vol. 84, no. 1, pp. 30–39, Mar. 2013, doi: 10.1893/0005-3155-84.1.30.

[103] M. M. Harriott and M. C. Noverr, "*Candida albicans* and *Staphylococcus aureus* Form Polymicrobial Biofilms: Effects on Antimicrobial Resistance," *Antimicrob Agents Chemother*, vol. 53, no. 9, pp. 3914–3922, Sep. 2009, doi: 10.1128/AAC.00657-09.

[104] I. Reigada *et al.*, "Surfaceome and Exoproteome Dynamics in Dual-Species *Pseudomonas aeruginosa* and *Staphylococcus aureus* Biofilms," *Front Microbiol*, vol. 12, Jun. 2021, doi: 10.3389/fmicb.2021.672975.

[105] S. C. Chew *et al.*, "Matrix Polysaccharides and SiaD Diguanylate Cyclase Alter Community Structure and Competitiveness of *Pseudomonas aeruginosa* during Dual-Species Biofilm Development with *Staphylococcus aureus*," *mBio*, vol. 9, no. 6, Dec. 2018, doi: 10.1128/mBio.00585-18.

[106] E. Y. Trizna *et al.*, "Bidirectional alterations in antibiotics susceptibility in *Staphylococcus aureus–Pseudomonas aeruginosa* dual-species biofilm," *Sci Rep*, vol. 10, no. 1, p. 14849, Sep. 2020, doi: 10.1038/s41598-020-71834-w.

[107] P. Phuengmaung *et al.*, "Coexistence of *Pseudomonas aeruginosa* With *Candida albicans* Enhances Biofilm Thickness Through Alginate-Related Extracellular Matrix but Is Attenuated by N-acetyl-l-cysteine," *Front Cell Infect Microbiol*, vol. 10, Nov. 2020, doi: 10.3389/fcimb.2020.594336.

[108] S. Kasetty, D. L. Mould, D. A. Hogan, and C. D. Nadell, "Both *Pseudomonas aeruginosa* and *Candida albicans* Accumulate Greater Biomass in Dual-Species Biofilms under Flow," *mSphere*, vol. 6, no. 3, Jun. 2021, doi: 10.1128/mSphere.00416-21.

[109] A. S. Setiyawan, A. Nur, Mhd. Fauzi, K. Oginawati, and P. Soewondo, "Effects of Different Polymeric Materials on the Bacterial Attachment and Biofilm Formation in Anoxic Fixed-Bed Biofilm Reactors," *Water Air Soil Pollut*, vol. 234, no. 3, p. 147, Mar. 2023, doi: 10.1007/s11270-023-06174-2.

[110] B. Battulga, M. Kawahigashi, and B. Oyuntsetseg, "Characterization of biofilms formed on polystyrene microplastics (PS-MPs) on the shore of the Tuul River, Mongolia," *Environ Res*, vol. 212, p. 113329, Sep. 2022, doi: 10.1016/j.envres.2022.113329.

[111] R. B. Shinde, J. S. Raut, and M. S. Karuppayil, "Biofilm formation by *Candida albicans* on various prosthetic materials and its fluconazole sensitivity: a kinetic study," *Mycoscience*, vol. 53, no. 3, pp. 220–226, May 2012, doi: 10.1007/S10267-011-0155-Y.

[112] C. Almeida, N. F. Azevedo, S. Santos, C. W. Keevil, and M. J. Vieira, "Discriminating Multi-Species Populations in Biofilms with Peptide Nucleic Acid Fluorescence In Situ Hybridization (PNA FISH)," *PLoS One*, vol. 6, no. 3, p. e14786, Mar. 2011, doi: 10.1371/journal.pone.0014786.